

Astronomy 233 Spring 2011

Physical Cosmology

Week 5

*Dark Matter, CMB, and
Structure Formation*

Joel Primack

University of California, Santa Cruz

Types of Dark Matter

Ω_i represents the fraction of the critical density $\rho_c = 10.54 h^2 \text{ keV/cm}^3$ needed to close the Universe, where h is the Hubble constant H_0 divided by 100 km/s/Mpc.

Dark Matter Type	Fraction of Critical Density	Comment
Baryonic	$\Omega_b \sim 0.04$	about 10 times the visible matter
Hot	$\Omega_\nu \sim 0.001-0.1$	light neutrinos
Cold	$\Omega_c \sim 0.3$	most of the dark matter in galaxy halos

Dark Matter and Associated Cosmological Models

Ω_m represents the fraction of the critical density in all types of matter.
 Ω_Λ is the fraction contributed by some form of "dark energy."

Acronym	Cosmological Model	Flourished
HDM	hot dark matter with $\Omega_m = 1$	1978–1984
SCDM	standard cold dark matter with $\Omega_m = 1$	1982–1992
CHDM	cold + hot dark matter with $\Omega_c \sim 0.7$ and $\Omega_\nu = 0.2-0.3$	1994–1998
Λ CDM	cold dark matter $\Omega_c \sim 1/3$ and $\Omega_\Lambda \sim 2/3$	1996–today

WHAT IS THE DARK MATTER?

Prospects for DIRECT and INDIRECT detection of **WIMPs** are improving.

With many upcoming experiments

- Production at Large Hadron Collider

- Better CMB data from PLANCK

- Direct Detection

 - Spin Independent - CDMS-II, XENON50, LUX

 - Spin Dependent - COUPP, PICASSO

- Indirect detection via

 - GLAST and larger ACTs

 - PAMELA and ATIC

-- there could well be a big discovery in the next year or two!

Four roads to dark matter: *catch it, infer it, make it, weigh it*

Direct:



Production:



LHC

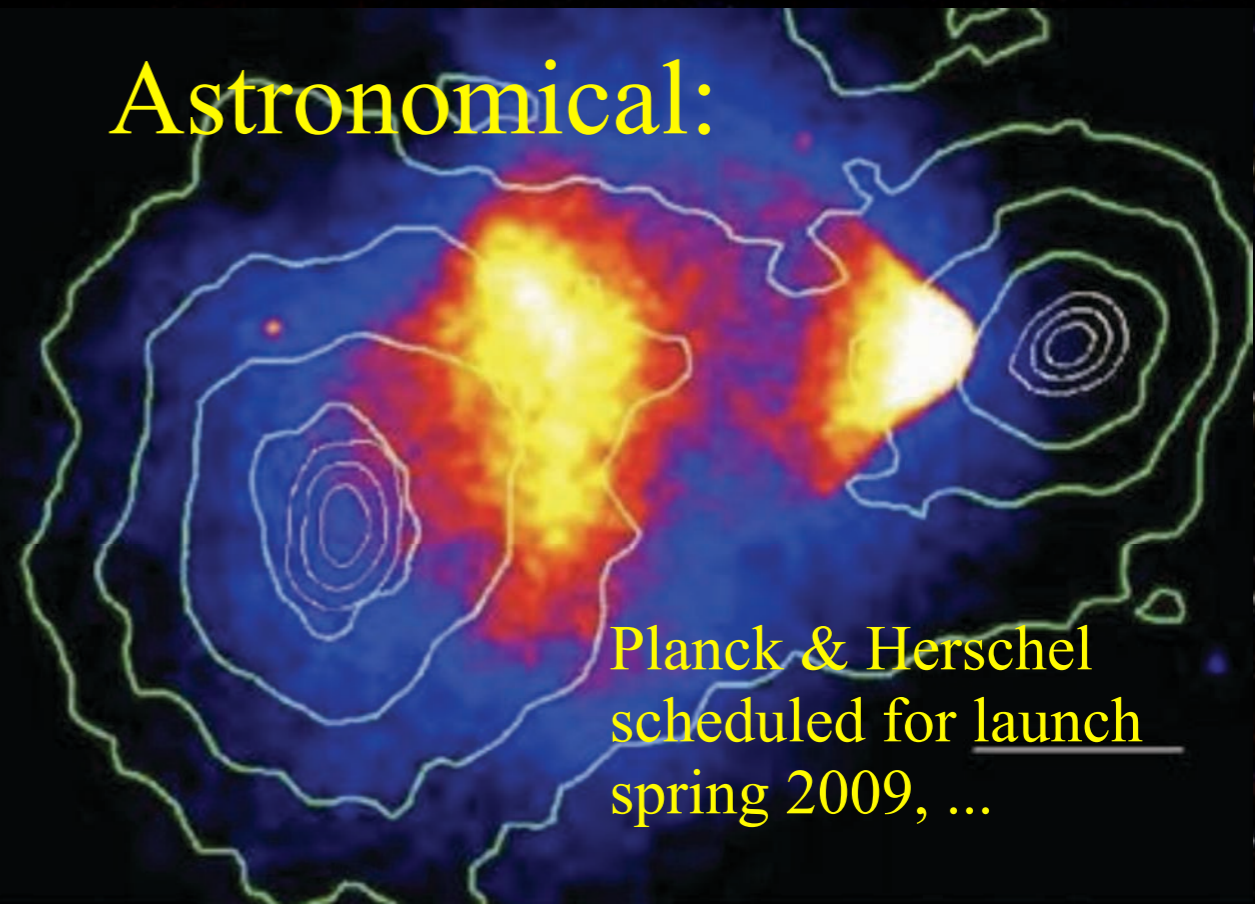
With all these upcoming experiments, the next few years will be very exciting!

Indirect:



Fermi (GLAST) launched June 11, 2008

Astronomical:

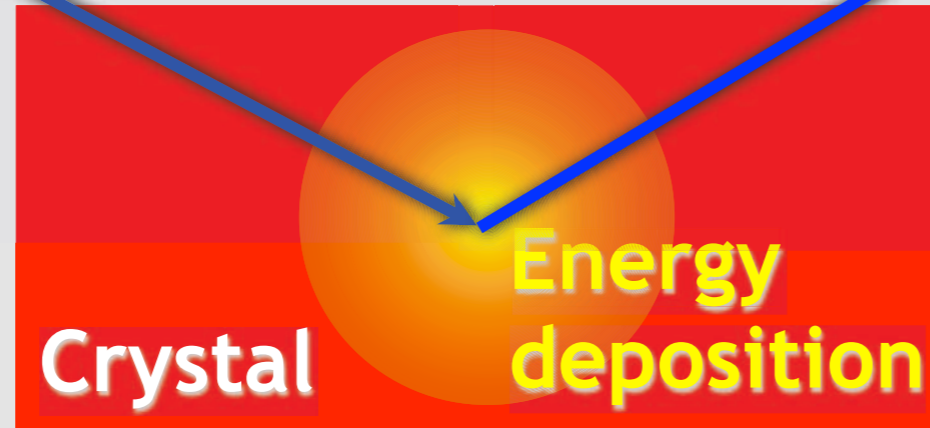


Planck & Herschel scheduled for launch spring 2009, ...

Search for Neutralino Dark Matter

Direct Method (Laboratory Experiments)

Galactic dark matter particle (e.g. neutralino)

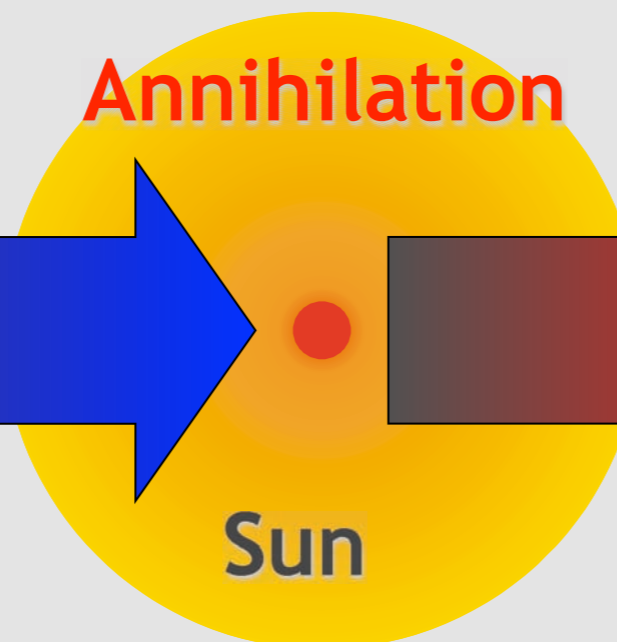


Recoil energy (few keV) is measured by

- Ionisation
- Scintillation
- Cryogenic

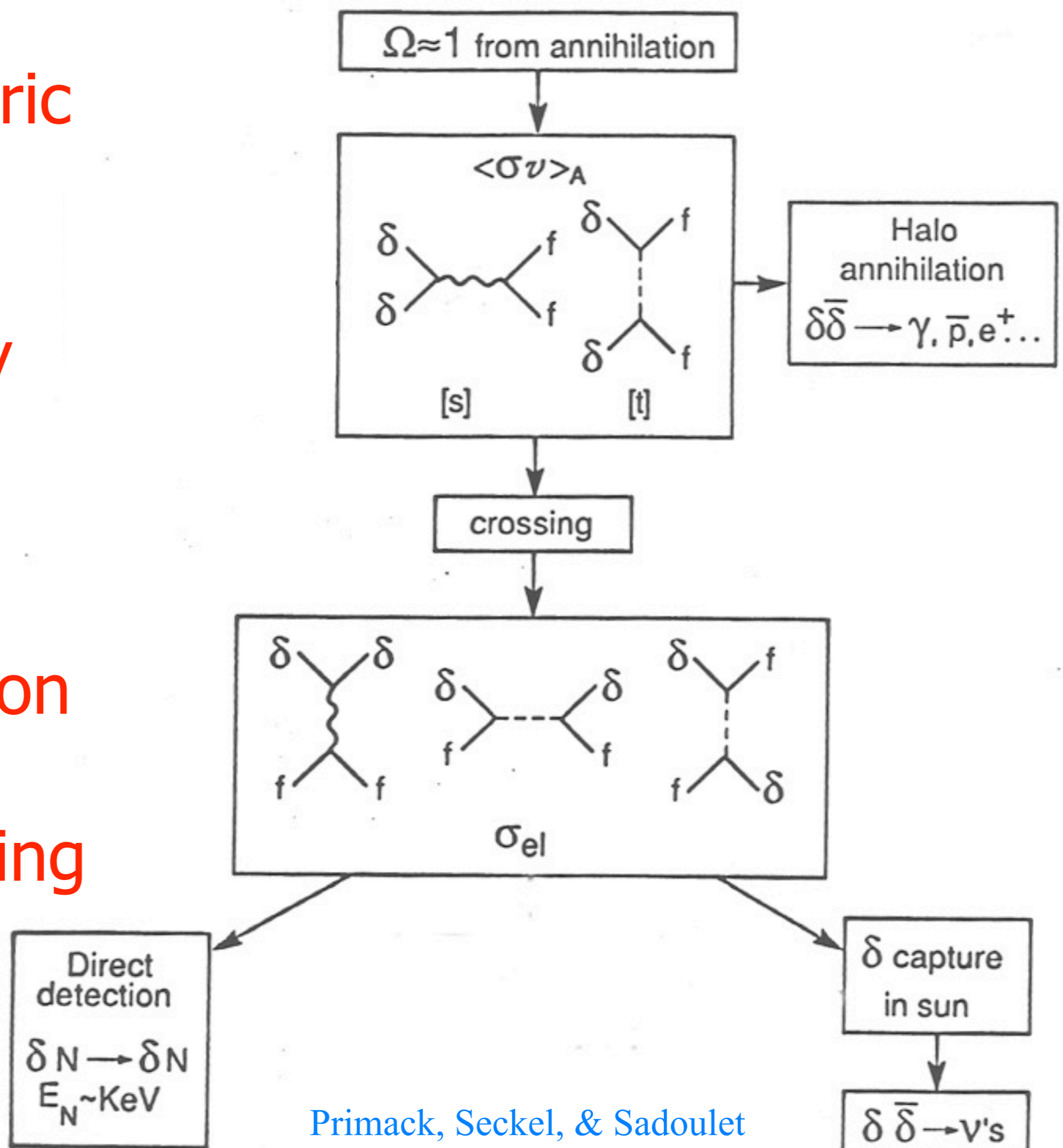
Indirect Method (Neutrino Telescopes)

Galactic dark matter particles are accreted



High-energy neutrinos (GeV-TeV) can be measured

Supersymmetric
WIMP (δ)
annihilation
is related by
crossing
to
WIMP
Direct Detection
by
Elastic Scattering



Primack, Seckel, & Sadoulet
Ann Rev Nucl Part Sci 1988

Future WIMP Sensitivities

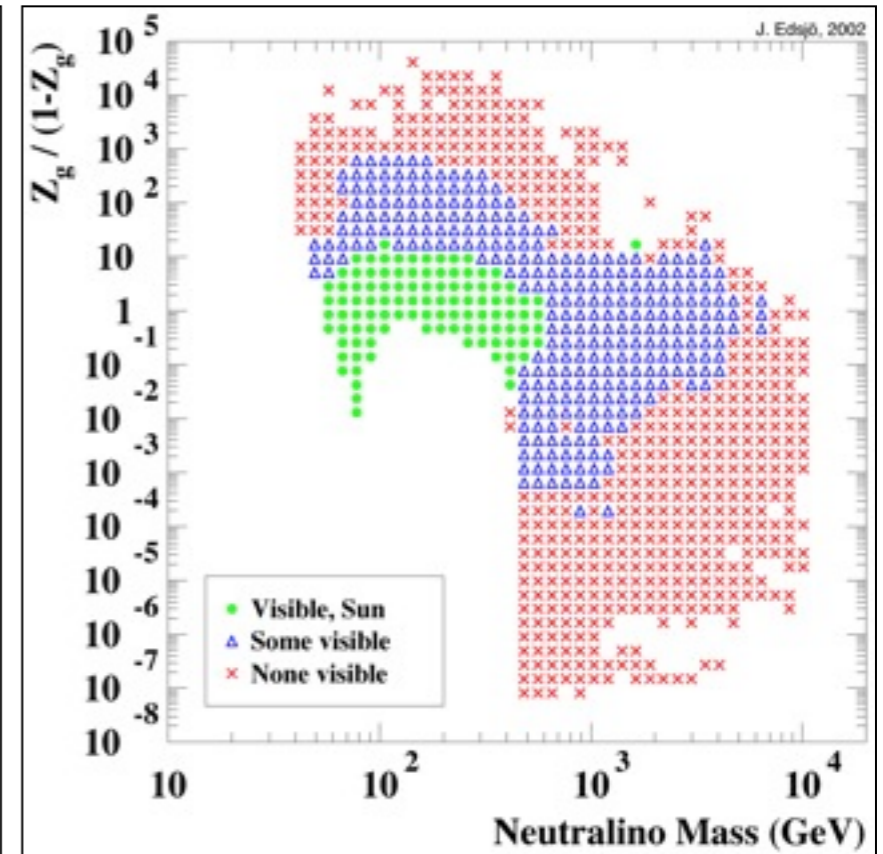
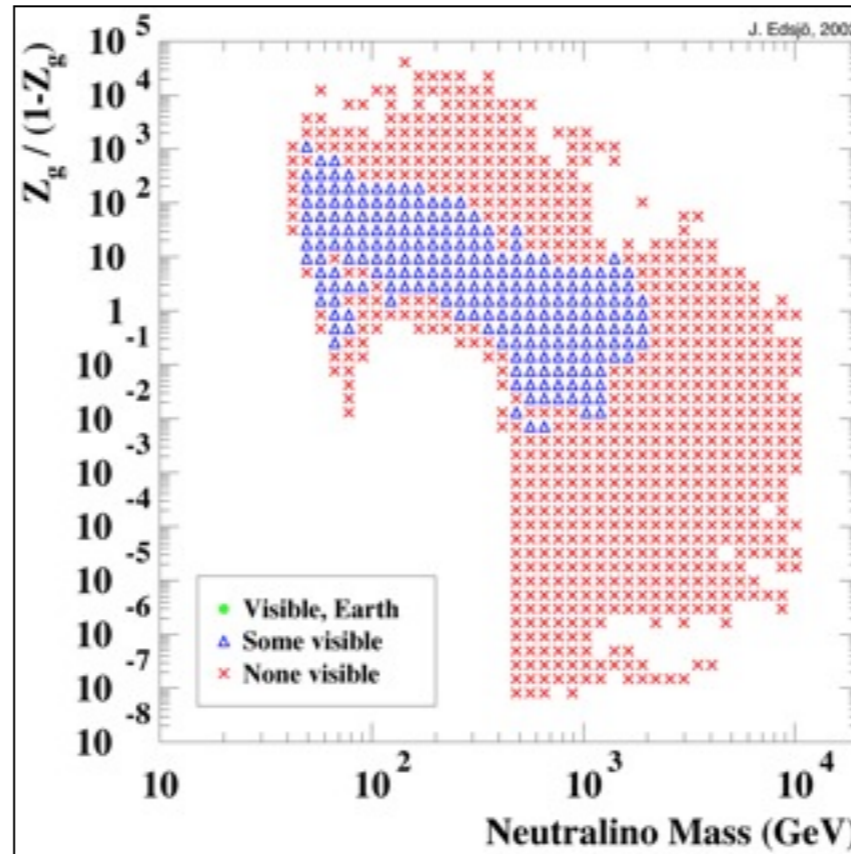
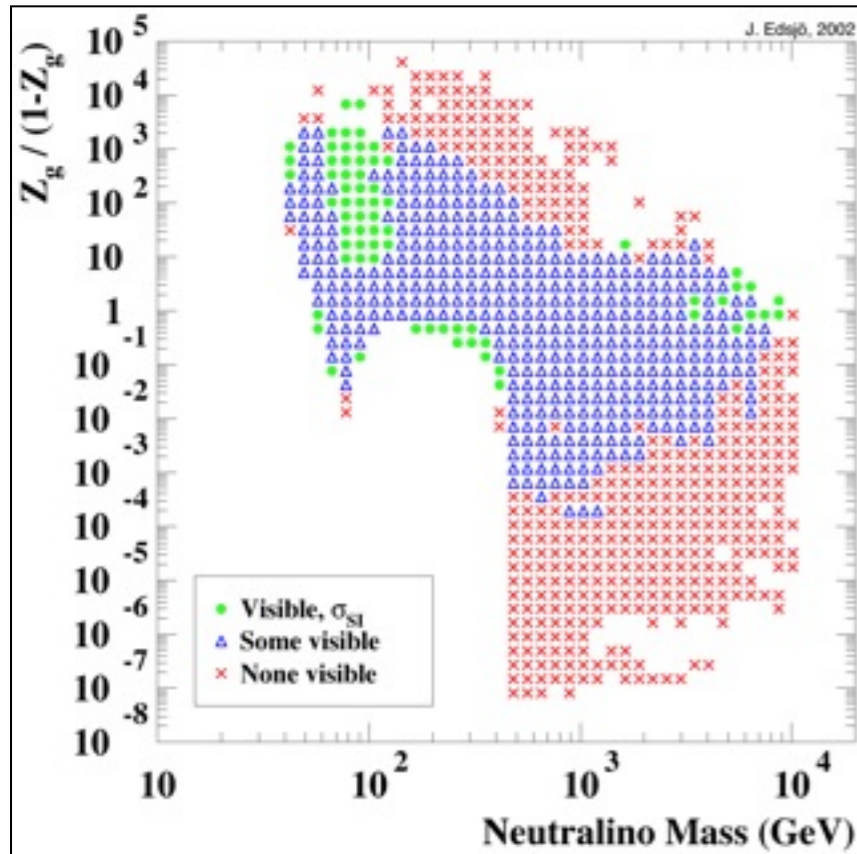
Direct Detection

Indirect, km³ Detector

Genius/CRESST

Earth

Sun



Annihilation



Sun



High-energy neutrinos (GeV-TeV) can be measured

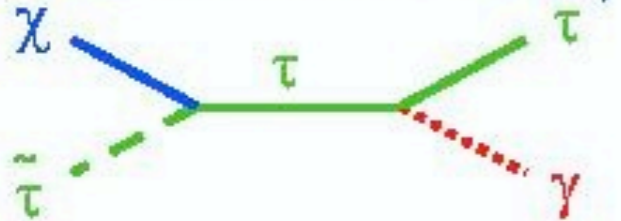
Relic Density

- Cosmology: $\Omega_{\text{DM}} = 0.23$

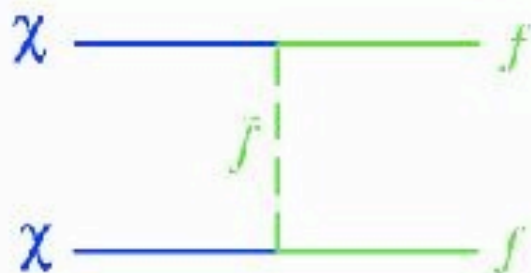
Freeze out when annihilation rate \approx expansion rate

$$\Rightarrow \Omega_x h^2 = \frac{3 \cdot 10^{-27} \text{ cm}^3 / \text{s}}{\langle \sigma_A v \rangle} \Rightarrow \sigma_A \approx \frac{\alpha^2}{M_{EW}^2} \quad \sim 100 \text{ GeV Weak Scale!}$$

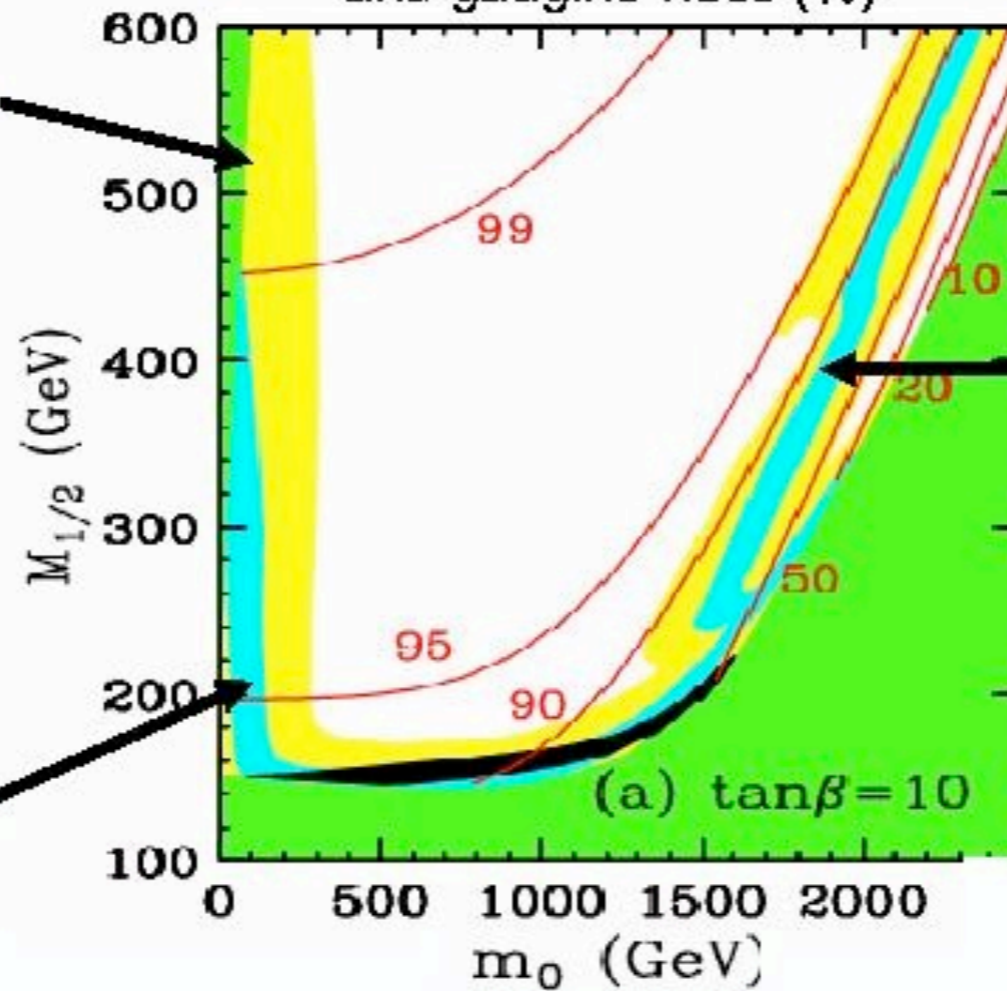
Co-annih. region
 $\chi \approx$ pure Bino
 Very sensitive to $m_{\tilde{\tau}}$



Bulk region
 $\chi \approx$ pure Bino
 Sensitive to $m_{\tilde{f}}$

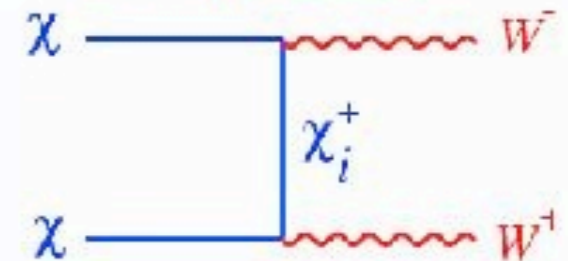


Relic density regions and gaugino-ness (%)



Feng, Matchev, Wilczek (2000)

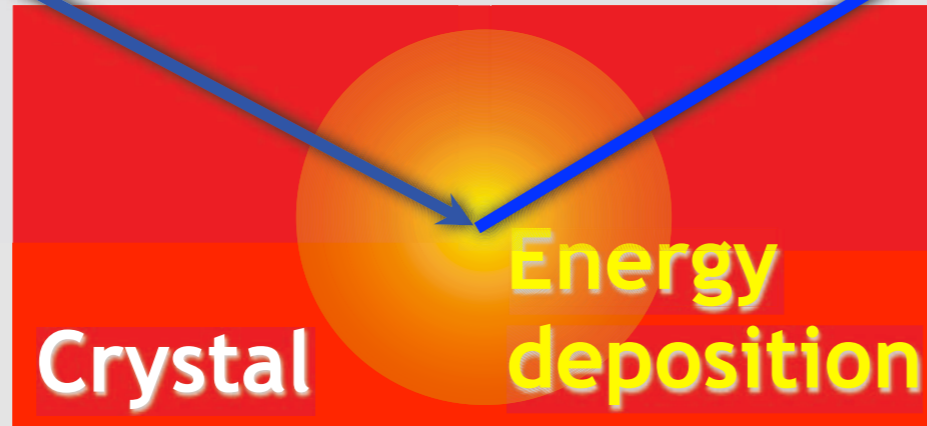
Focus point region
 $\chi \approx$ Bino-Higgsino
 Sensitive to χ composition



Search for Neutralino Dark Matter

Direct Method (Laboratory Experiments)

Galactic dark matter particle (e.g. neutralino)



Recoil energy (few keV) is measured by

- Ionisation
- Scintillation
- Cryogenic

PHYSICAL REVIEW D

VOLUME 31, NUMBER 12

15 JUNE 1985

Detectability of certain dark-matter candidates

Mark W. Goodman and Edward Witten

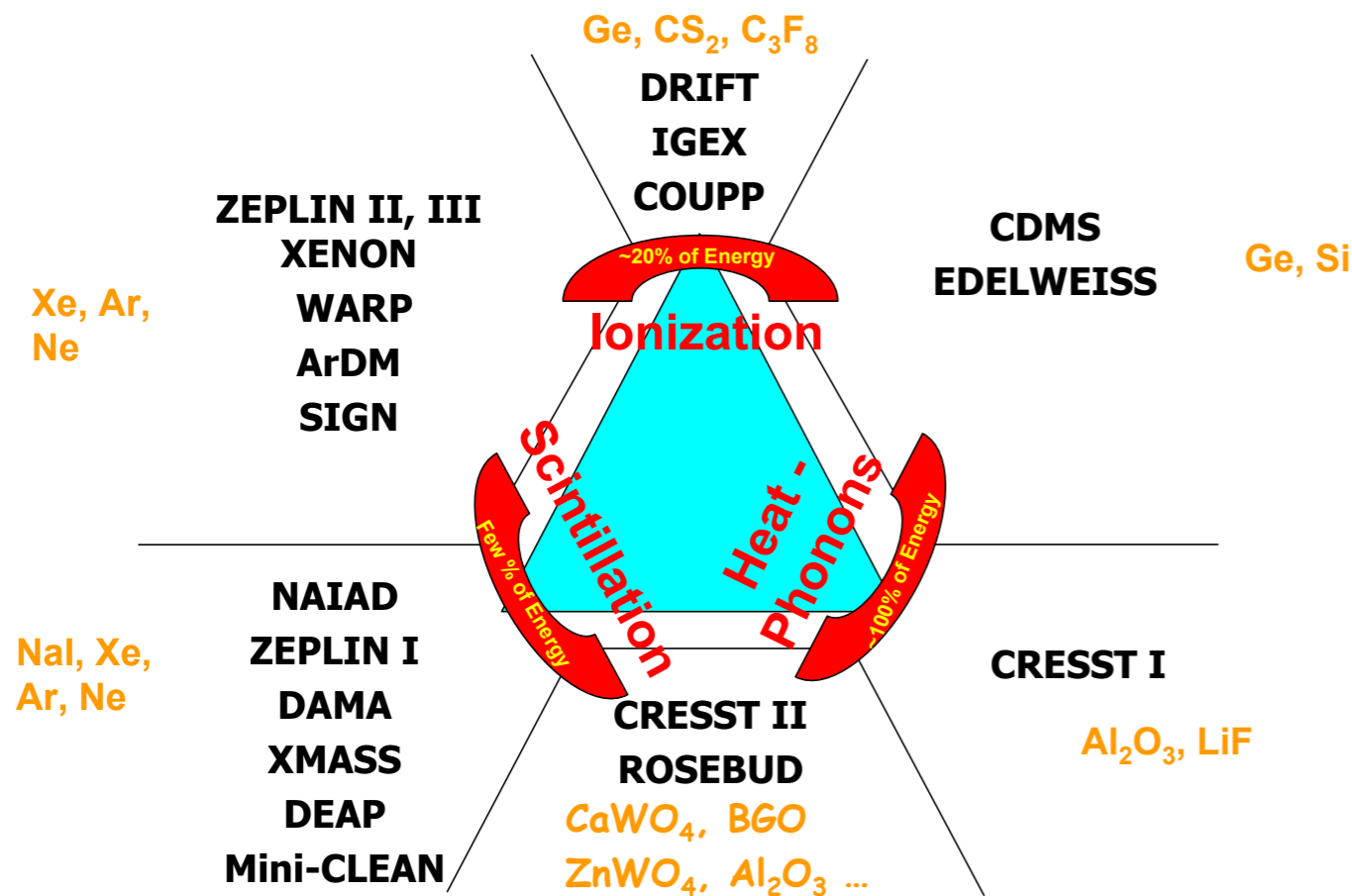
Joseph Henry Laboratories, Princeton University, Princeton, New Jersey 08544

(Received 7 January 1985)

We consider the possibility that the neutral-current neutrino detector recently proposed by Drukier and Stodolsky could be used to detect some possible candidates for the dark matter in galactic halos. This may be feasible if the galactic halos are made of particles with coherent weak interactions and masses $1-10^6$ GeV; particles with spin-dependent interactions of typical weak strength and masses $1-10^2$ GeV; or strongly interacting particles of masses $1-10^{13}$ GeV.

Experimental Approaches

Direct Detection Techniques

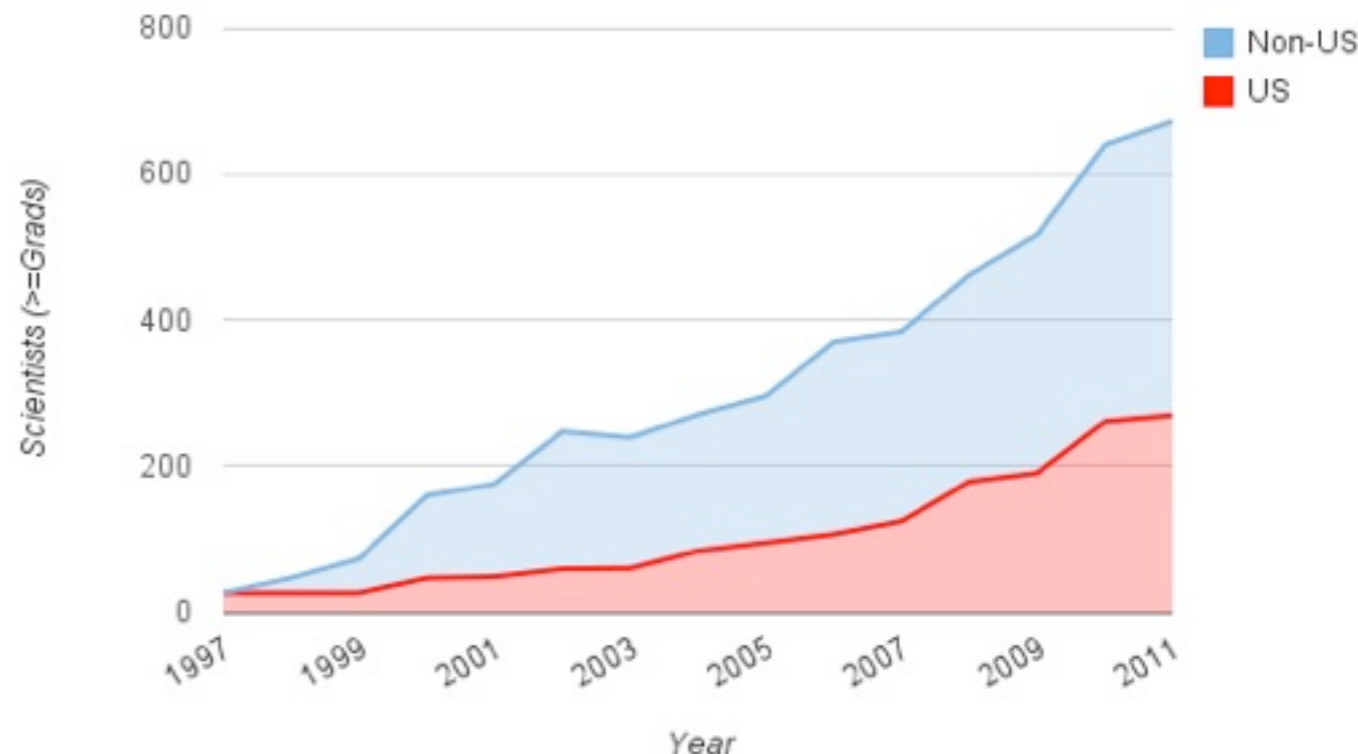


Need as large as possible:
amount of information and
signal to noise ratio

An expanding community

U.S. ≈ 270 physicists
≈ 40% of world

Dark Matter Direct Detection (Personnel >= Grads) v3.2



At least **two** pieces of information in order
to recognize nuclear recoil
extract rare events from background
(self consistency)
+ fiducial cuts (self shielding, bad
regions)

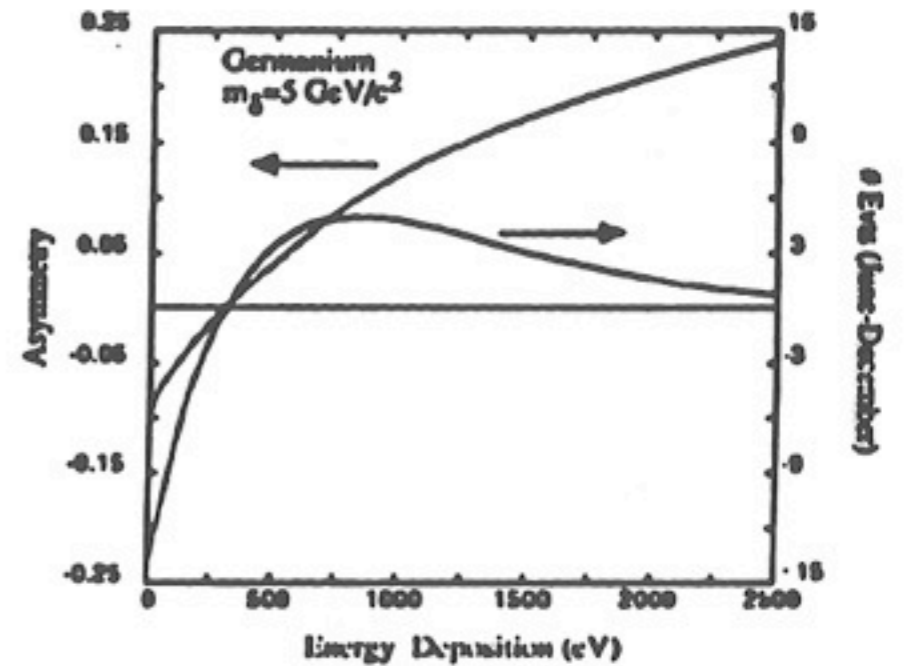
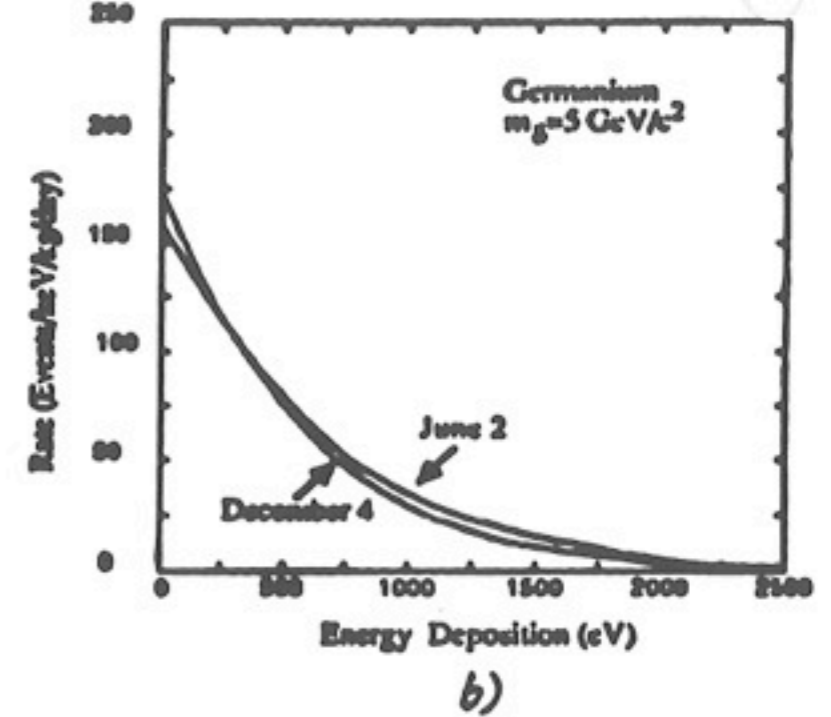
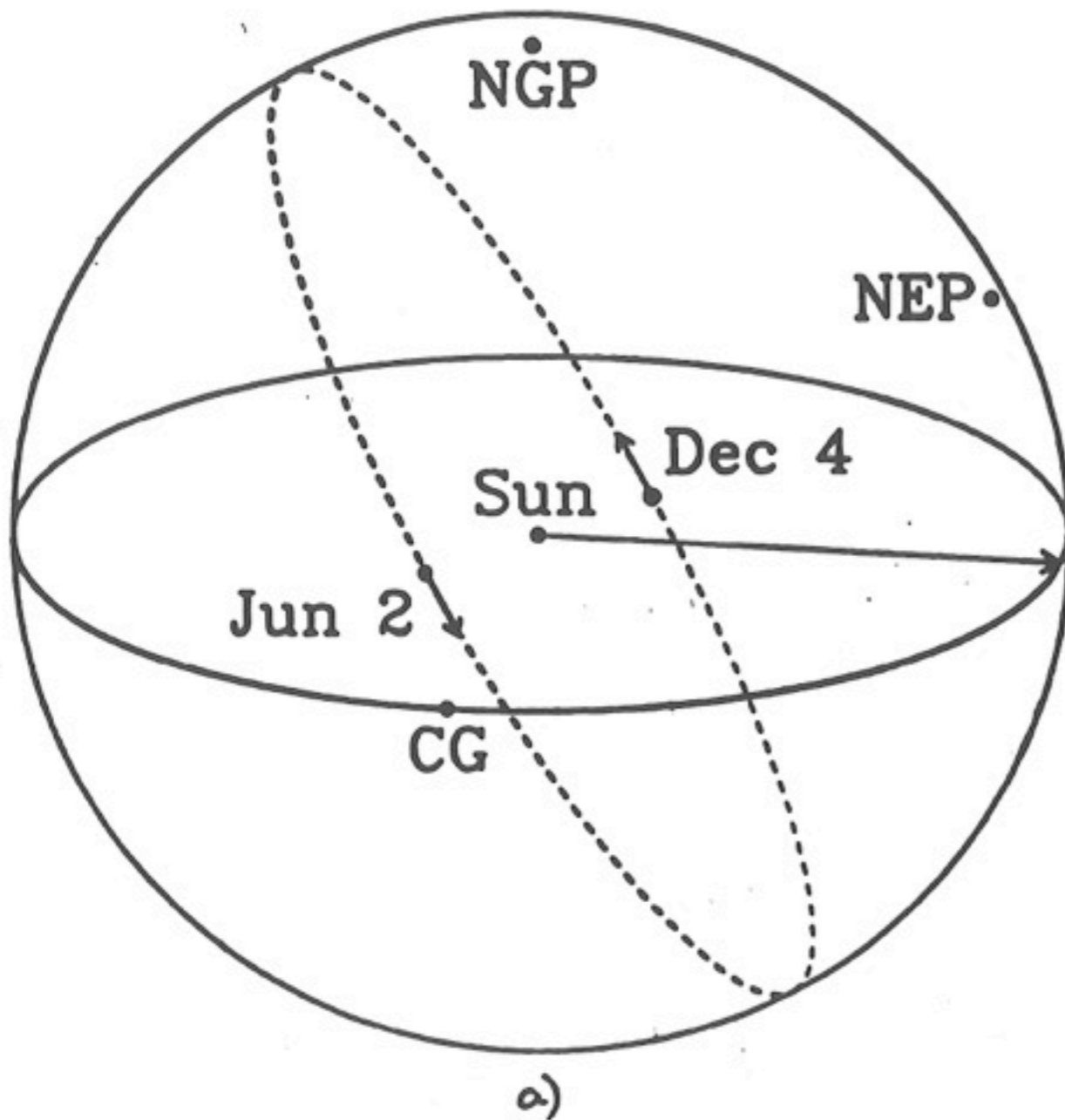


Figure 3. Annual effect in WIMP detection by elastic scattering. (a) Why expected: The solid line (darker in the front) shows the plane of the galactic disk and the Sun's orbit; the dashed circle is the orbit of the Earth (ecliptic plane). NGP and NEP are the north galactic and ecliptic poles. CG shows the direction toward the galactic center, and the long and short arrows show the Sun's and the Earth's velocities. The sum of the Sun's and Earth's velocities reaches its maximum on June 2 (248 km s^{-1}) and minimum on December 4 (219 km s^{-1}). (These velocities with respect to the galactic center are obtained neglecting the small eccentricity of the Earth's orbit, and assuming that the Sun's peculiar velocity is 16.5 km s^{-1} in the galactic direction $l = 53^\circ$, $b = 25^\circ$ with respect to the local standard of rest (cf. 118). Event rates in WIMP detectors actually depend on the Earth's velocity with respect to the DM halo, whose rotational velocity is uncertain.) (b) Rate for June 2 and December 4 vs. deposited energy. (c) June - December difference (right axis) and asymmetry (left axis) vs. deposited energy. Note that although the asymmetry increases with the energy deposition, the rate and therefore also the June - December rate difference both decrease at high energy deposition.

Primack, Seckel, & Sadoulet, Ann Rev Nucl Part Sci 1988

DAMA

Clear summer-winter modulation

13 years 1.17 ton year

2 different experiments
(same electronics)

right phase for WIMP

If WIMP $\approx 4\%$ asymmetry,

Very large signal

Surprisingly low background

Wide suspicion that this is instrumental

but no convincing explanation so far! Subtle problem!

David Nygren's suggestion

After-pulsing after μ 's

Keep our eyes open!

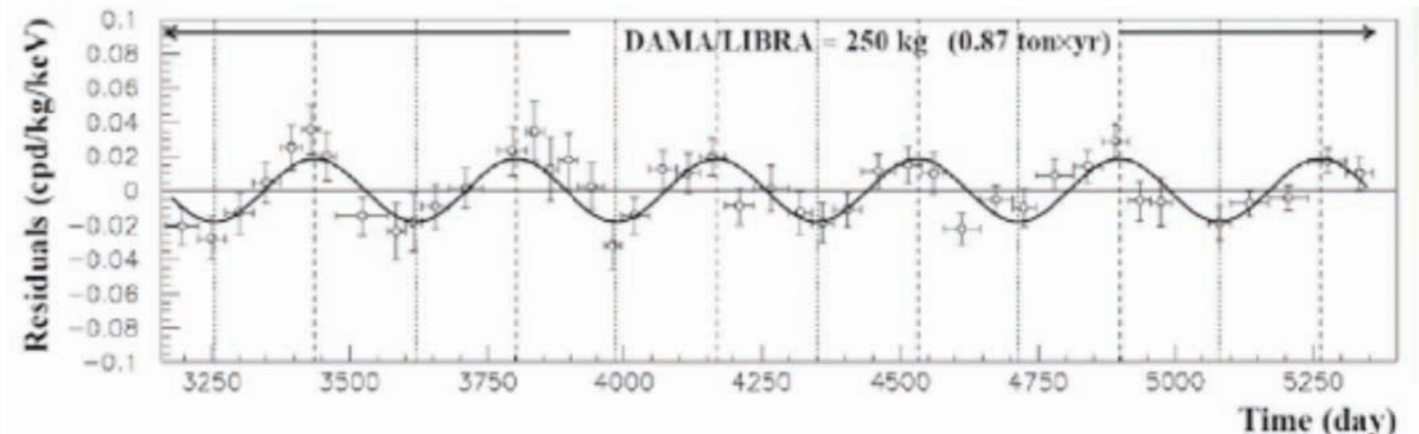
Repeat experiment

South Pole

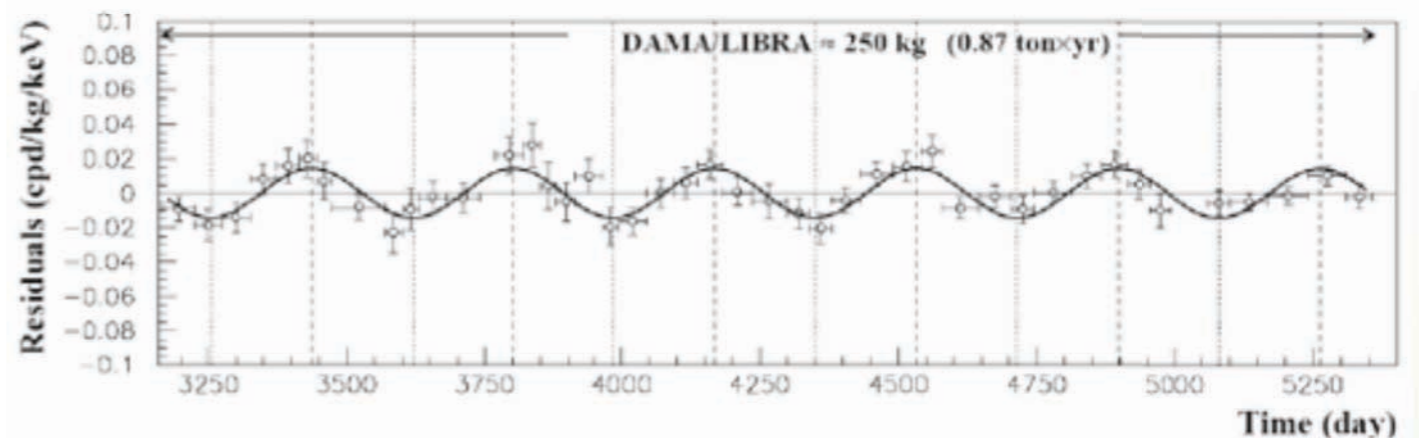
Princeton

KIMS (100kg CsI, 3 keVee)

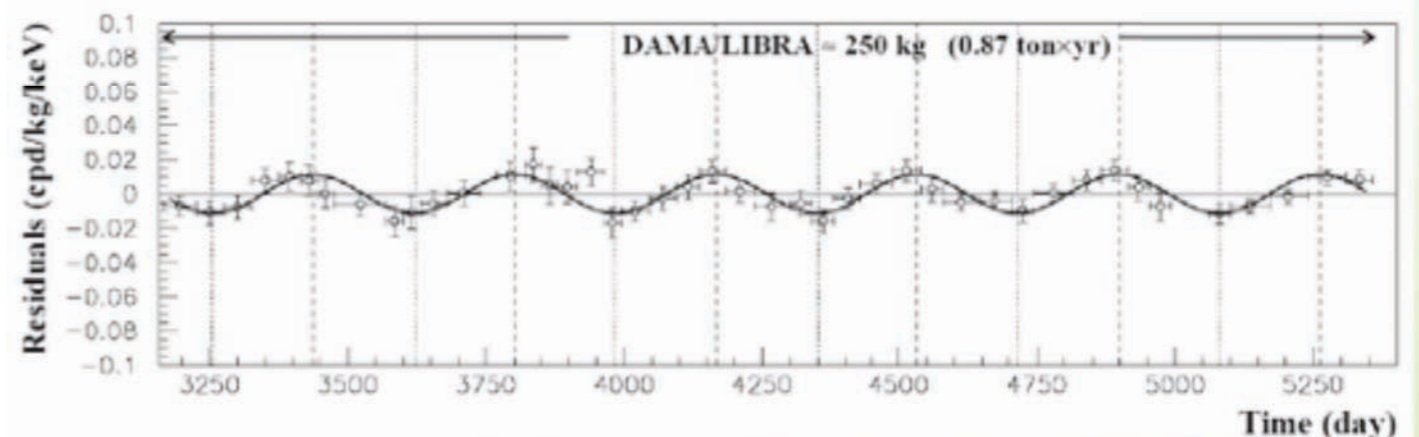
2-4 keV Latest Princeton Nov 2011



2-5 keV



2-6 keV



CDMS - Cryogenic DM Search

Berkeley-Stanford-led experiment
has been at forefront

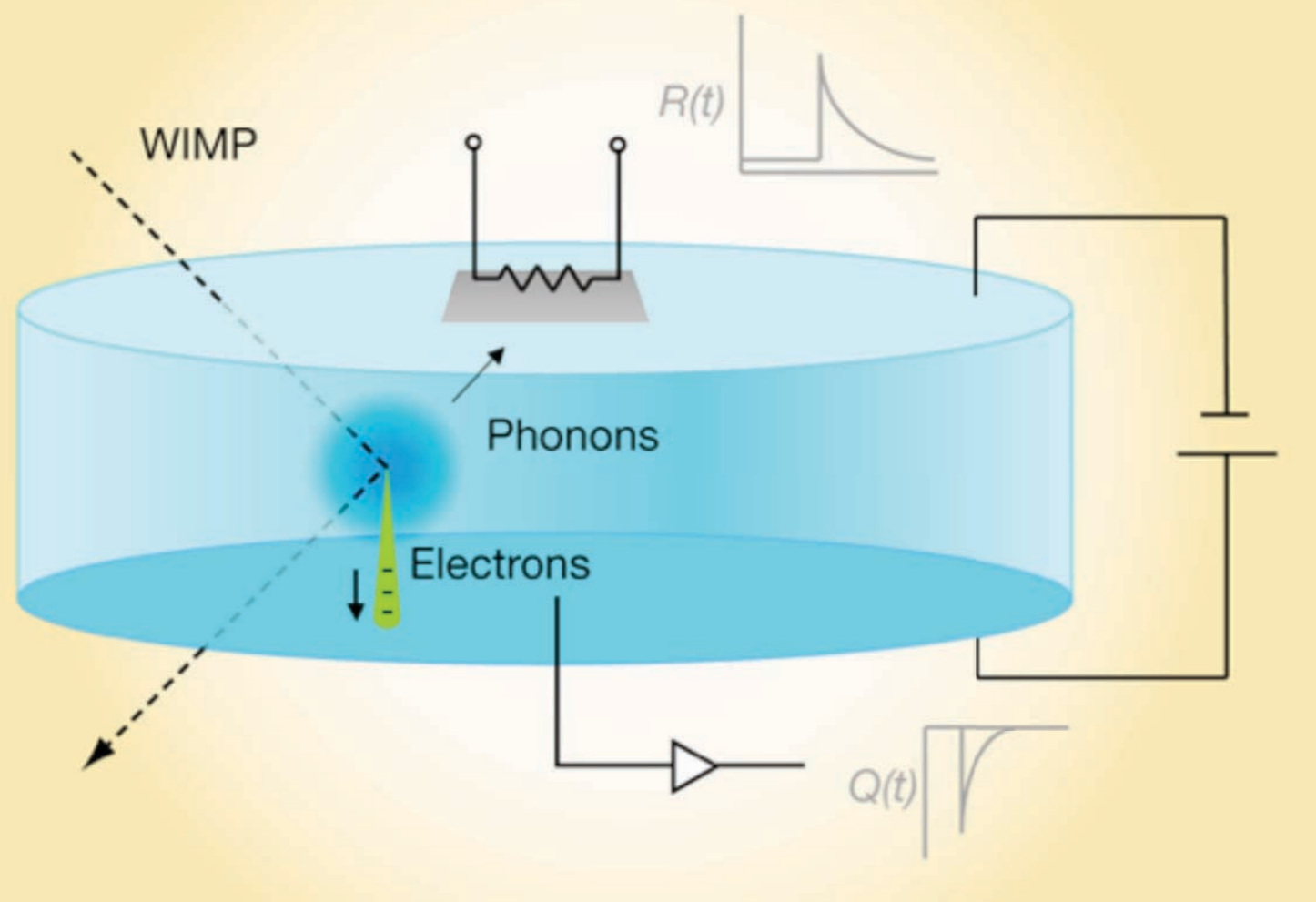


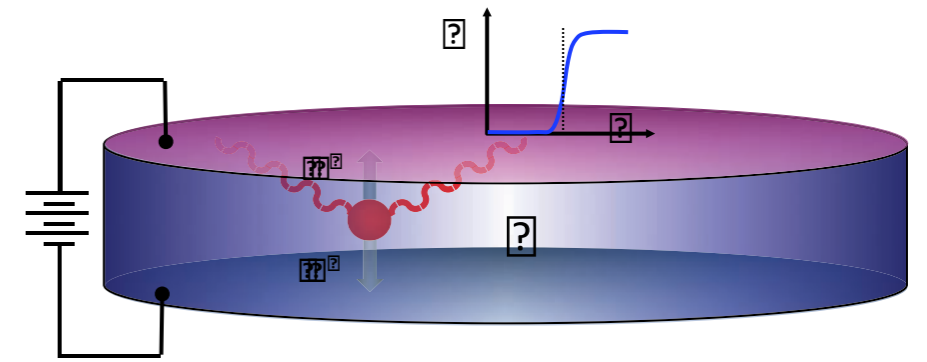
Figure from: Perspective by Karl van Bibber
<http://physics.aps.org/viewpoint-for/10.1103/PhysRevLett.102.011301> on
Z. Ahmed et al. CDMS Collaboration, "Search for Weakly Interacting Massive Particles with the First Five-Tower Data from the Cryogenic Dark Matter Search at the Soudan Underground Laboratory," *Phys. Rev. Lett.* 102, 011301 (2009) – Published January 05, 2009

Schematic of an individual detector within CDMS. A WIMP scattering from a germanium nucleus produces a low-energy nuclear recoil, resulting in both ionization and athermal phonons. Charge carriers drift out to one face of the detector under the influence of a small electric field, and are detected with a sensitive amplifier [signal shown as $Q(t)$]. Phonons reaching the other face break Cooper pairs in a thin superconducting aluminum layer; the resulting quasiparticles heat a transition-edge sensor (TES) bonded to the aluminum layer, causing a measurable momentary change in its resistance $R(t)$. In reality, the readout elements on both sides are highly segmented, and the relative timing of the ionization and phonon signals recorded, to provide good event localization.

CDMS II December 2009

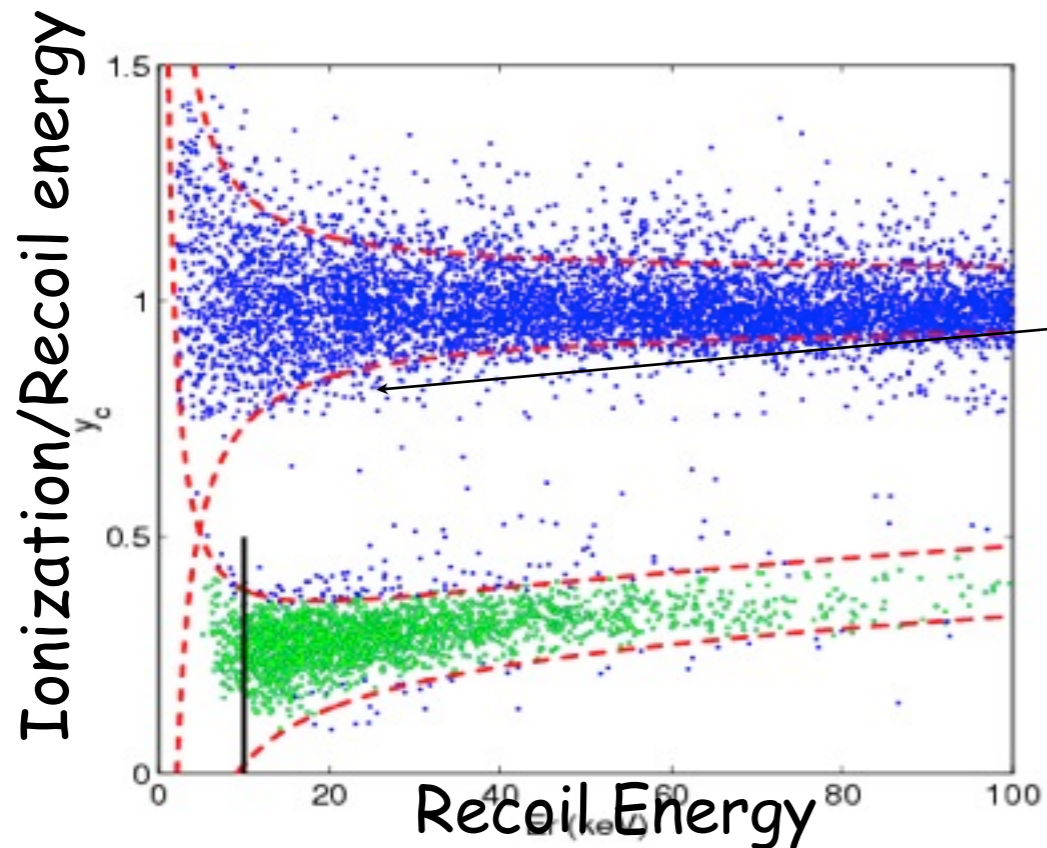
Ionization + Athermal Phonons

7.5 cm \varnothing 1 cm thick \approx 250g
4 phonon sensors on 1 face
2 ionization channel

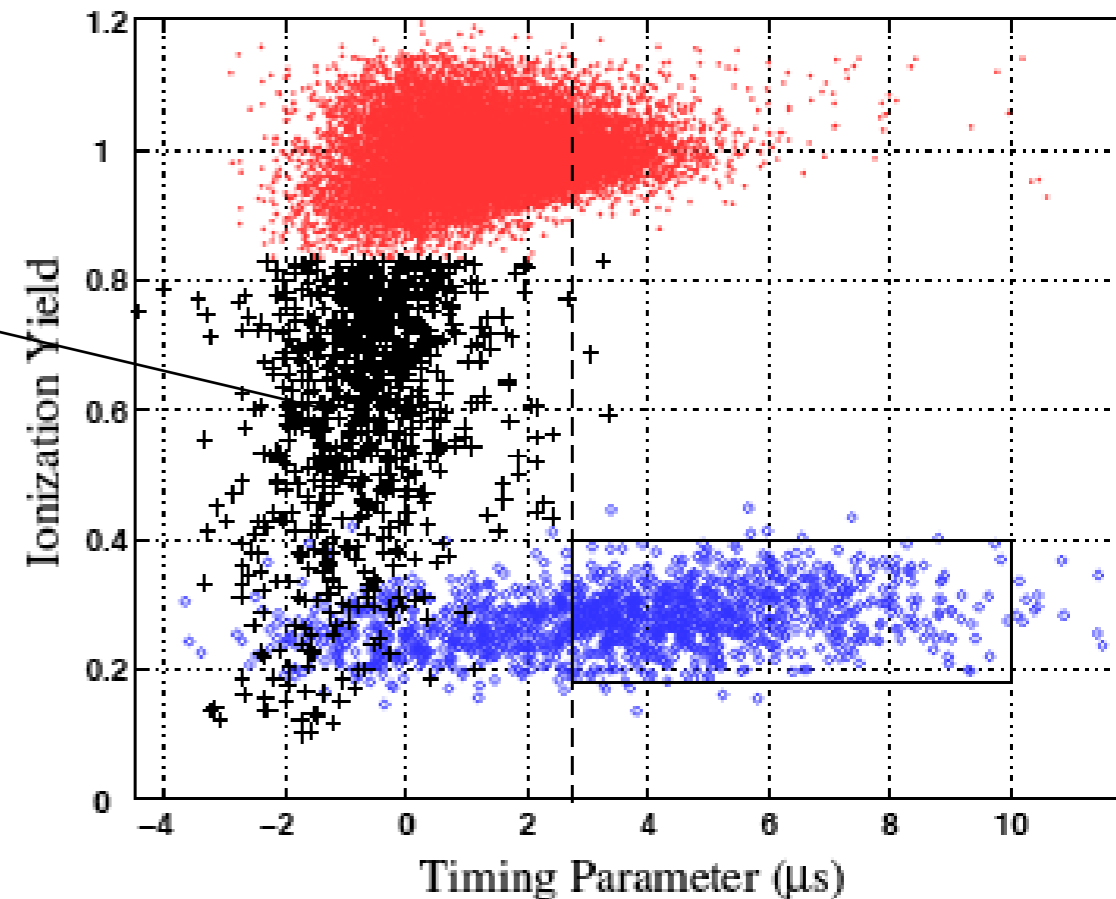


Ionization yield

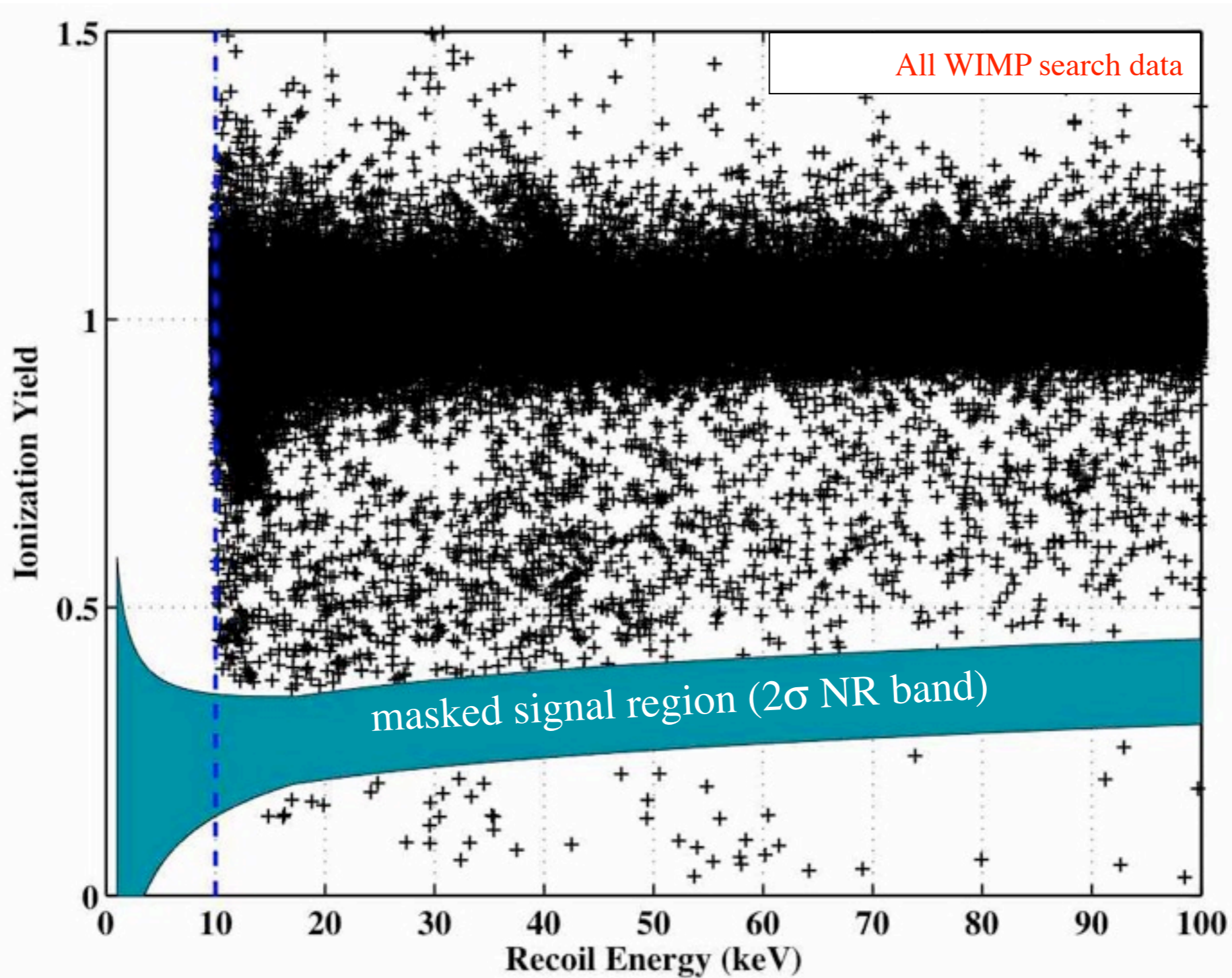
Timing -> surface discrimination



Surface
Electrons

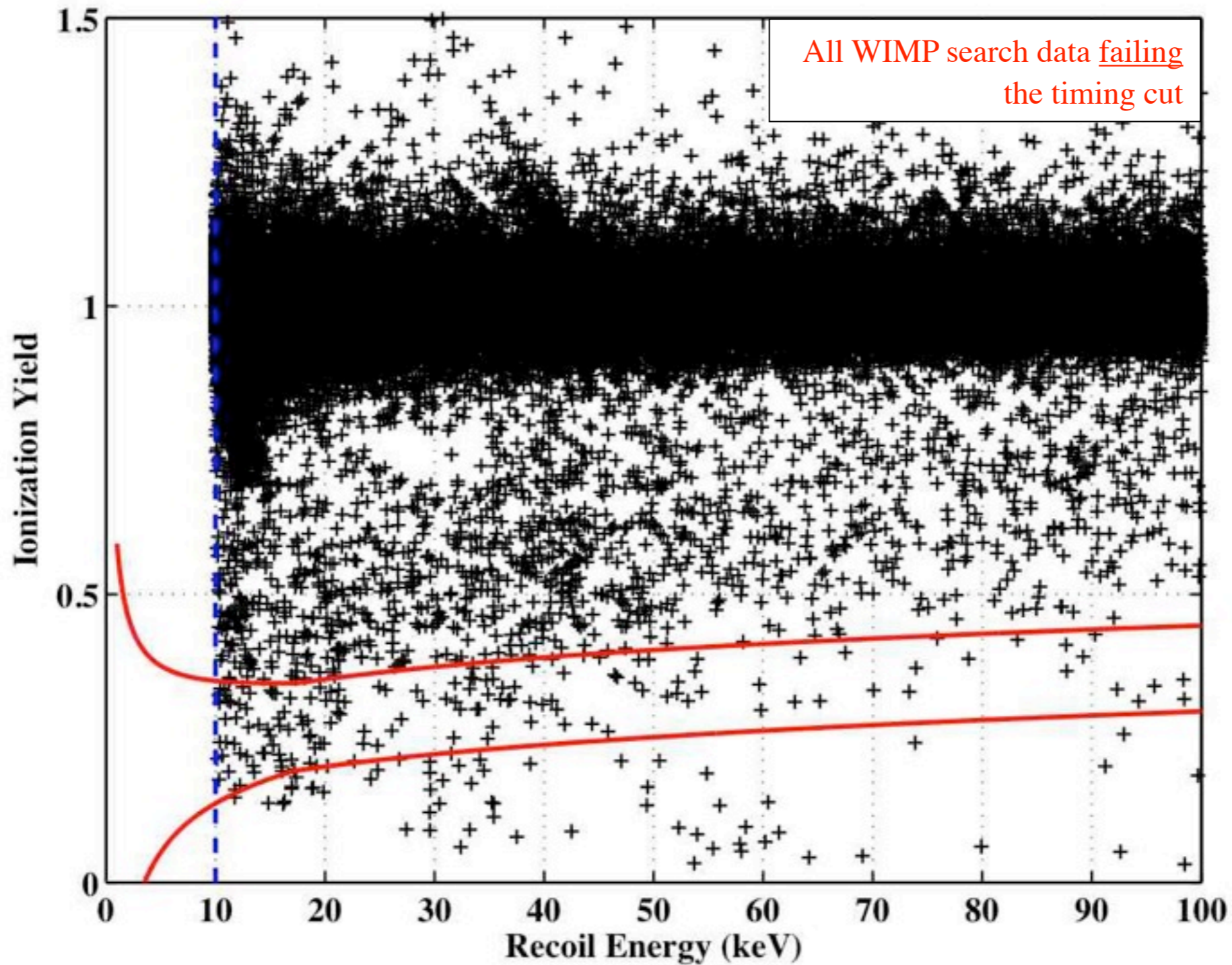


CDMS Blind Analysis



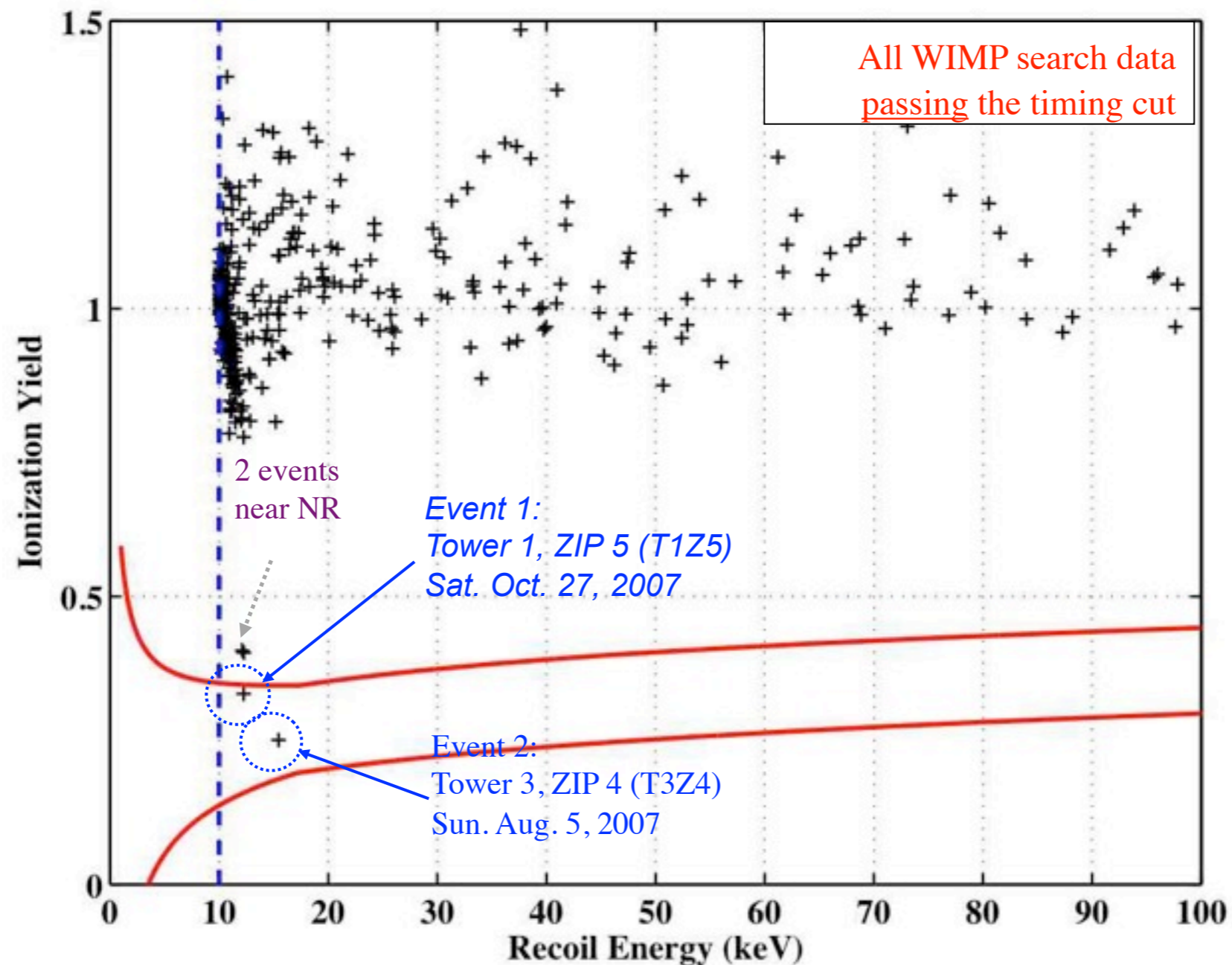
We unblinded the signal region November 5, 2009

Unblind Events Failing Timing Cut



150 events in the NR band fail the timing cut, consistency checks deemed ok

Unblind Events Passing Timing Cut

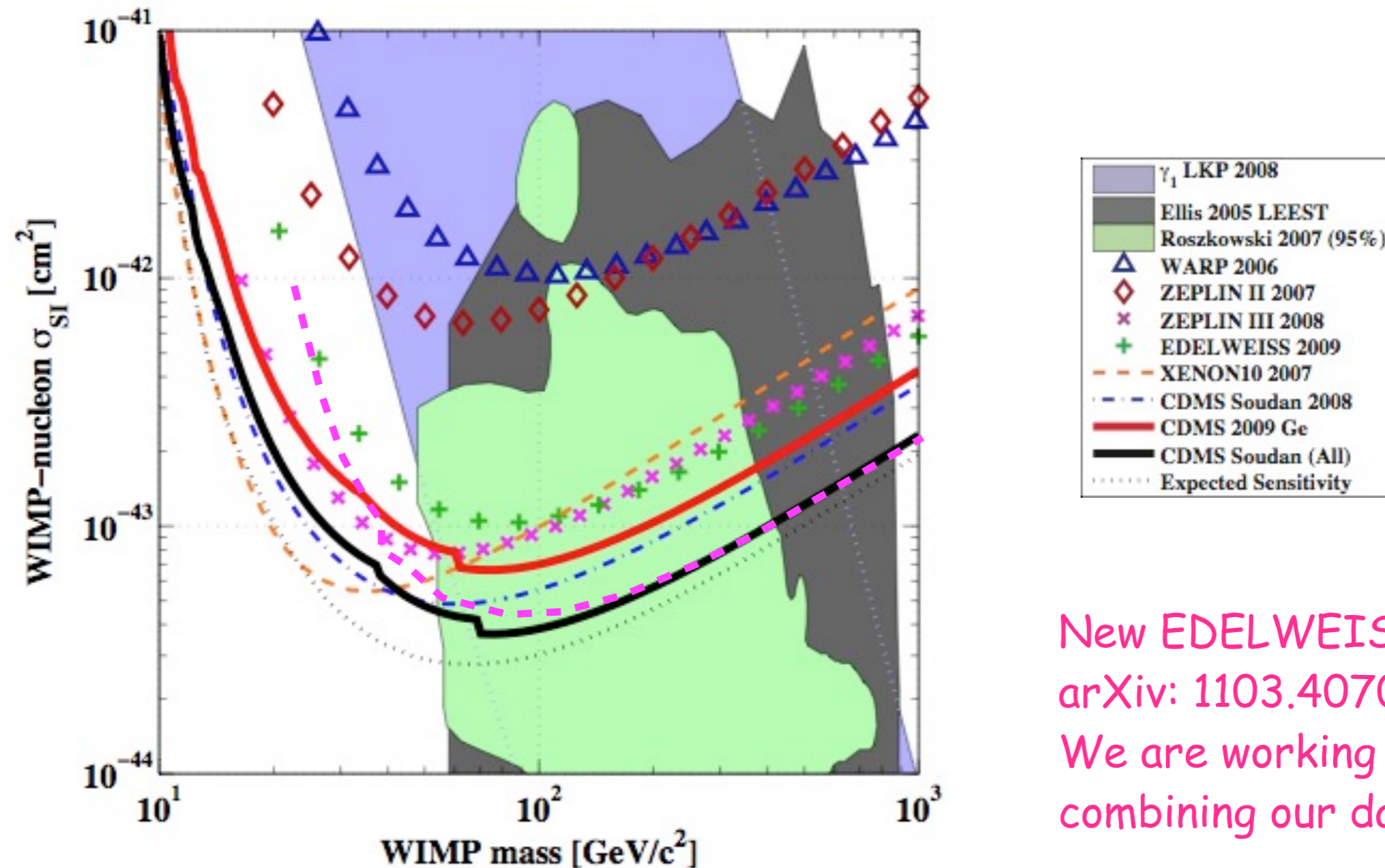


2 events in the NR band pass the timing cut!

Background 0.8 ± 0.1 (stat) ± 0.2 (syst) surface events
+ 0.1 ± 0.05 (syst) neutron \Rightarrow 23% Probability

90% C.L. Spin-Independent Limit

Science 12 February 2010

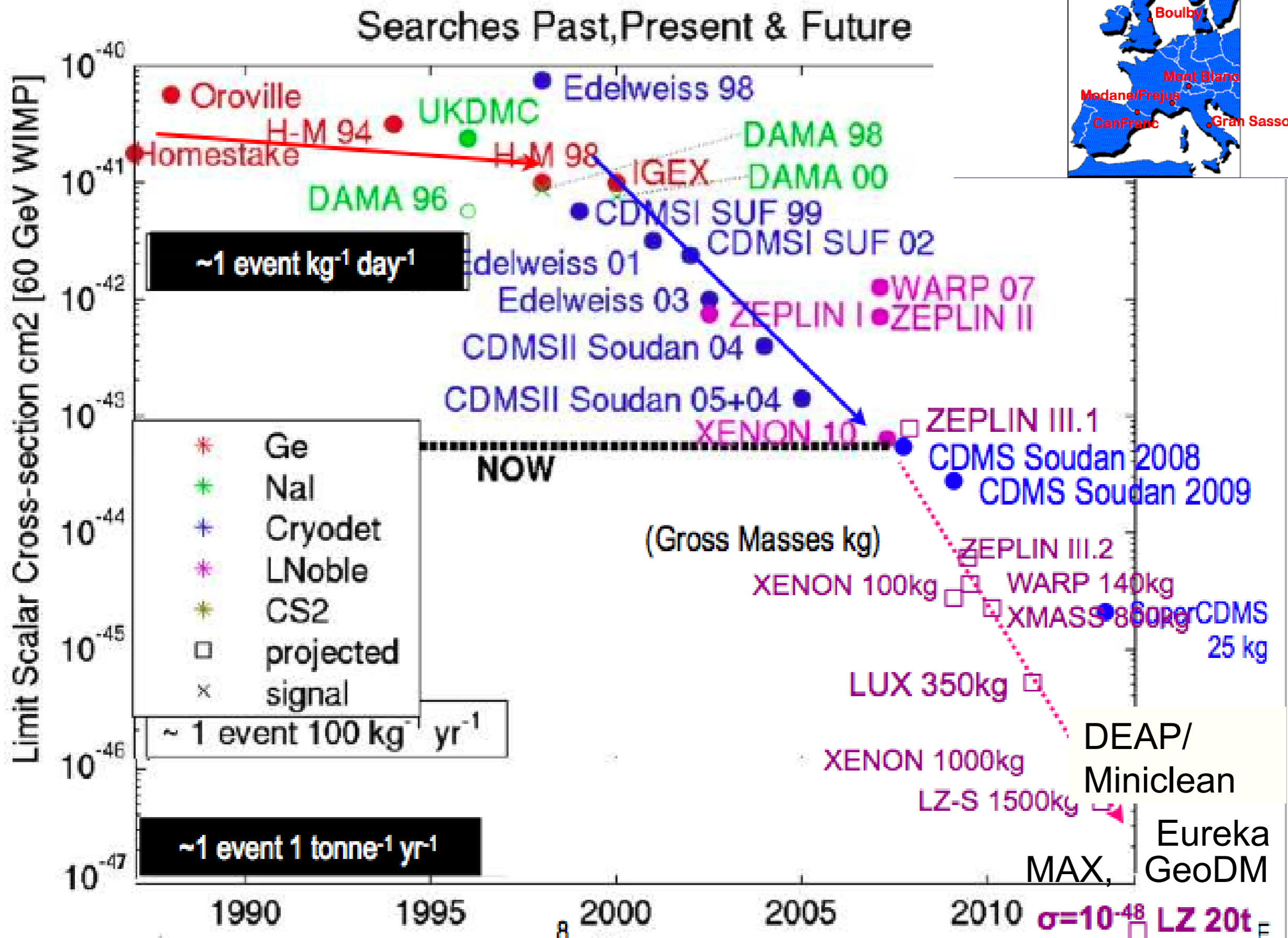
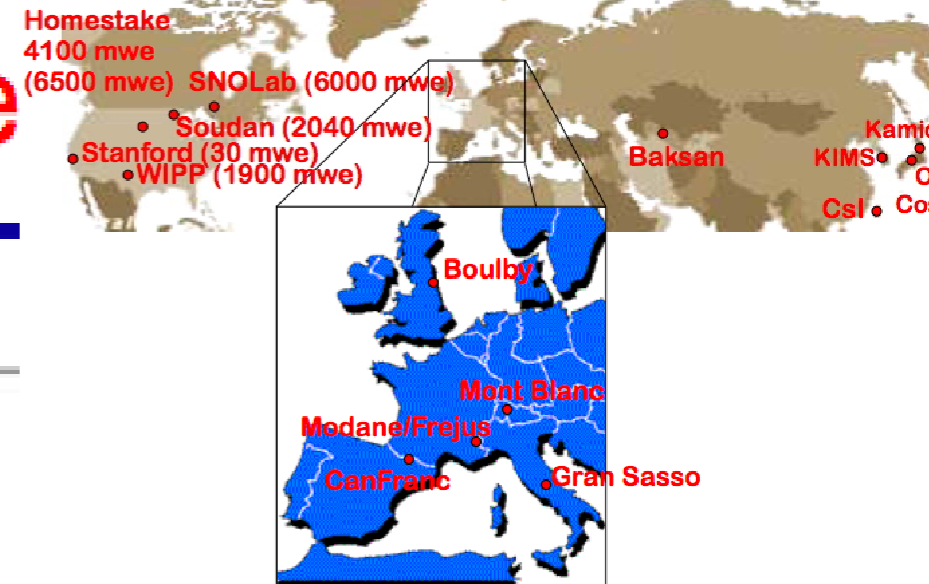


New EDELWEISS limit
arXiv: 1103.4070
We are working on a paper
combining our data!

Upper limit at the 90% C.L. on the WIMP-nucleon cross section :

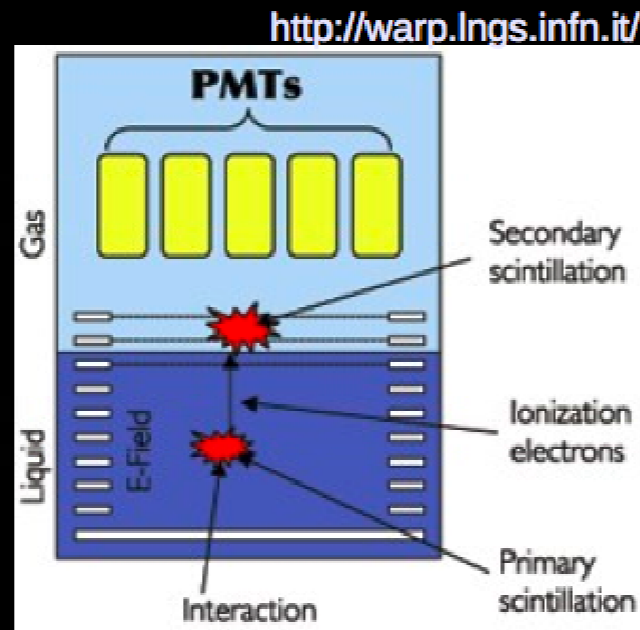
$$3.8 \times 10^{-44} \text{ cm}^2 \text{ for a WIMP of mass } 70 \text{ GeV}/c^2$$

DM Direct Search Progress Over Time



Liquid noble detectors

- WIMP-nucleus elastic scattering produces ionization electrons and photons.
- Photons (primary scintillation) are detected by PMTs
- Electrons are drifted (by E field) to gas region, where they are accelerated and collide with gas atoms, producing secondary scintillation
- Shape of primary and ratio of primary to secondary signal depend on ionizing particle (WIMP looks different from ex. beta decay electron)

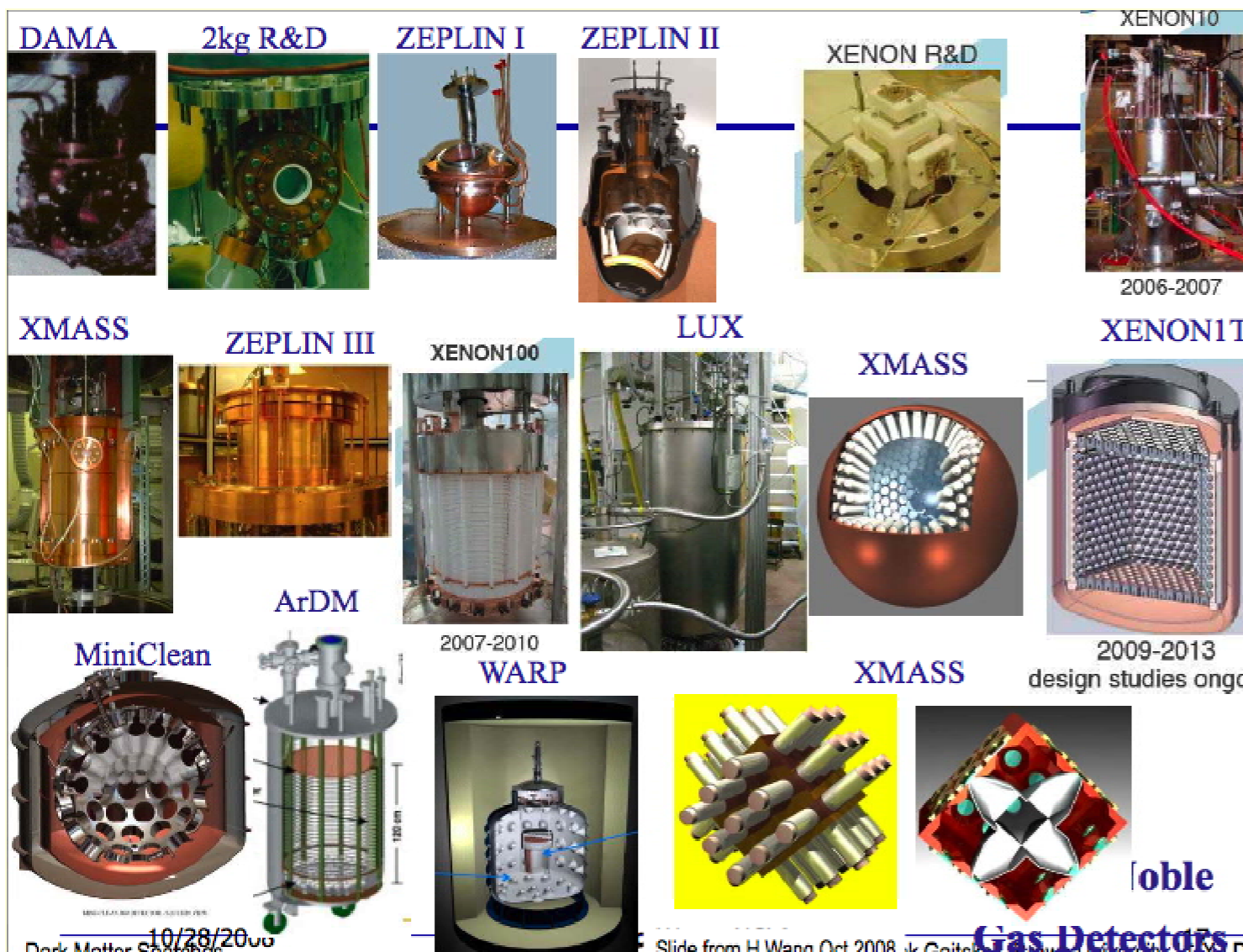


Noble Liquid Comparison (DM Detectors)

	Scintillation Light	Intrinsic Backgrounds	WIMP (100 GeV) Sensitivity vs Ge >10 keVr
Ne (A=20) \$60/kg 100% even-even nucleus	85 nm Requires wavelength Shifter	Low BP (20K) - all impurities frozen out No radioactive isotopes	Scalar Coupling: Eth>50 keVr, 0.02x Axial Coupling: 0 (no odd isotope)
Ar (A=40) \$2/kg (isotope separation >\$1000/kg) ~100% even-even	125 nm Requires wavelength shifter	Nat Ar contains ~39Ar 1 Bq/kg == ~150 evts/keVee/kg/day at low energies. Requires isotope separation, low 39Ar source, or very good discrimination (~10 ⁶ to match CDMS II)	Scalar Coupling: Eth>50 keVr, 0.10x Axial Coupling: 0 (no odd isotope)
Xe (A=131) \$1000/kg 50% odd isotope	175 nm UV quartz PMT window	136Xe double beta decay is only long lived isotope - below pp solar neutrino signal. Relevant for DM search below ~10 ⁻²⁷ cm ² . 85Kr can be removed by charcoal or distillation separation.	Scalar Coupling: Eth>5 keVr, 1.30x Axial Coupling: ~5x (model dep) Xe is 50% odd n isotope 129Xe, 131Xe

Future of Direct Detection

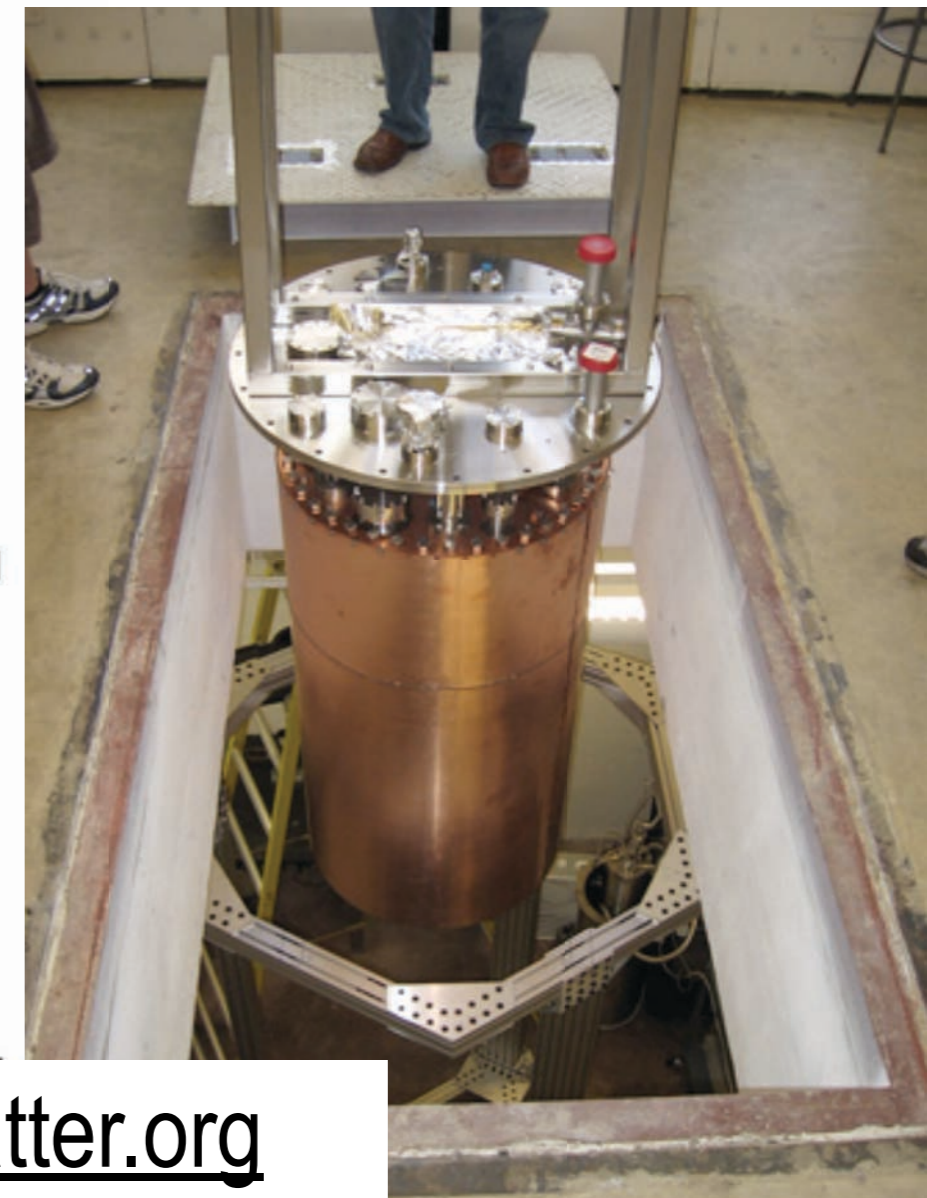
- Experiments under construction, to release results in 2009-2010
 - Target masses 10-300 kg
 - Expect 10-100x better reach than existing limits.
- Next Round, for results in 2011-2013
 - Target masses 1-3 tonne, 10³ x better reach
 - Project cost \$5-15M
- “Ultimate” Detectors, for results ~2014+
 - Target masses 3-50 tonne, 10⁴ x better reach
 - Project cost \$20-50M
- Labs with 1-20 tonne dm experiments on roadmap
 - Gran Sasso, Italy
 - Frejus, France
 - Canfranc, Spain
 - Kamioka, Japan
 - SNOLab, Canada
 - Sanford Lab/DUSEL (Homestake), US



LUX Dark Matter Experiment

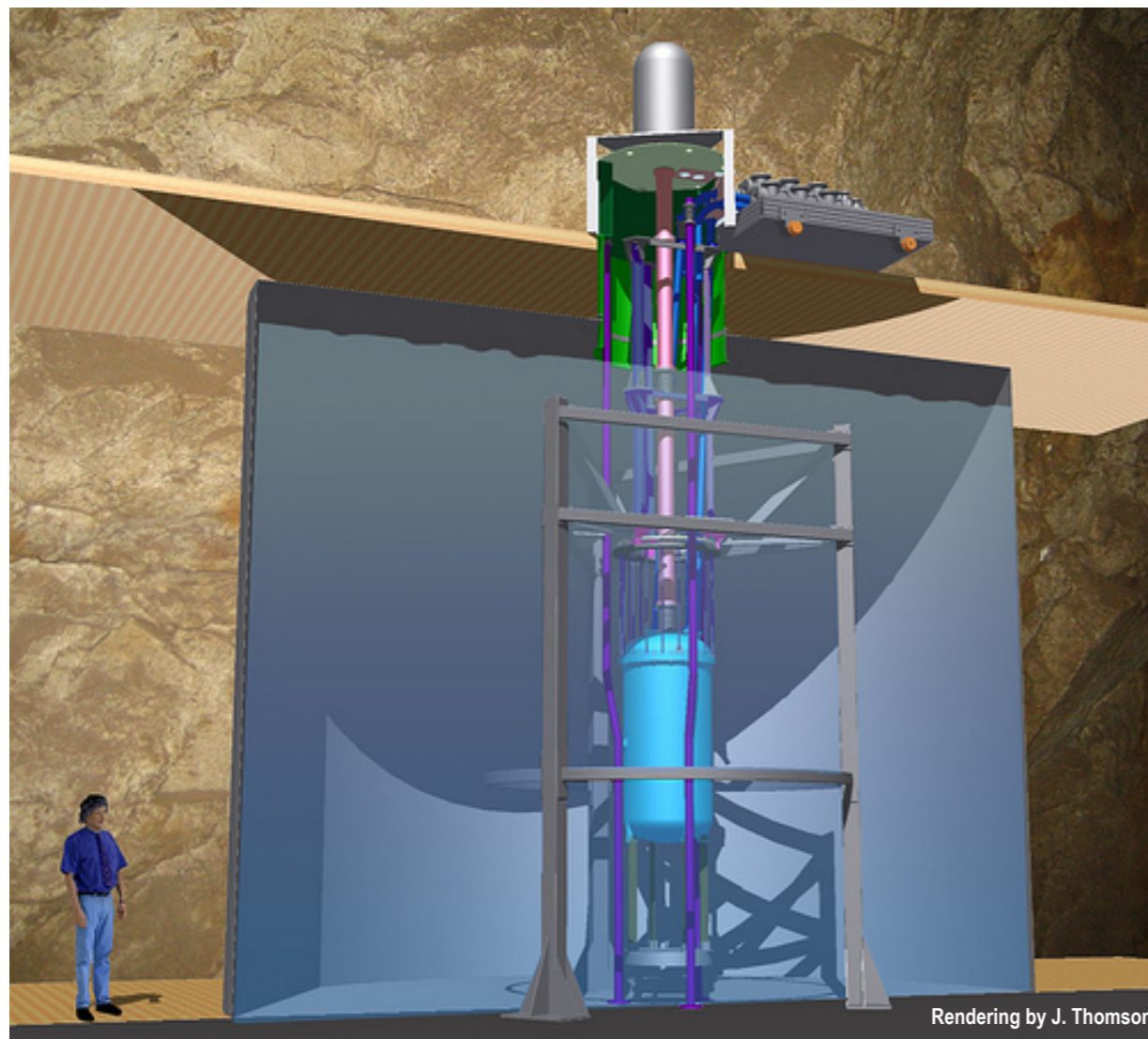
- Brown [Gaitskell], Case [Shutt], LBNL [Lesko], LLNL [Bernstein], Maryland [Hall], Rochester [Wolfs], Texas A&M [White], UC Davis [Svoboda/Tripathi], U South Dakota [Mei], Yale [McKinsey]
 - ◆ XENON10, ZEPLIN II (US), CDMS; ν Detectors (Kamland/SuperK/SNO/Borexino); HEP/ γ -ray astro
 - ◆ Also ZEPLIN III Groups in next phase
 - ◆ Co-spokespersons: Gaitskell (Brown) / Shutt (Case)
- 300 kg Dual Phase liquid Xe TPC with 100 kg fiducial
 - ◆ Using conservative assumptions: >99.4% ER background rejection for 50% NR acceptance, $E > 5$ keVr (ER rejection is energy dependent)
(Case+Columbia/Brown Prototypes + XENON10 + ZEPLIN II)
 - ◆ 3D-imaging TPC eliminates surface activity, defines fiducial
- Backgrounds:
 - ◆ Internal: strong self-shielding of PMT activity
 - Can achieve BG $\gamma + \beta < 8 \times 10^{-4}$ /keVee/kg/day, dominated by PMTs (Hamamatsu R8778).
 - Neutrons (α, n) & fission subdominant
 - ◆ External: large water shield with muon veto.
 - Very effective for cavern $\gamma + n$, and HE n from muons
 - Very low gamma backgrounds with readily achievable $< 10^{-11}$ g/g purity.
- DM reach: 7×10^{-46} cm² in 10 months

In DUSEL
(Deep Underground Science
and Engineering Laboratory)
Homestake Mine
Lead, South Dakota, USA
2012?

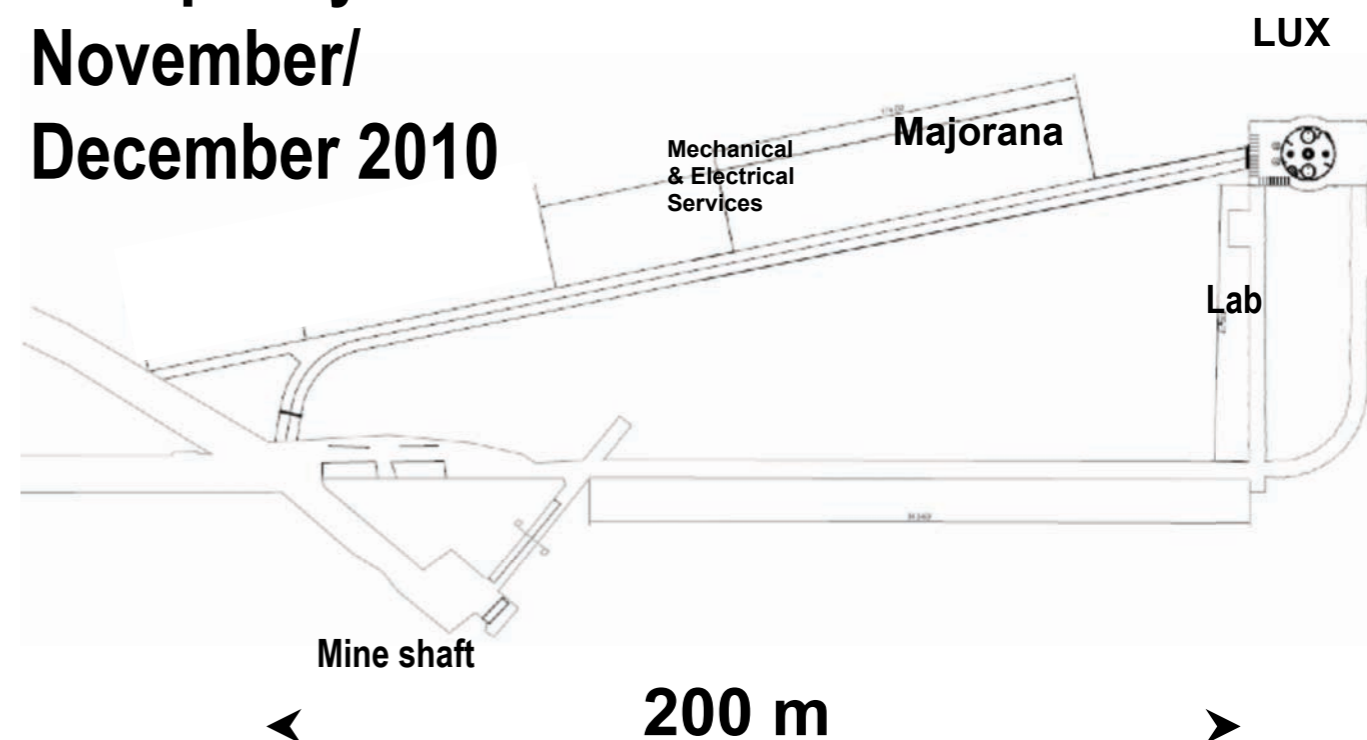


LUX in the Davis Laboratory at the Homestake Mine in South Dakota (4850)

- Construction/excavation design completed
- New 300' access/safety tunnel being excavated
- Shared with Majorana facility
- Two story, dedicated LUX 55' x 30' x 32' facility being built now



- Beneficial occupancy: November/December 2010



WIMP Signals in a Dual-Phase Xenon Detector



2005-2007



XENON10

Achieved (2007) $\sigma_{SI} = 8.8 \times 10^{-44} \text{ cm}^2$ Projected (2010) $\sigma_{SI} \sim 2 \times 10^{-45} \text{ cm}^2$

Phys. Rev. Lett. **100**, 021303 (2008)

Phys. Rev. Lett. **101**, 091301 (2008)

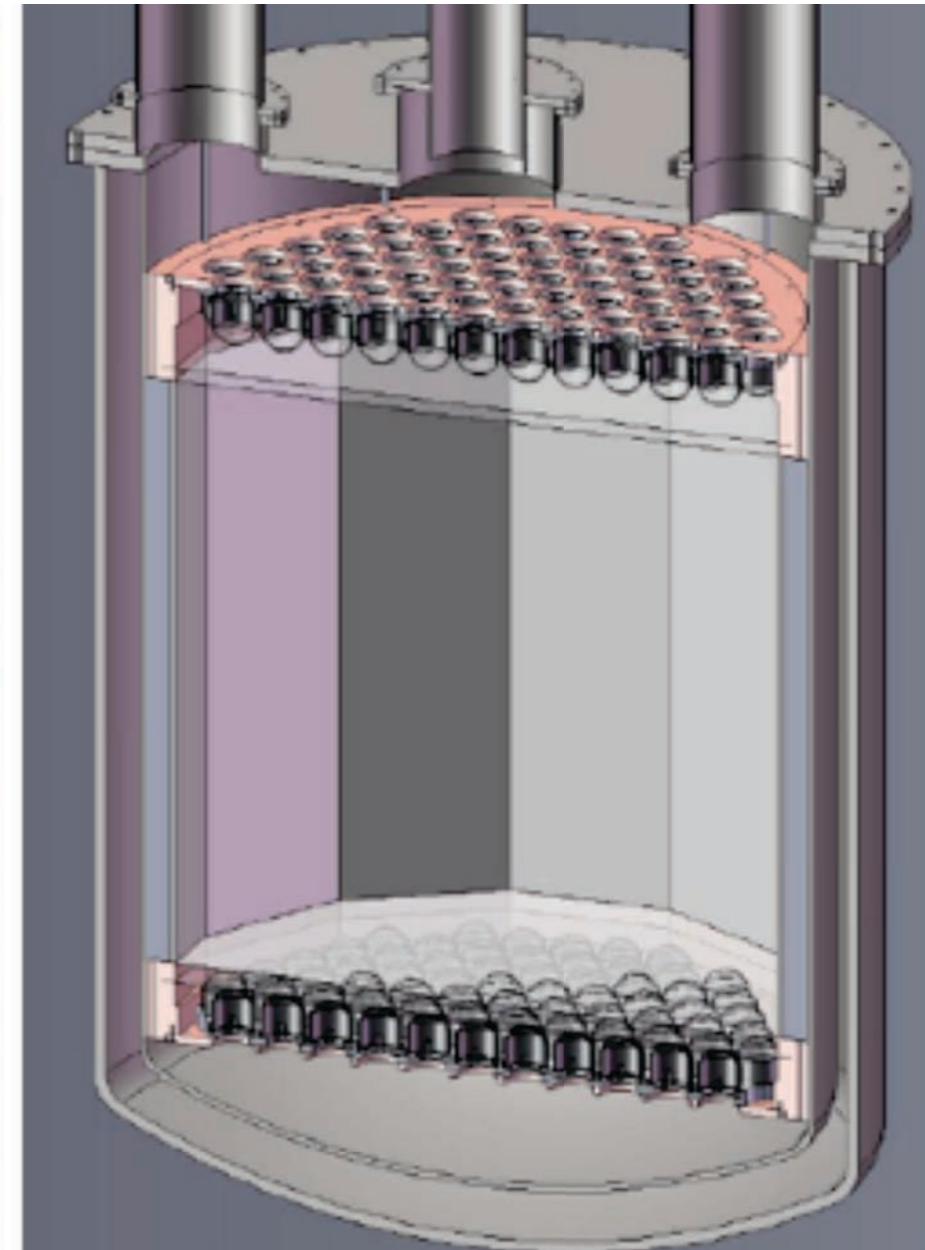
2008-2011



XENON100

XENON100 is a collaboration of Columbia and Rice universities, University of Zurich, University of Coimbra and Gran Sasso National Laboratory. UCLA joined the XENON100 effort in April 2008.

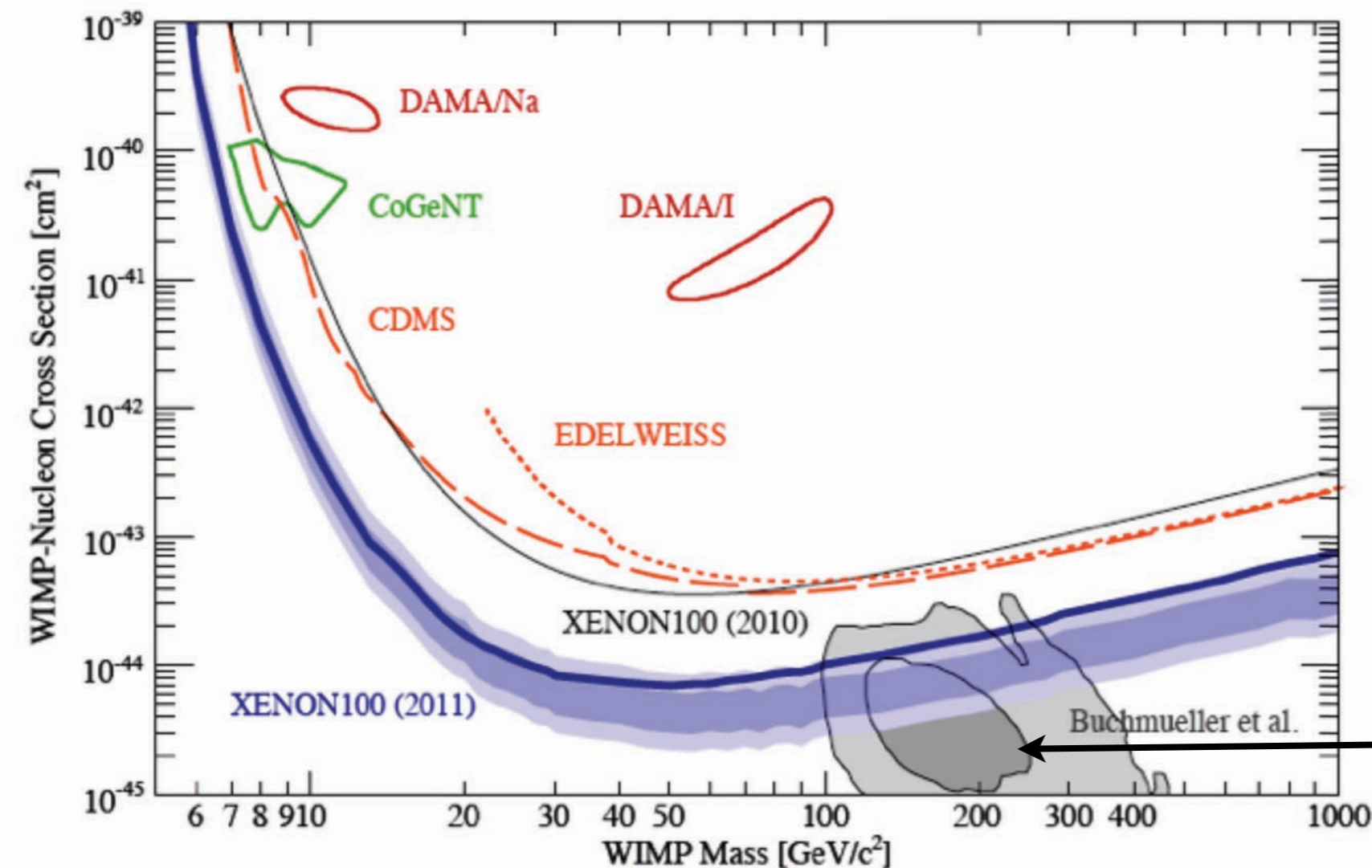
2011-2012



XENON1T

Goal: $\sigma_{SI} < 10^{-46} \text{ cm}^2$

We present results from the direct search for dark matter with the XENON100 detector, installed underground at the Laboratori Nazionali del Gran Sasso of INFN, Italy. XENON100 is a two-phase time projection chamber with a 62 kg liquid xenon target. Interaction vertex reconstruction in three dimensions with millimeter precision allows to select only the innermost 48 kg as ultra-low background fiducial target. In 100.9 live days of data, acquired between January and June 2010, no evidence for dark matter is found. Three candidate events were observed in a pre-defined signal region with an expected background of (1.8 ± 0.6) events. This leads to the most stringent limit on dark matter interactions today, excluding spin-independent elastic WIMP-nucleon scattering cross-sections above $7.0 \times 10^{-45} \text{ cm}^2$ for a WIMP mass of $50 \text{ GeV}/c^2$ at 90% confidence level.



Spin-independent elastic WIMP-nucleon cross-section as function of WIMP mass. The new XENON100 limit at 90% CL, as derived with the Profile Likelihood method taking into account all relevant systematic uncertainties, is shown as the thick (blue) line together with the 1σ and 2σ sensitivity of this run (shaded blue band).

LHC favored region

Implications on Inelastic Dark Matter from 100 Live Days of XENON100 Data

E. Aprile et al. 4/15/11

The XENON100 experiment has recently completed a dark matter run with 100.9 live-days of data, taken from January to June 2010. Events in a 48kg fiducial volume in the energy range between 8.4 and 44.6 keV_{nr} have been analyzed. A total of three events have been found in the predefined signal region, compatible with the background prediction of (1.8 ± 0.6) events. Based on this analysis we present limits on the WIMP-nucleon cross section for inelastic dark matter. With the present data we are able to rule out the explanation for the observed DAMA/LIBRA modulation as being due to inelastic dark matter scattering off iodine at a 90% confidence level.

A search for light dark matter in XENON10 data

E. Aprile et al. 4/15/11

We report results of a search for light ($\lesssim 10$ GeV) particle dark matter with the XENON10 detector. The event trigger was sensitive to a single electron, with the analysis threshold of 5 electrons corresponding to 1.4 keV nuclear recoil energy. Considering spin-independent dark matter-nucleon scattering, we exclude cross sections $\sigma_n > 3.5 \times 10^{-42}$ cm², for a dark matter particle mass $m_\chi = 8$ GeV. We find that our data strongly constrain recent elastic dark matter interpretations of excess low-energy events observed by CoGeNT and CRESST-II, as well as the DAMA annual modulation signal.

DAMA

Clear summer-winter modulation

13 years 1.17 ton year

2 different experiments
(same electronics)

right phase for WIMP

If WIMP $\approx 4\%$ asymmetry,

Very large signal

Surprisingly low background

Wide suspicion that this is instrumental

but no convincing explanation so far! Subtle problem!

David Nygren's suggestion

After-pulsing after μ 's

Keep our eyes open!

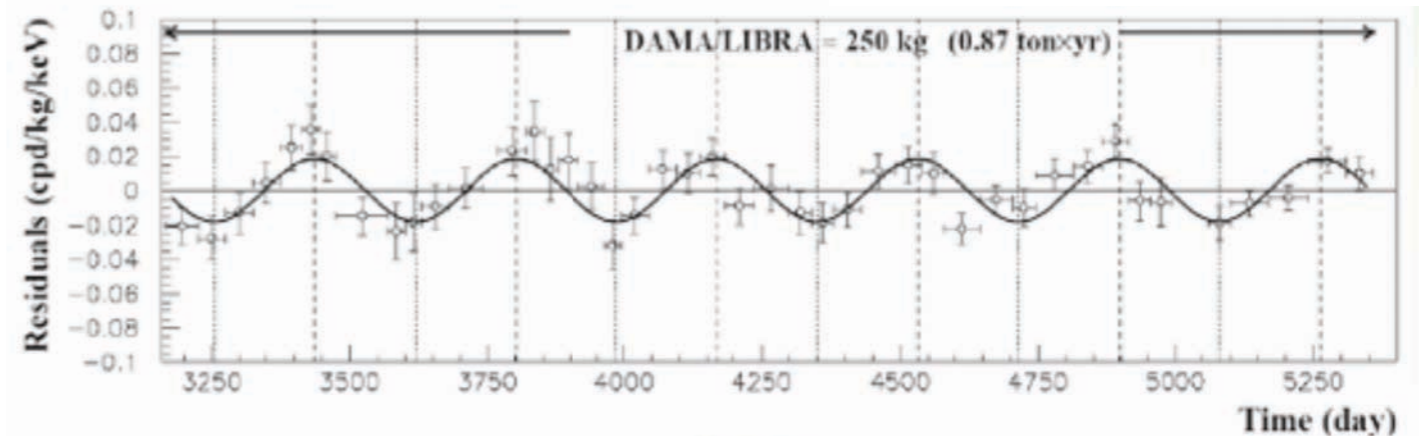
Repeat experiment

South Pole

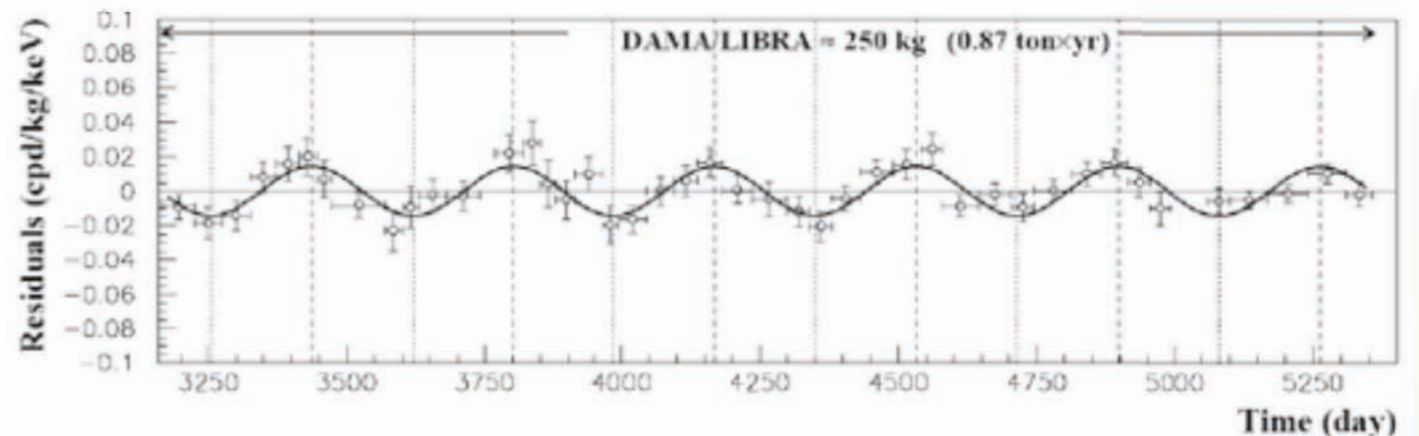
Princeton

KIMS (100kg CsI, 3 keVee)

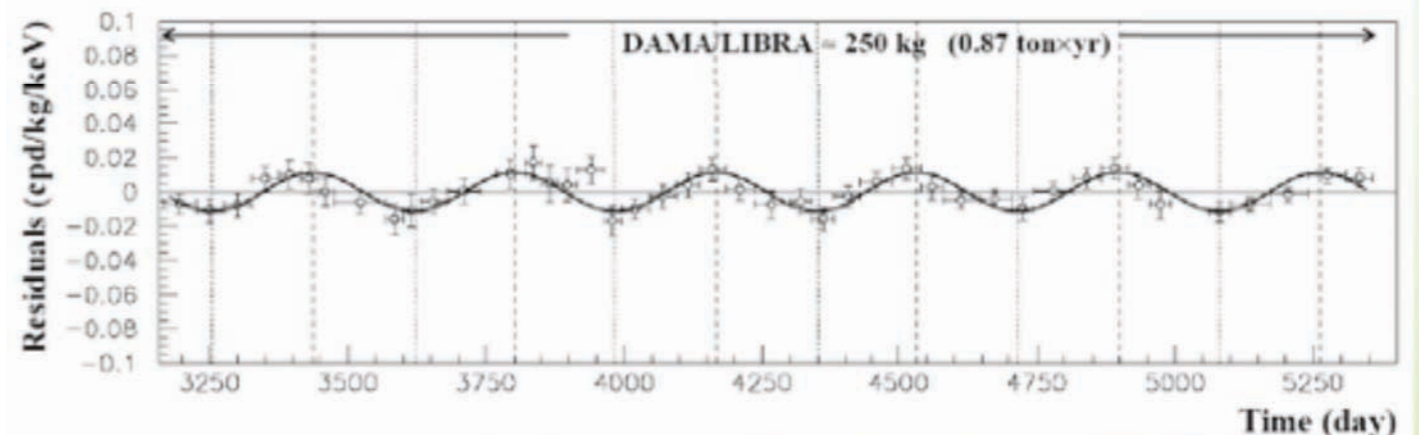
2-4 keV Latest Princeton Nov 2011



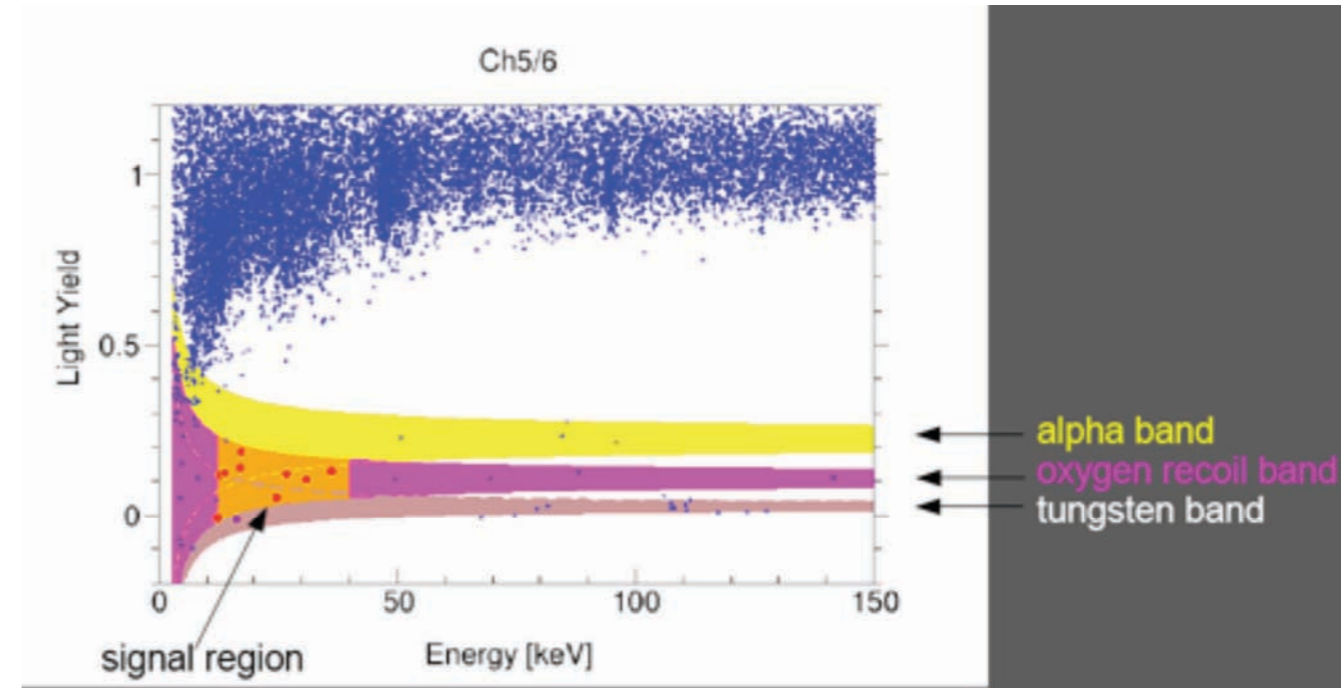
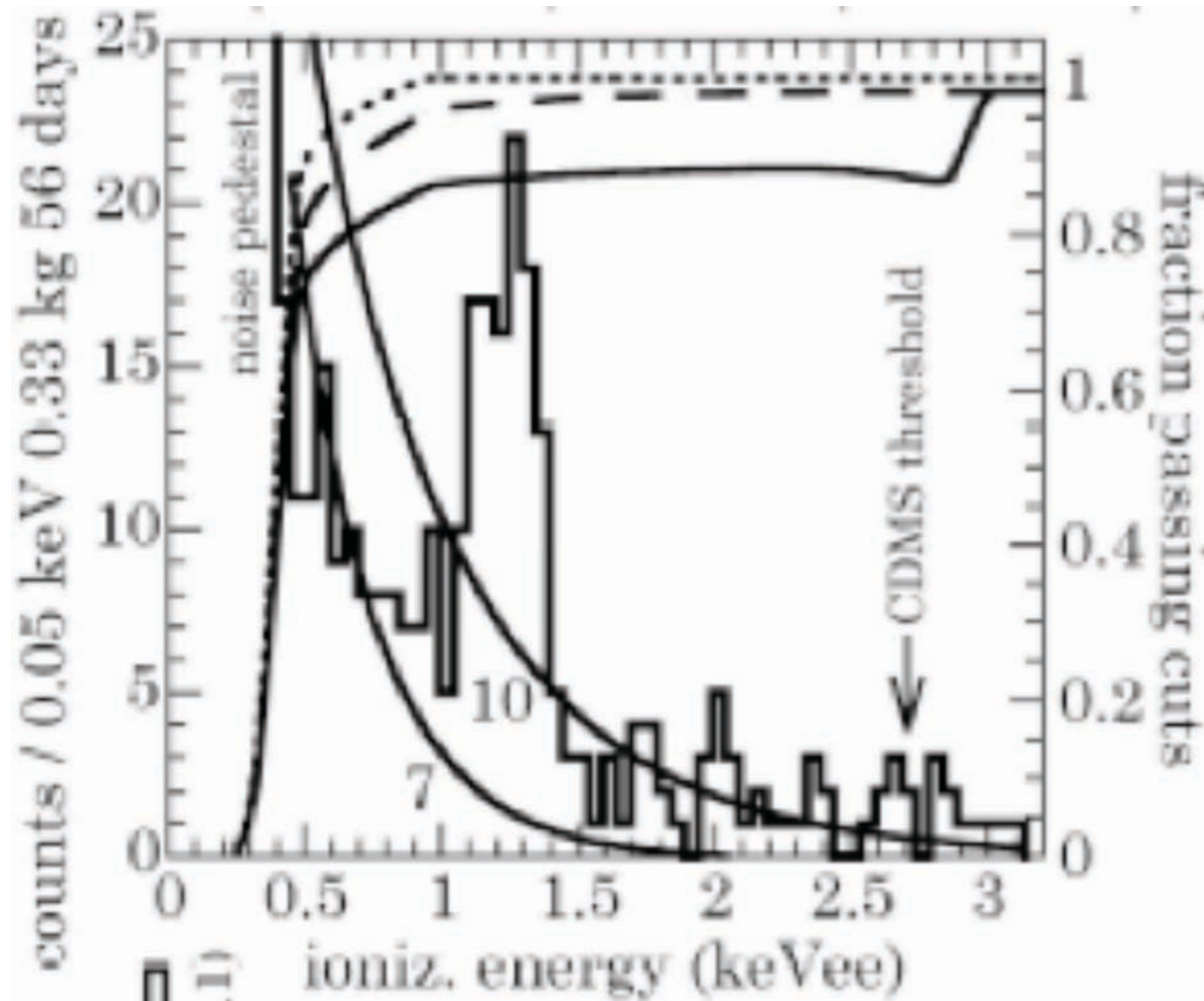
2-5 keV



2-6 keV



A 7 GeV/c² WIMP?



CoGeNT

Evidence for a signal ?

Detailed shape of the background: very weak!

CRESST

Events in Oxygen band

57 events

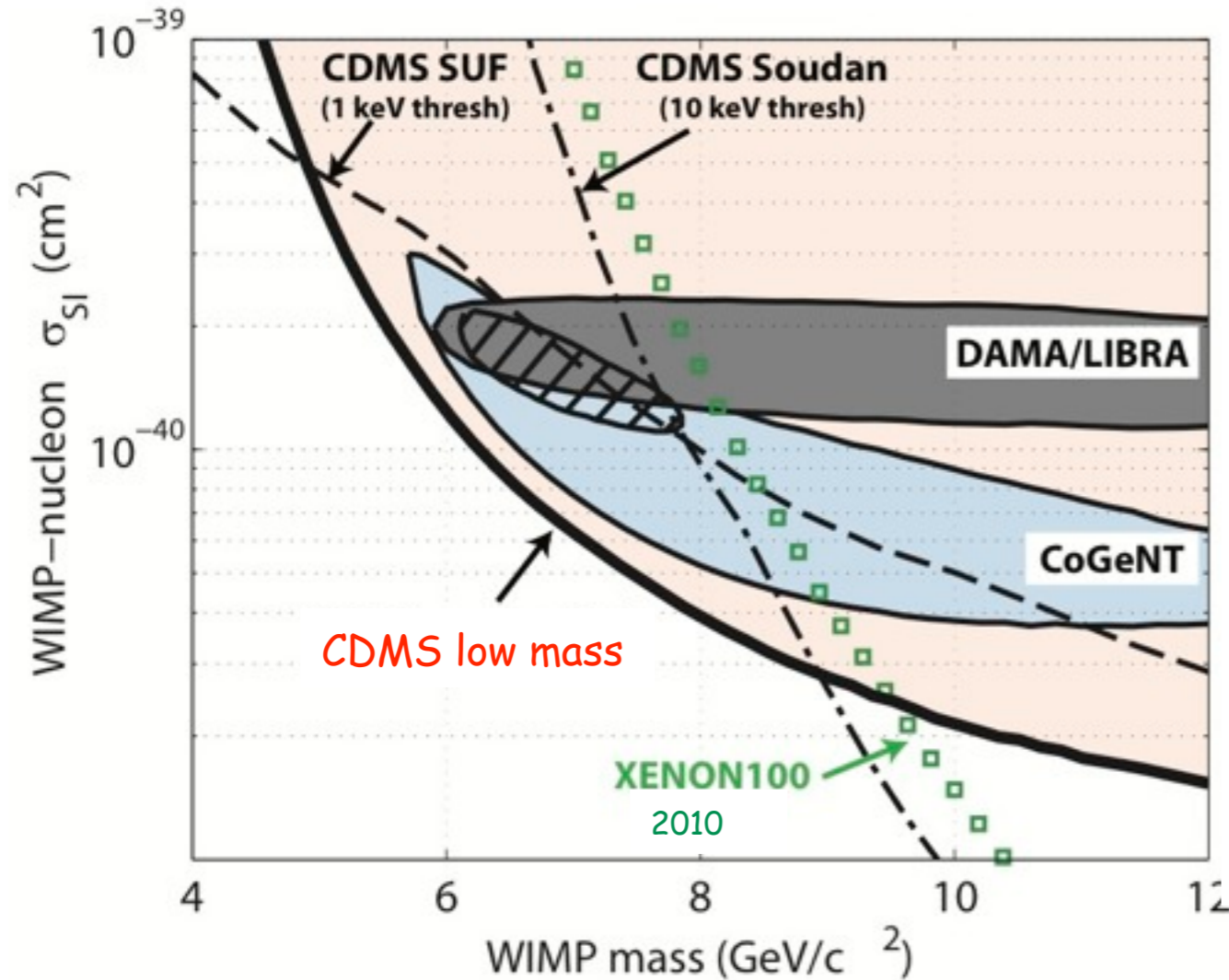
Claim that they cannot be fully explained by n, alphas, gamma 22 events

Claim 4.6 sigma effect ????

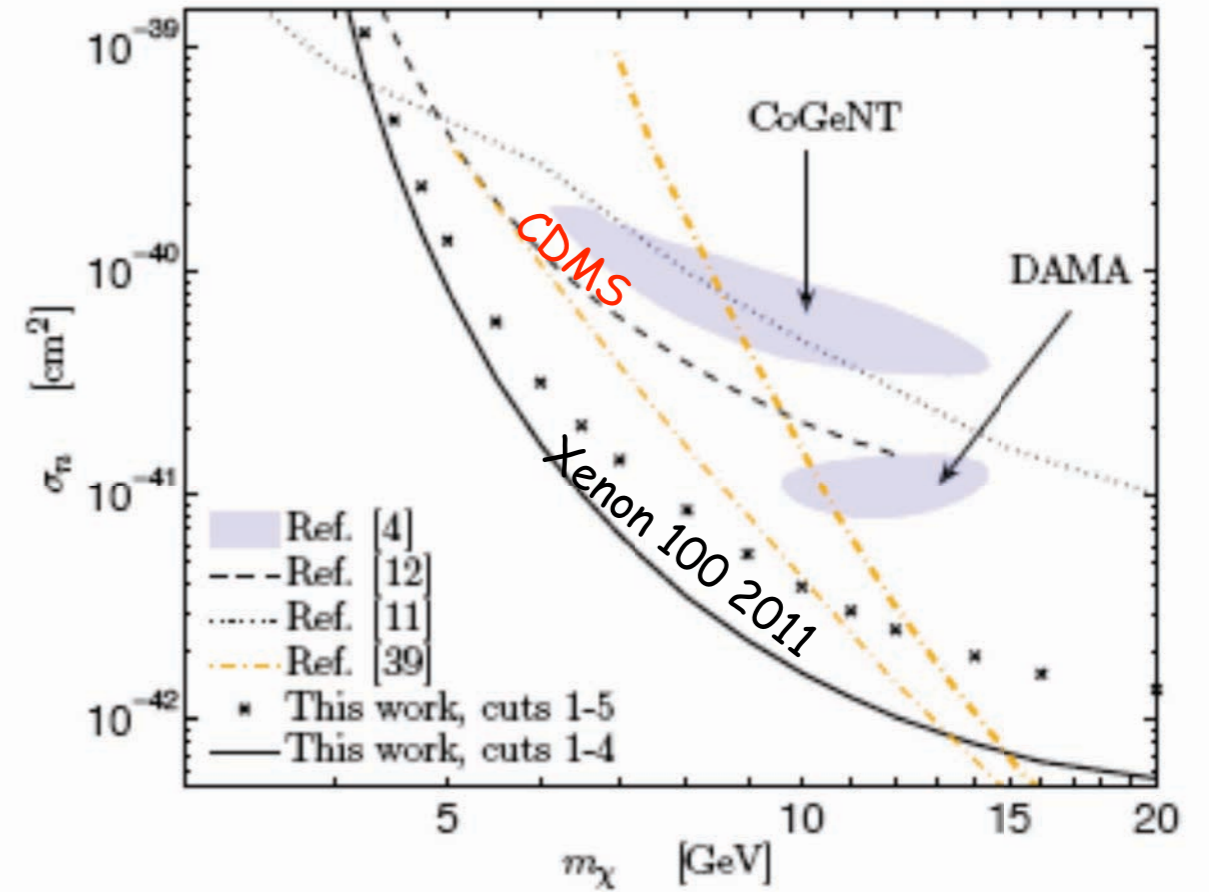
Hooper, Collar, Hall, McKinsey arXiv 1007.1005

A 7 GeV/c² WIMP could explain CoGeNT, DAMA and CRESST!

Alas!



Ahmed et al ArXiv:1011.2482
PRL 2011



Xenon 100 ArXiv:1104.3088

Can we have a WIMP excited state?

Idea by Neal Weiner

CDMS and Zeplin had already excluded most of the territory
Xenon 100 finishes the job

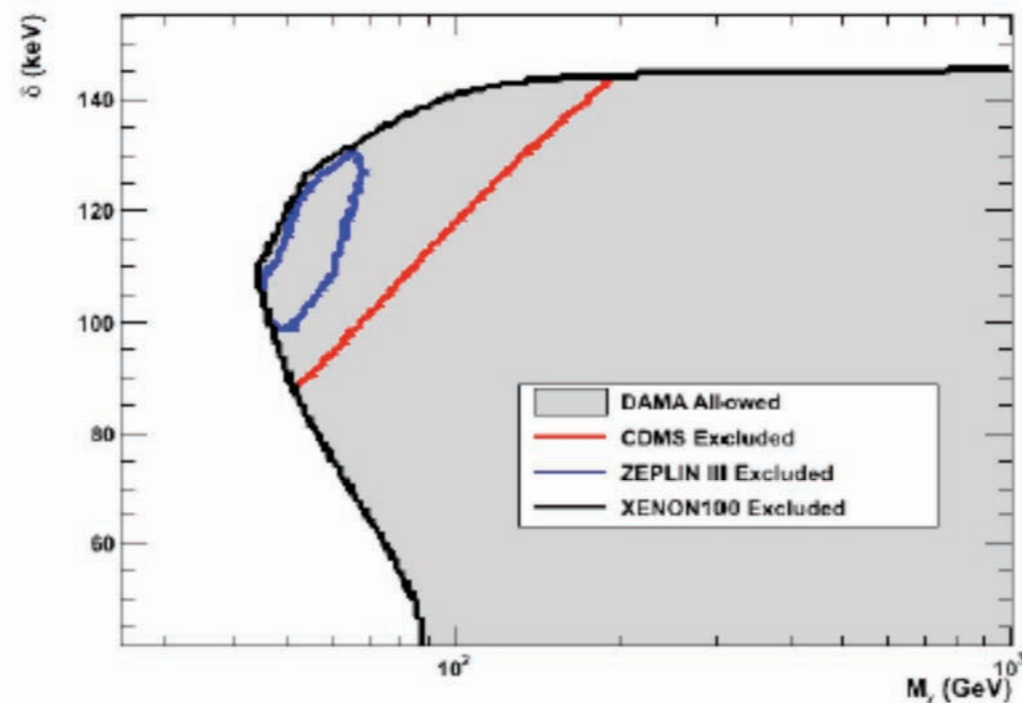


FIG. 4: Parameter space to explain the DAMA annual modulation with iDM (bounded area), and parameter space excluded by different experiments. The black line corresponding to XENON100 excludes the whole DAMA allowed region. $v_0 = 220$ km/s and $v_{esc} = 544$ km/s have been used. CDMS [14] (red) and ZEPLIN-III [15] (blue) exclusion curves are also shown.

Dark Matter and Terascale Physics

V. Barger

The Gold Standard: mSUGRA

- SUSY stabilizes radiative corrections to the Higgs mass and realizes GUT unification of electroweak and strong couplings
- Weird quantum numbers of particles explained by 16 representation of SO(10)
- mSUGRA: SUSY broken by gravity
 - predictive--small number of parameters: $m_0, m_{1/2}, A_0, \tan \beta, \text{sign}(\mu)$
- Find well defined regions of parameter space consistent with the relic density from WMAP

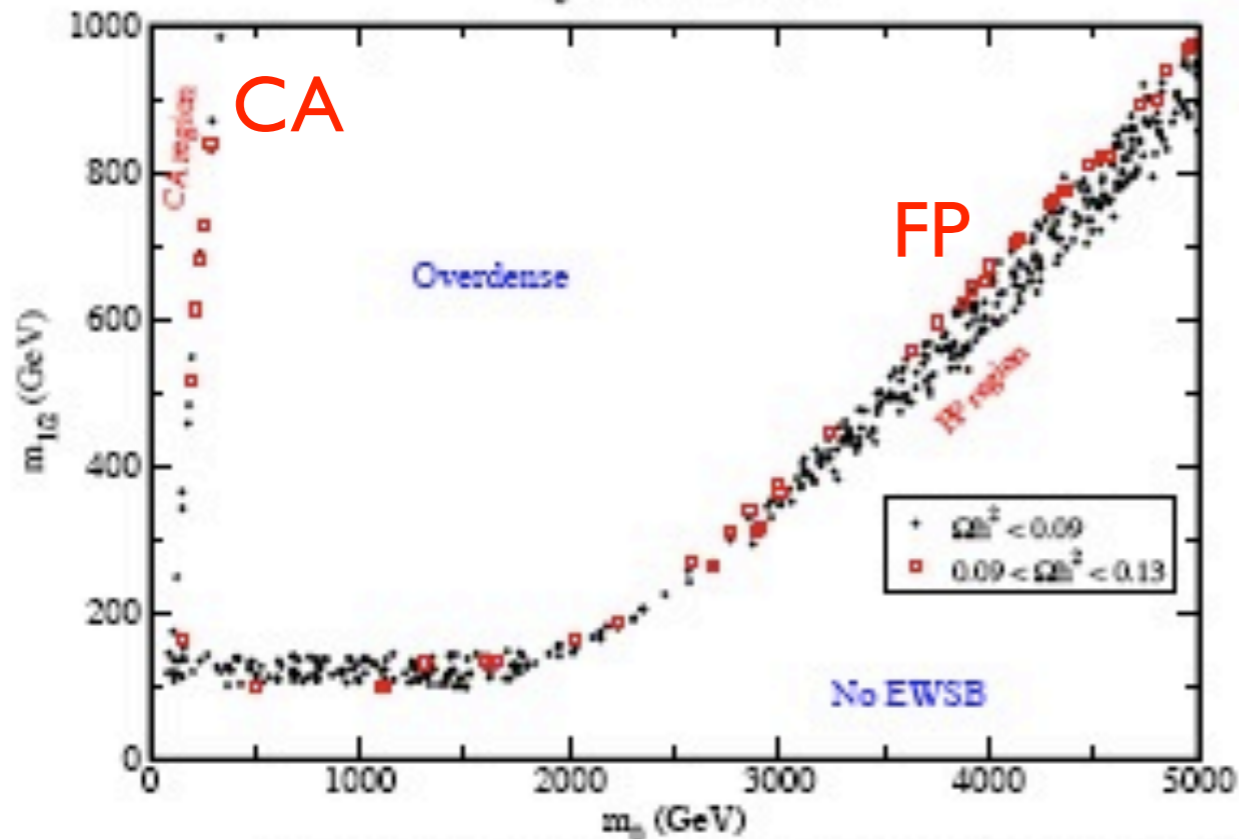
$$0.099 < \Omega_{DM} h^2 < 0.123 \quad (2\sigma)$$

- DM is associated with EWSB
 - weak scale cross section naturally gives Ω_{CDM}

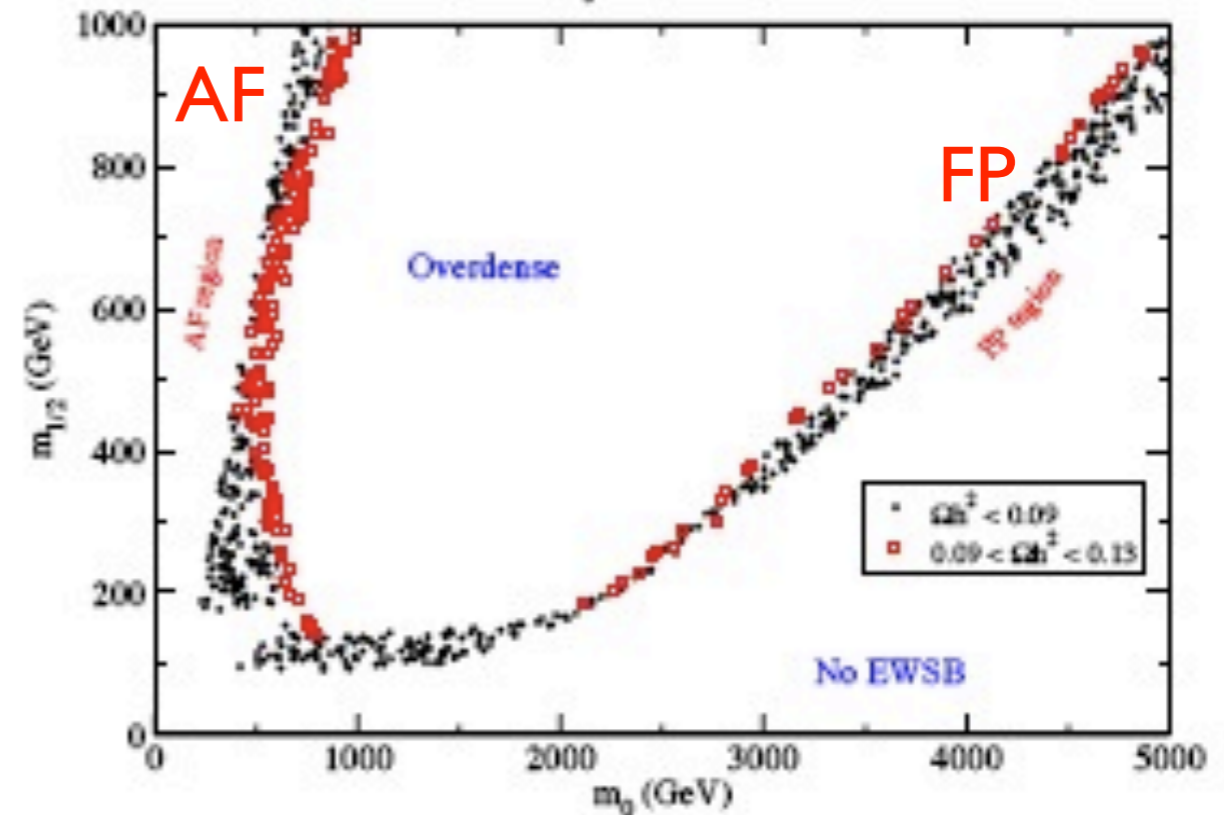
mSUGRA parameter space

- Representative regions in mSUGRA parameter space (red points fully account for Ω_{CDM})

$A_0 = 0, \tan\beta = 30, \mu > 0$



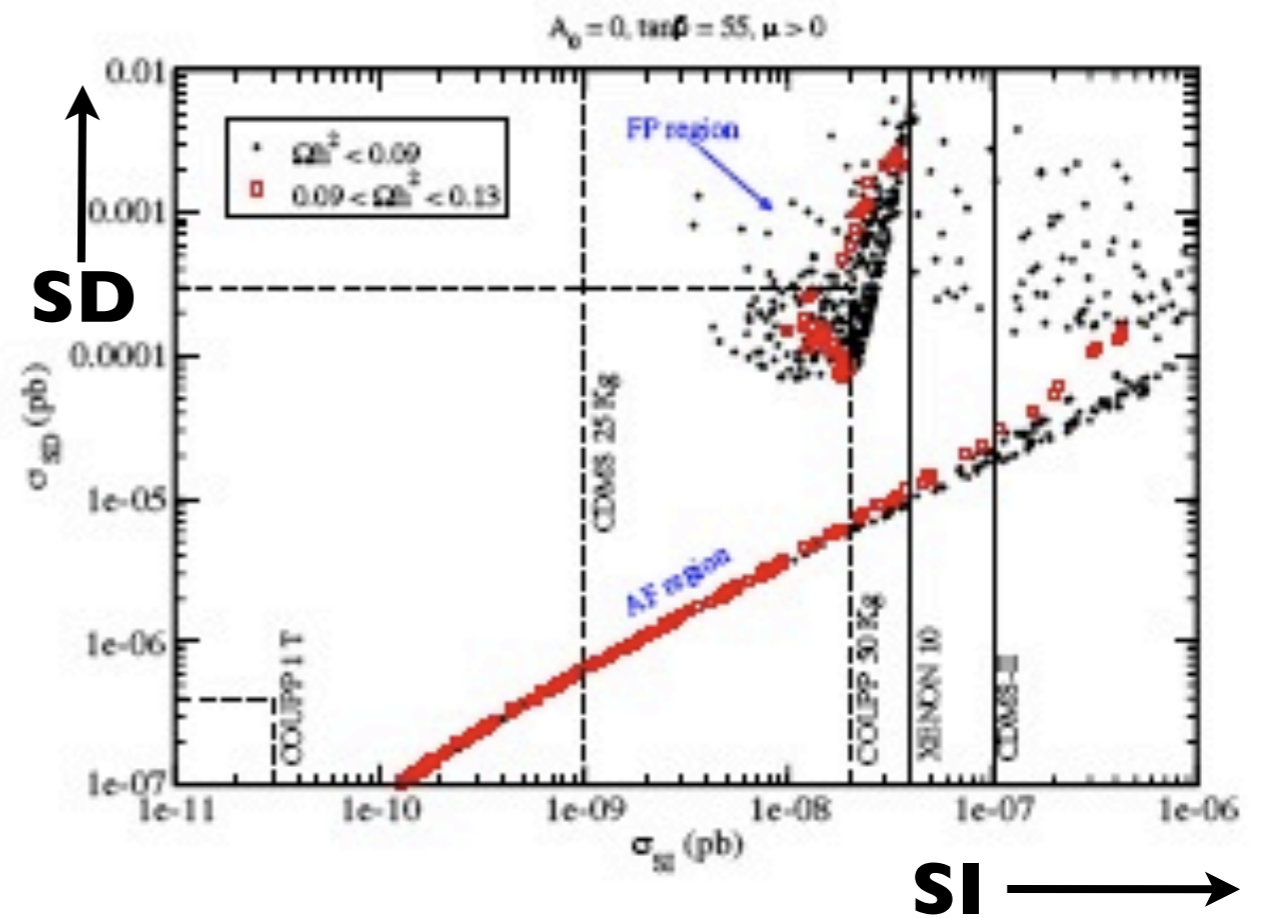
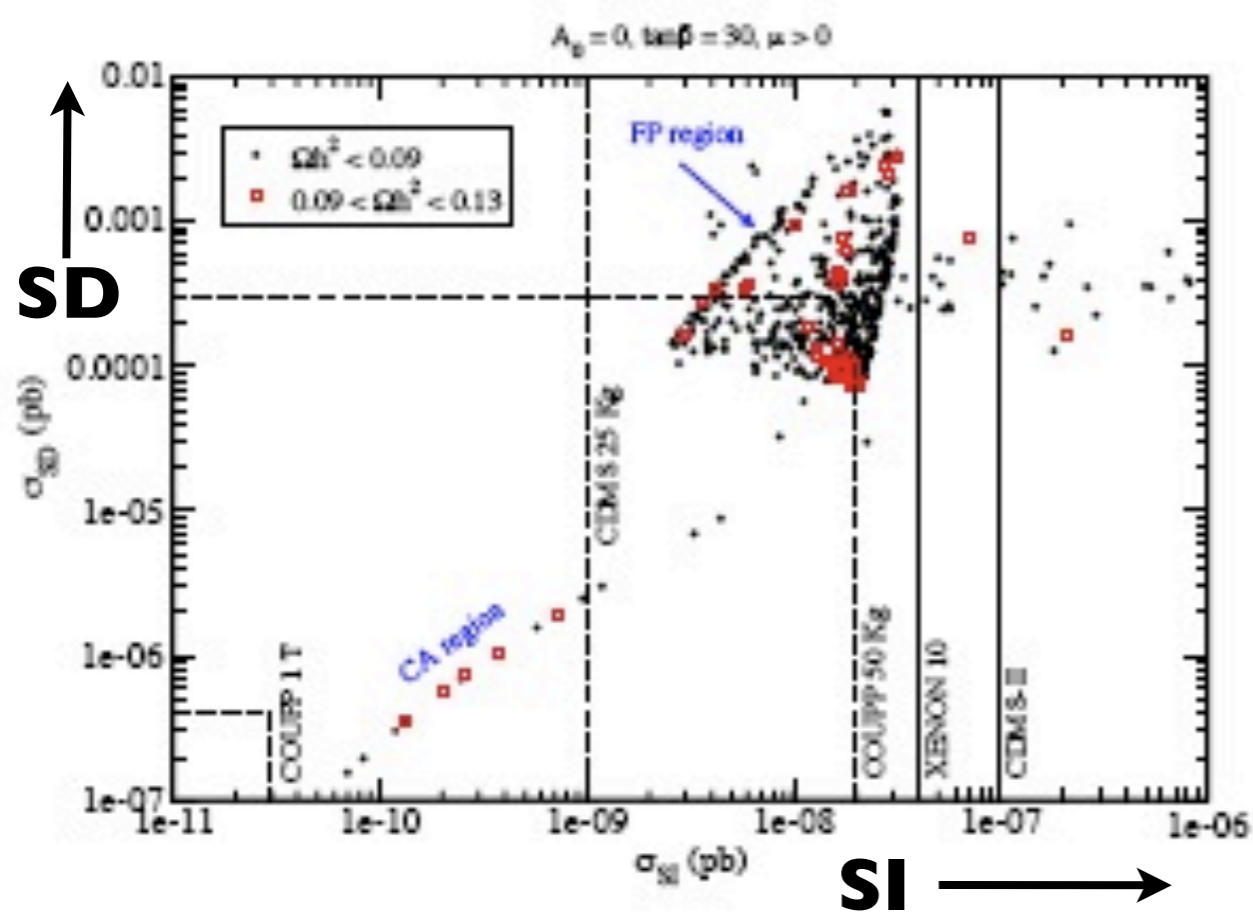
$A_0 = 0, \tan\beta = 55$



- Focus Point (FP) region: high mass scalar fermions
Preferred by $b - \tau$ unification
Solves SUSY FCNC and CP-violating problems
- A-funnel (AF) region: annihilation through CP-odd Higgs (A)
- $\tilde{\tau} - \chi_1^0$ coannihilation (CA) region
- Bulk region (BR) at low $m_0, m_{1/2}$ nearly excluded

Scattering rates in mSUGRA

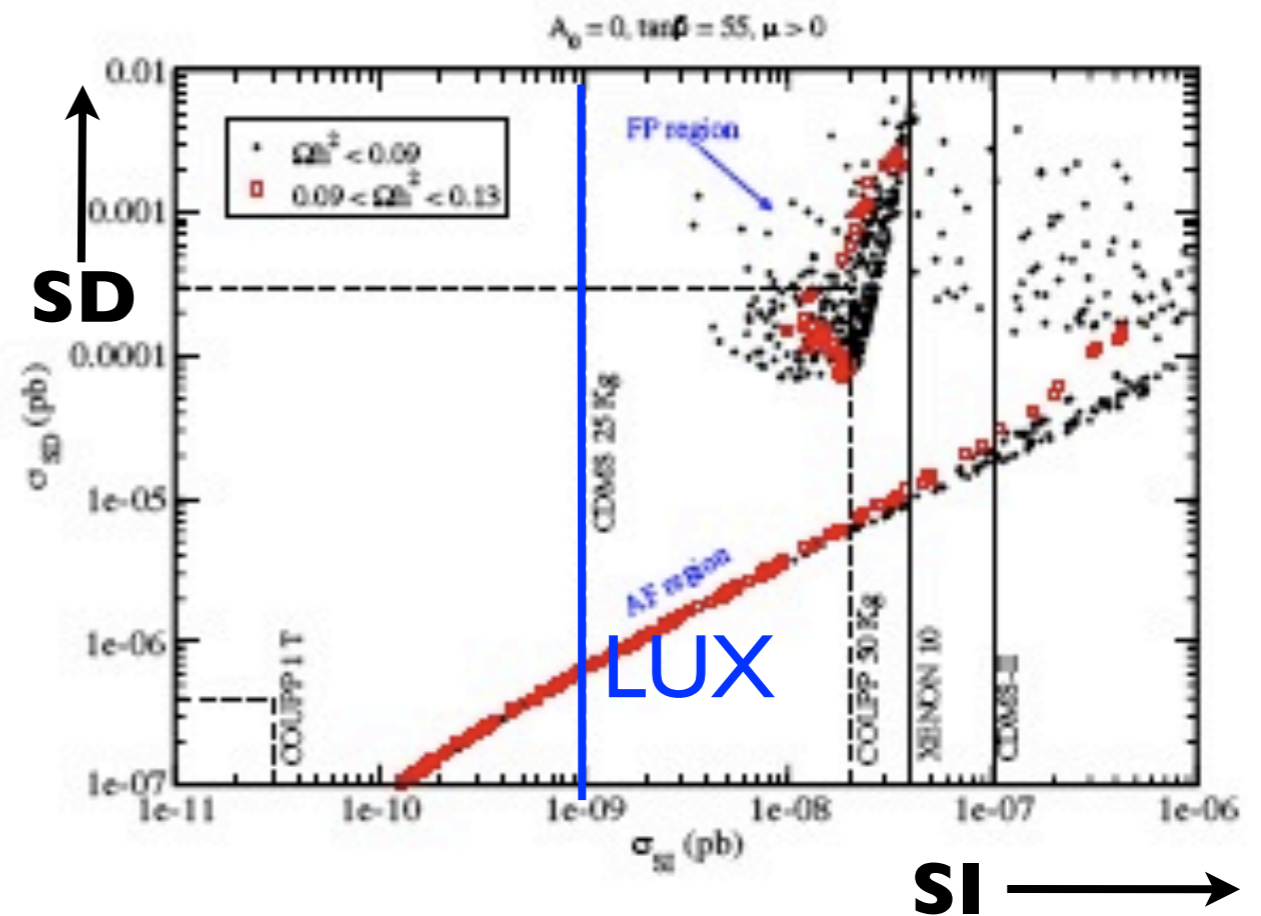
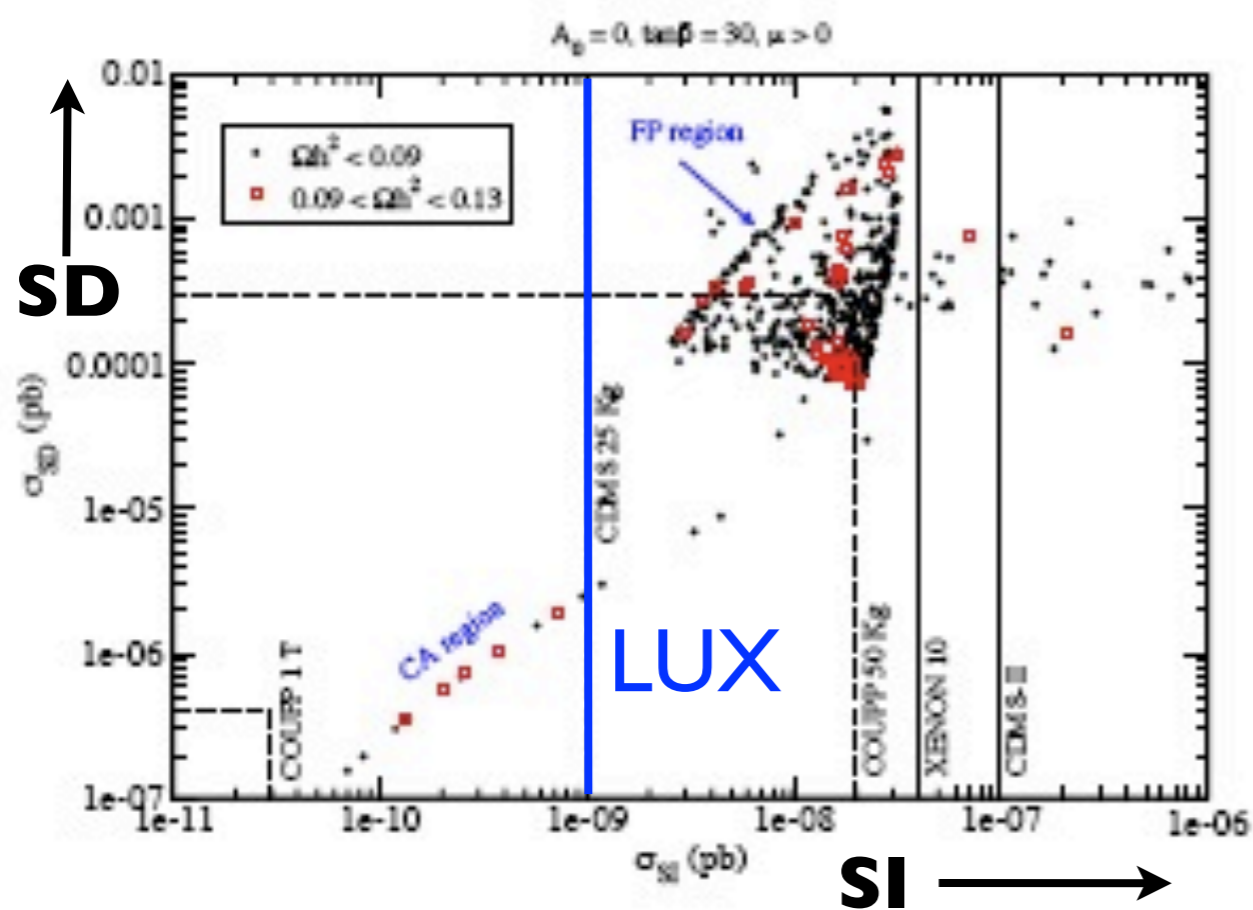
- Different solutions to DM relic density populate different regions of σ_{SD} VS. σ_{SI} Spin Dependent vs. Spin Independent



- FP region can be verified or disproved by both SD and SI measurements
- Detection in FP region would be of major significance for colliders (high mass scalars)

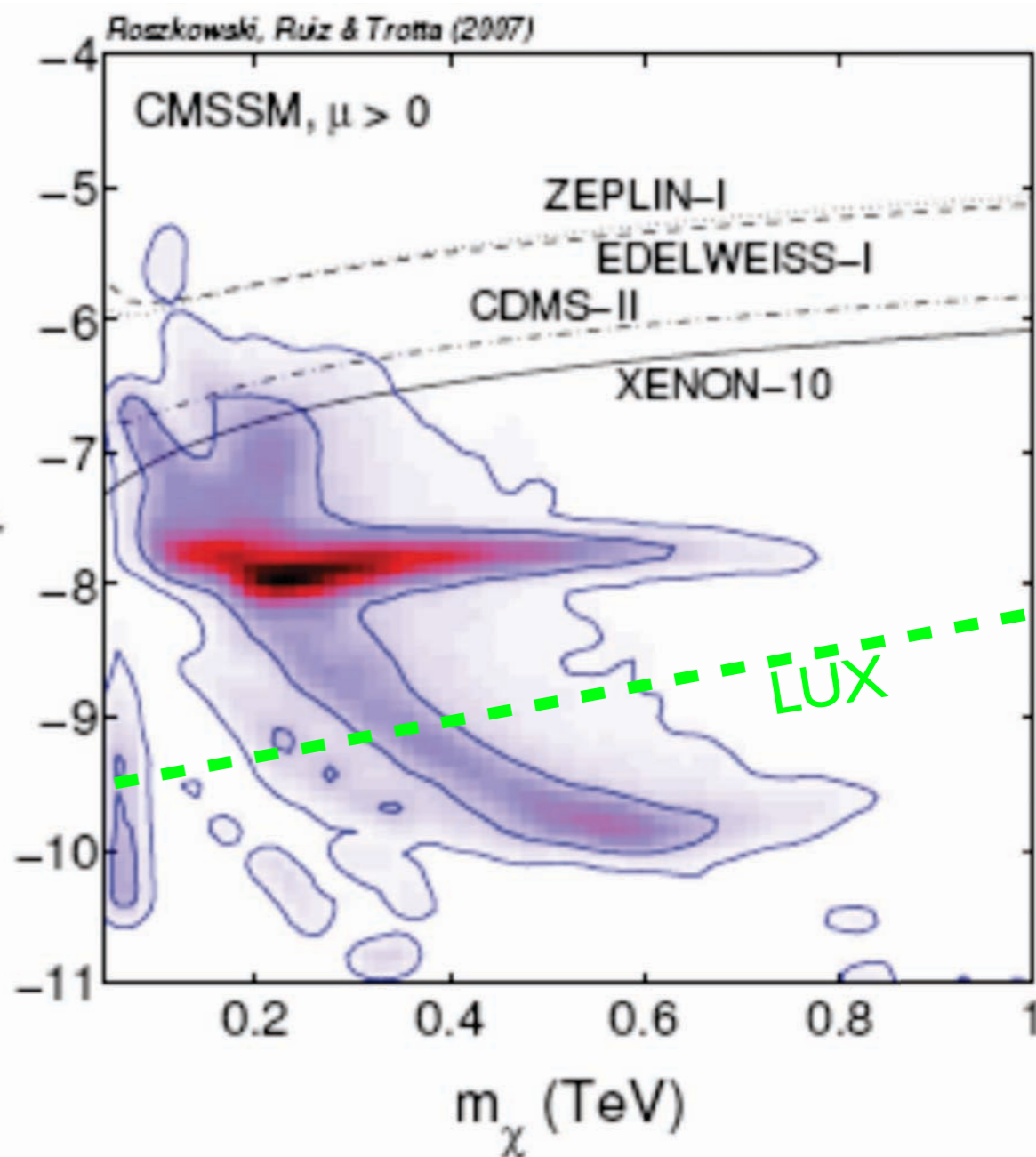
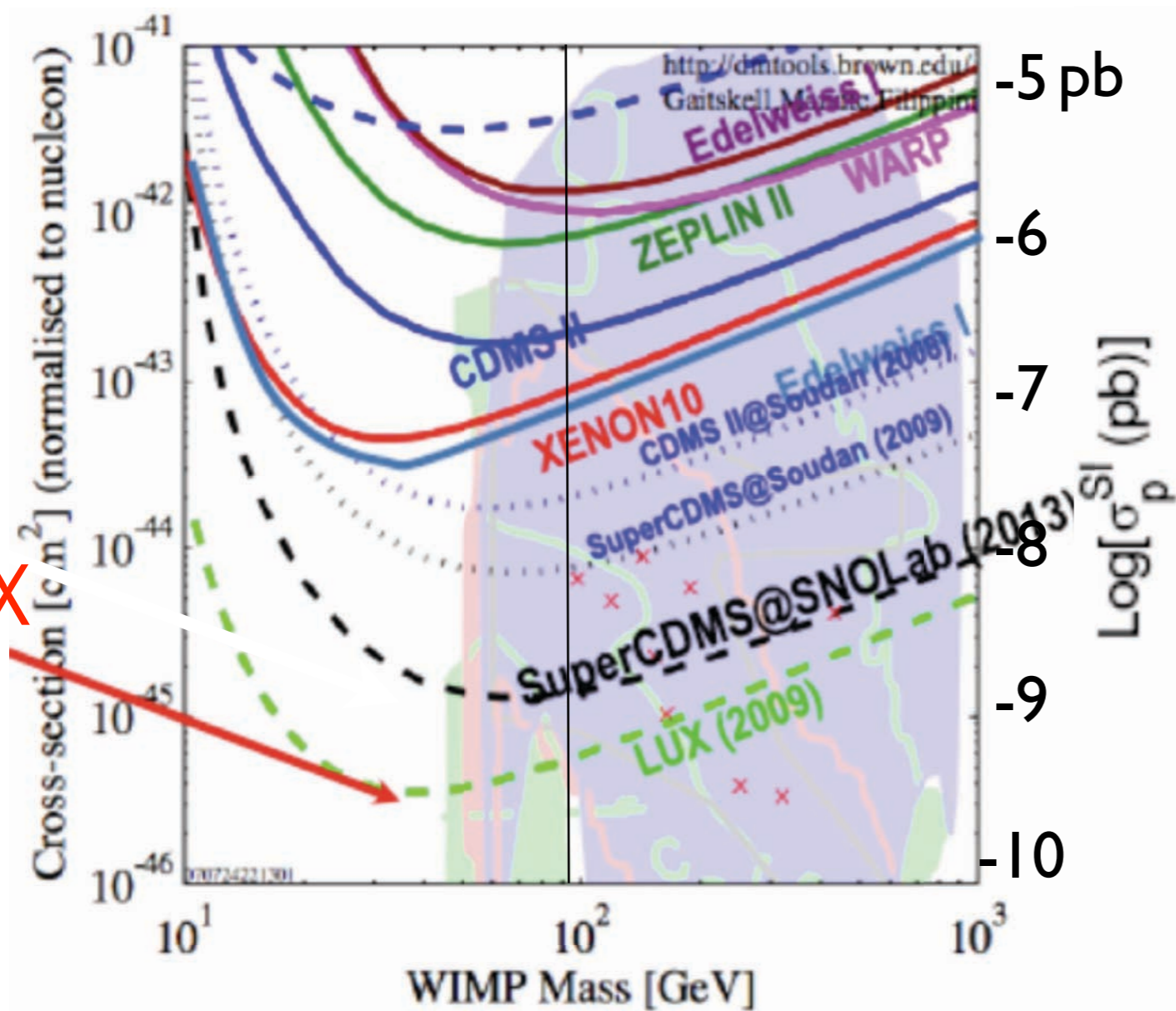
Scattering rates in mSUGRA

- Different solutions to DM relic density populate different regions of σ_{SD} VS. σ_{SI} Spin Dependent vs. Spin Independent



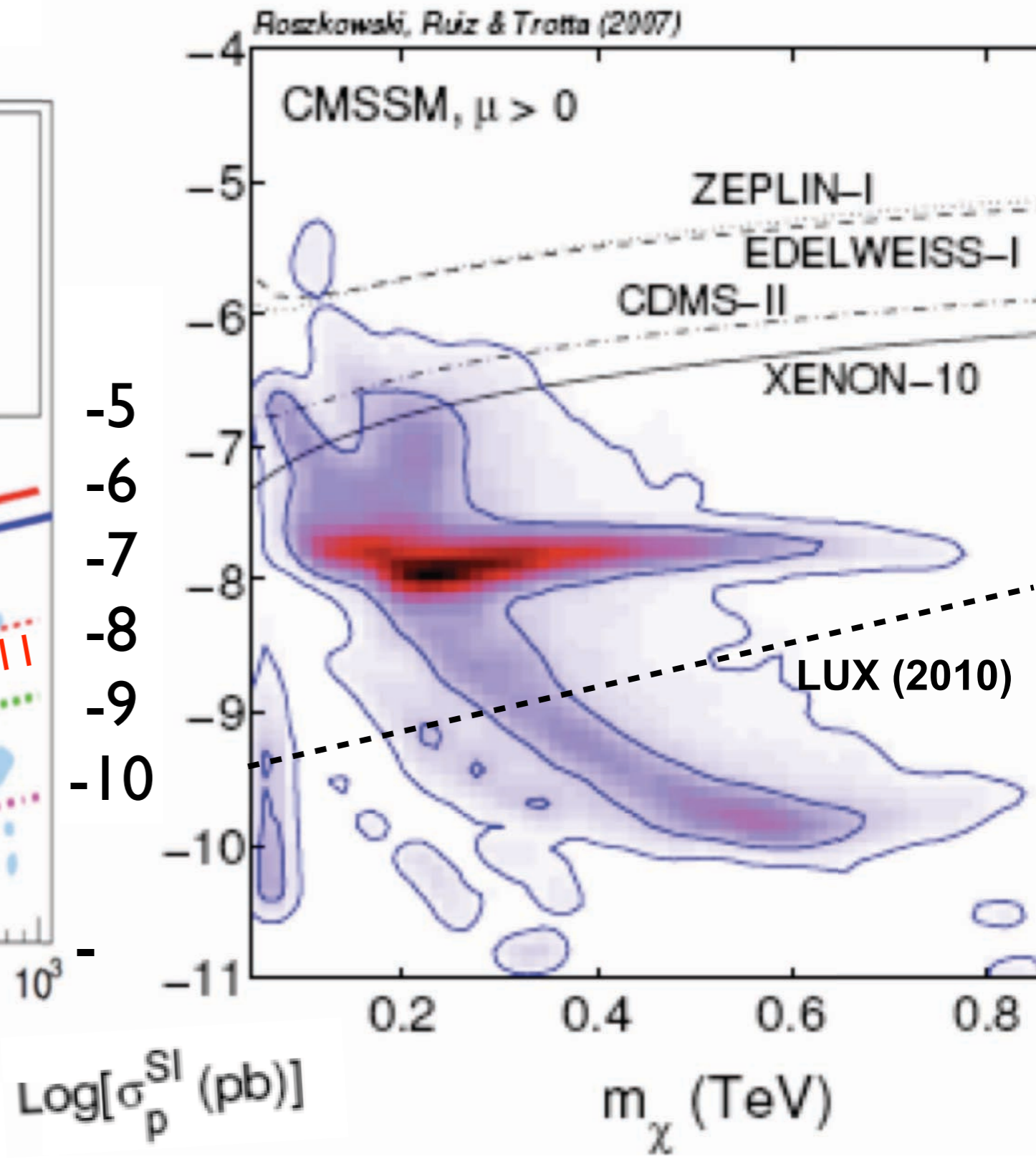
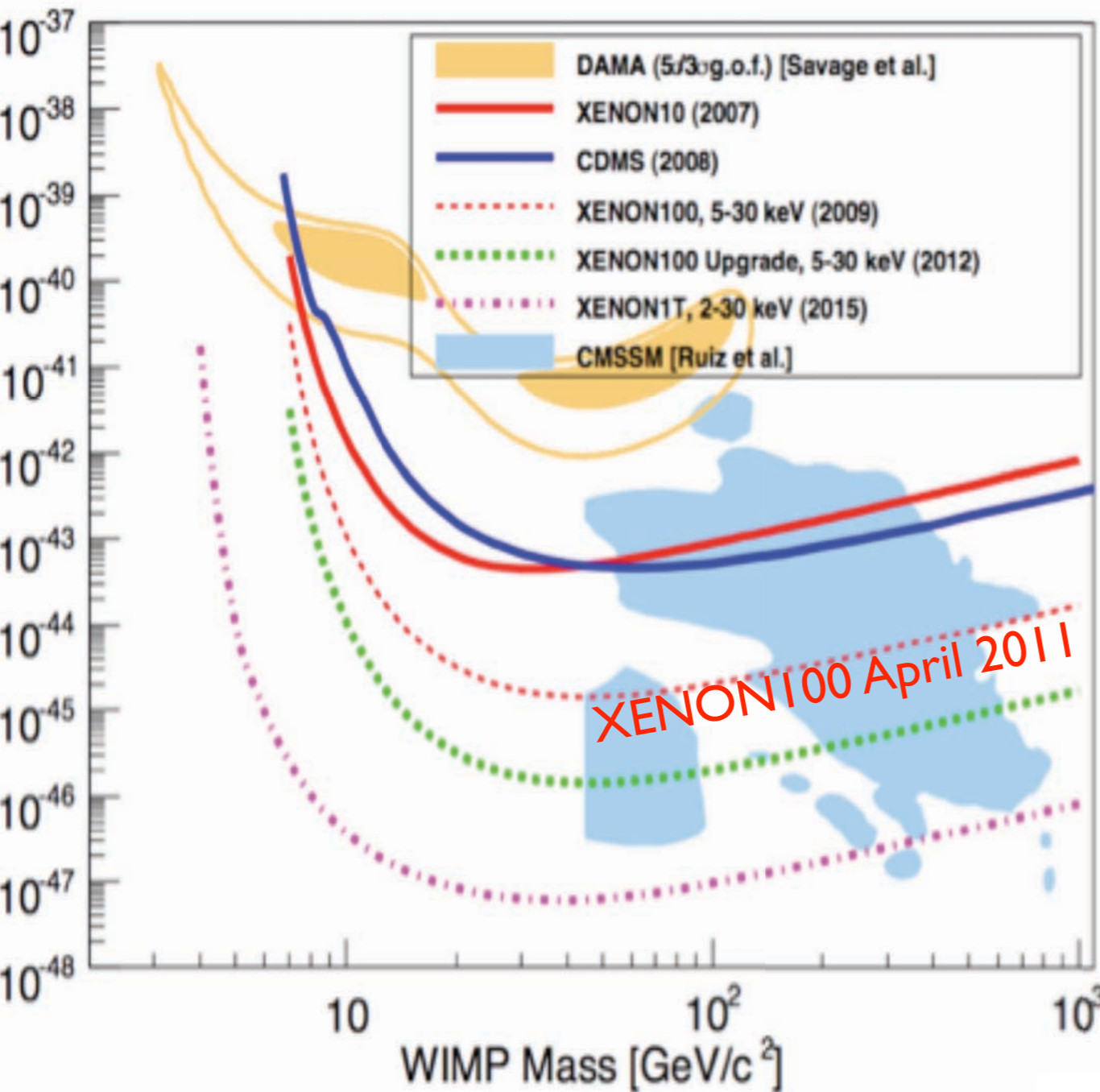
- FP region can be verified or disproved by both SD and SI measurements
- Detection in FP region would be of major significance for colliders (high mass scalars)

By ~2012 Direct Detection could probe most of the CMSSM (constrained minimal supersymmetric standard model) and mSUGRA (minimal supergravity) WIMP parameter space! If **LUX** and other large noble gas detectors succeed, they will leapfrog over CDMS and have great discovery potential during 2010-11.



$10^{-8} \text{ pb} = 10^{-44} \text{ cm}^2$ (barn = 10^{-24} cm^2 , pb = $10^{-12} \text{ b} = 10^{-36} \text{ cm}^2$)

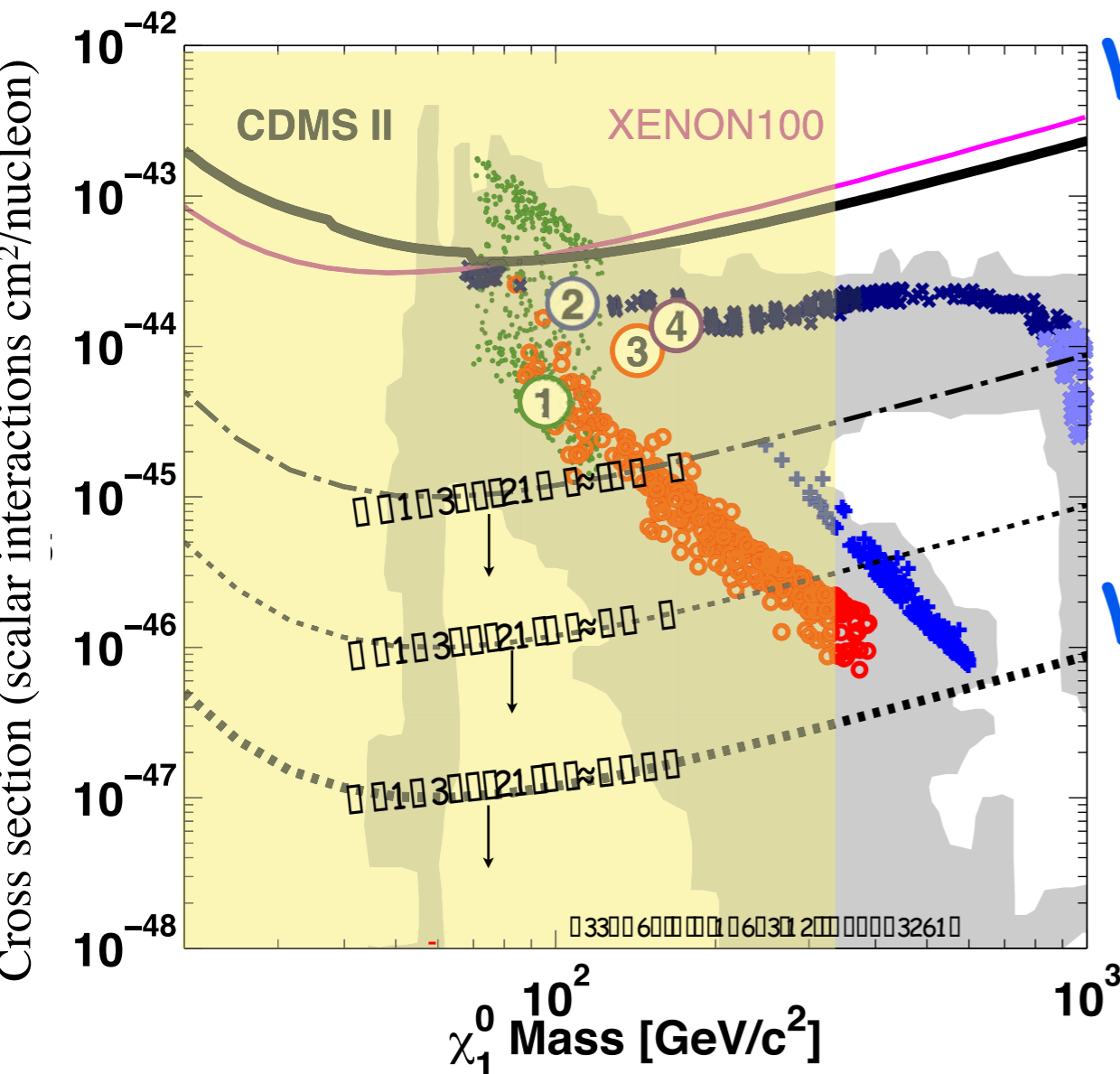
By ~2012 Direct Detection could probe most of the CMSSM (constrained minimal supersymmetric standard model) and mSUGRA (minimal supergravity) WIMP parameter space!



Where do we go next?

Strong consensus

Sensitivity = Mass + background free.



Why don't we pick a common technology now?

In spite of excellent progress, we do not know yet which are the best technologies...

We believe there is much to gain from at least two complementary technologies with different discrimination techniques and backgrounds

We propose instead a responsible common roadmap

Generation 1 -> 10^{-45} cm^2 Exploration of technology + science (Supersymmetry)

Generation 2 -> 10^{-46} cm^2 Push the most promising technologies to their limit + science

Generation 3 -> $<10^{-47} \text{ cm}^2$ 2 (US) 3or4 worldwide -> detailed understanding of the physics

≈ 2014 technology choice for ≈ 2018 deployment

WHAT IS THE DARK MATTER?

Prospects for DIRECT and INDIRECT detection of **WIMPs** are improving.

With many upcoming experiments

- Production at Large Hadron Collider

- Better CMB data from PLANCK

- Direct Detection

 - Spin Independent - CDMS-II, XENON50, LUX

 - Spin Dependent - COUPP, PICASSO

- Indirect detection via

 - GLAST and larger ACTs

 - PAMELA and ATIC

-- there could well be a big discovery in the next year or two!

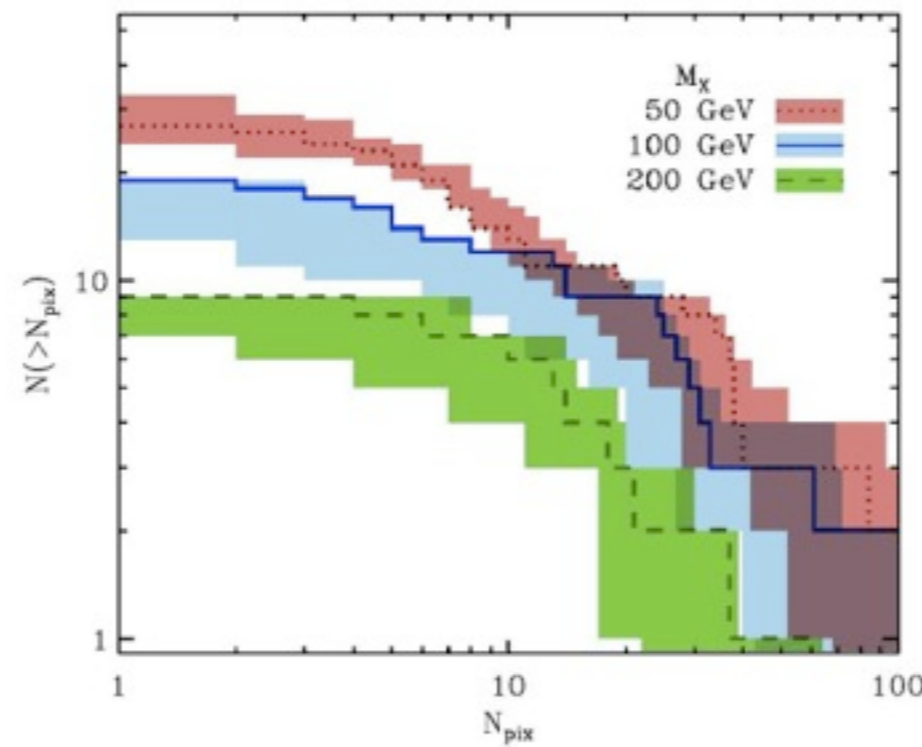
THE DARK MATTER ANNIHILATION SIGNAL FROM GALACTIC SUBSTRUCTURE: PREDICTIONS FOR GLAST

2008 [ApJ 686, 262](#)

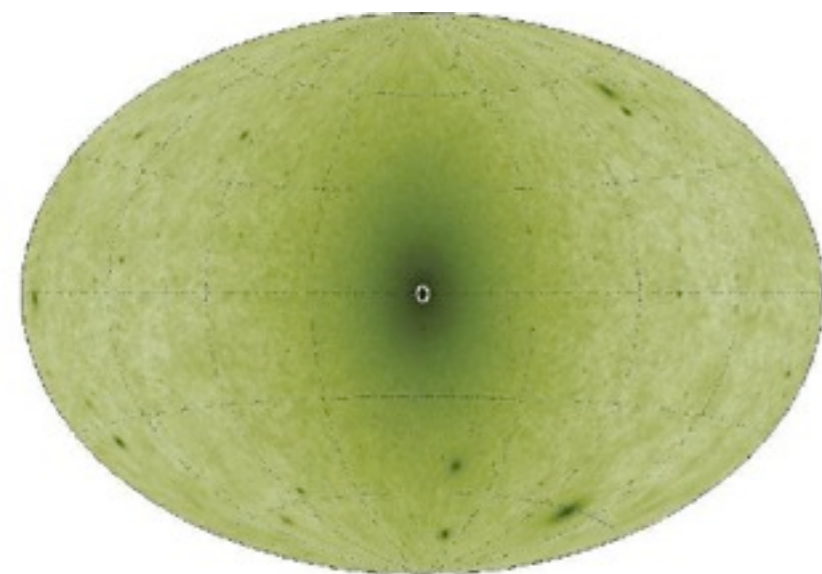
MICHAEL KUHLEN¹, JÜRIG DIEMAND^{2,3}, PIERO MADAU²

ABSTRACT

We present quantitative predictions for the detectability of individual Galactic dark matter subhalos in gamma-rays from dark matter pair annihilations in their centers. Our method is based on a hybrid approach, employing the highest resolution numerical simulations available (including the recently completed one billion particle Via Lactea II simulation) as well as analytical models for the extrapolation beyond the simulations' resolution limit. We include a self-consistent treatment of subhalo boost factors, motivated by our numerical results, and a realistic treatment of the expected backgrounds that individual subhalos must outshine. We show that for reasonable values of the dark matter particle physics parameters ($M_\chi \sim 50 - 500$ GeV and $\langle\sigma v\rangle \sim 10^{-26} - 10^{-25}$ cm³ s⁻¹) GLAST may very well discover a few, even up to several dozen, such subhalos, at 5σ significance, and some at more than 20σ . We predict that the majority of luminous sources would be resolved with GLAST's expected angular resolution. For most observer locations the angular distribution of detectable subhalos is consistent with a uniform distribution across the sky. The brightest subhalos tend to be massive (median V_{max} of 24 km s⁻¹) and therefore likely hosts of dwarf galaxies, but many subhalos with V_{max} as low as 5 km s⁻¹ are also visible. Typically detectable subhalos are 20 - 40 kpc from the observer, and only a small fraction are closer than 10 kpc. The total number of observable subhalos has not yet converged in our simulations, and we estimate that we may be missing up to 3/4 of all detectable subhalos.



The number of detectable ($S = 5$) subhalos with more than N_{pix} detectable pixels versus N_{pix} , for three different choices of M_χ (for $\langle\sigma v\rangle = 3 \times 10^{-26}$ cm³ s⁻¹). The shaded regions show the range of $N(>N_{\text{pix}})$ for ten randomly chosen observer locations and the solid lines refer to an observer placed along the intermediate axis of the host halo ellipsoid.

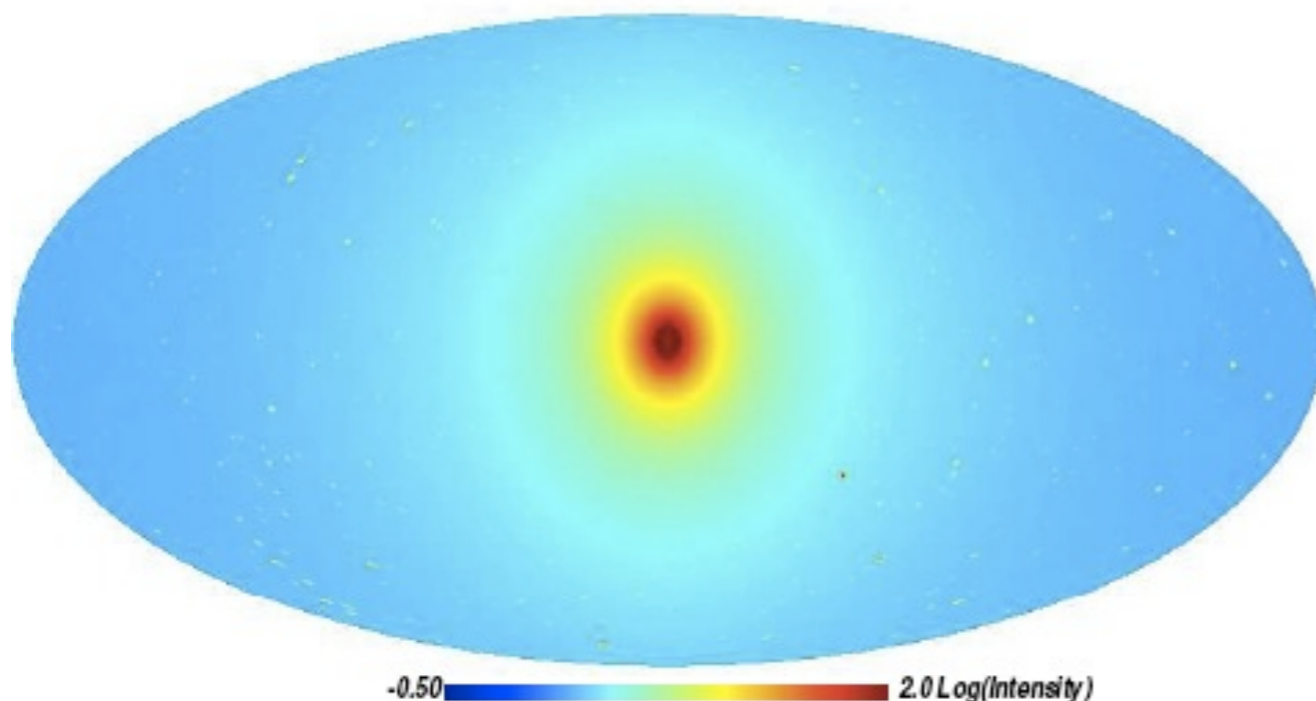


A blueprint for detecting supersymmetric dark matter in the Galactic halo

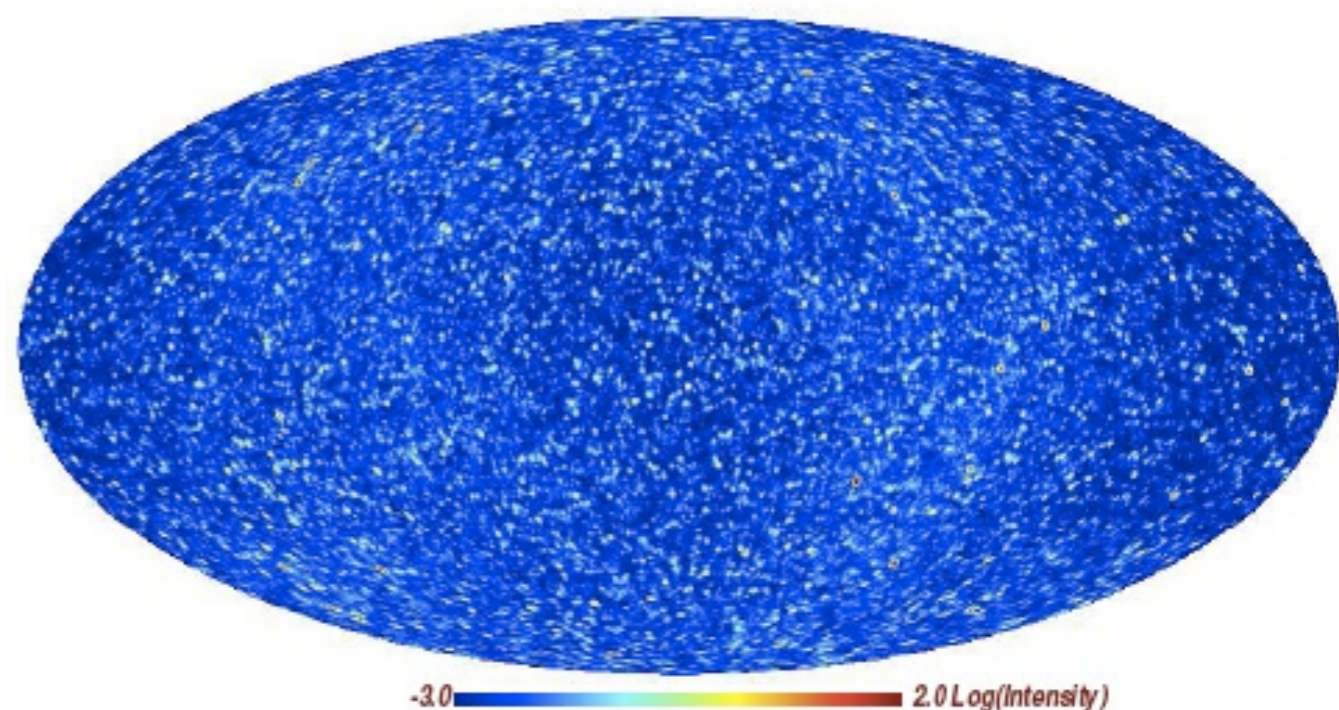
V. Springel et al. 2008 Nature 456, 73-76

Dark matter is the dominant form of matter in the universe, but its nature is unknown. It is plausibly an elementary particle, perhaps the lightest supersymmetric partner of known particle species¹. In this case, annihilation of dark matter in the halo of the Milky Way should produce γ -rays at a level which may soon be observable^{2,3}. Previous work has argued that the annihilation signal will be dominated by emission from very small clumps^{4,5} (perhaps smaller even than the Earth) which would be most easily detected where they cluster together in the dark matter halos of dwarf satellite galaxies⁶. Here we show, using the largest ever simulation of the formation of a galactic halo, that such small-scale structure will, in fact, have a negligible impact on dark matter detectability. Rather, the dominant and likely most easily detectable signal will be produced by diffuse dark matter in the main halo of the Milky Way^{7,8}. If the main halo is strongly detected, then small dark matter clumps should also be visible, but may well contain no stars, thereby confirming a key prediction of the Cold Dark Matter (CDM) model.

total emission



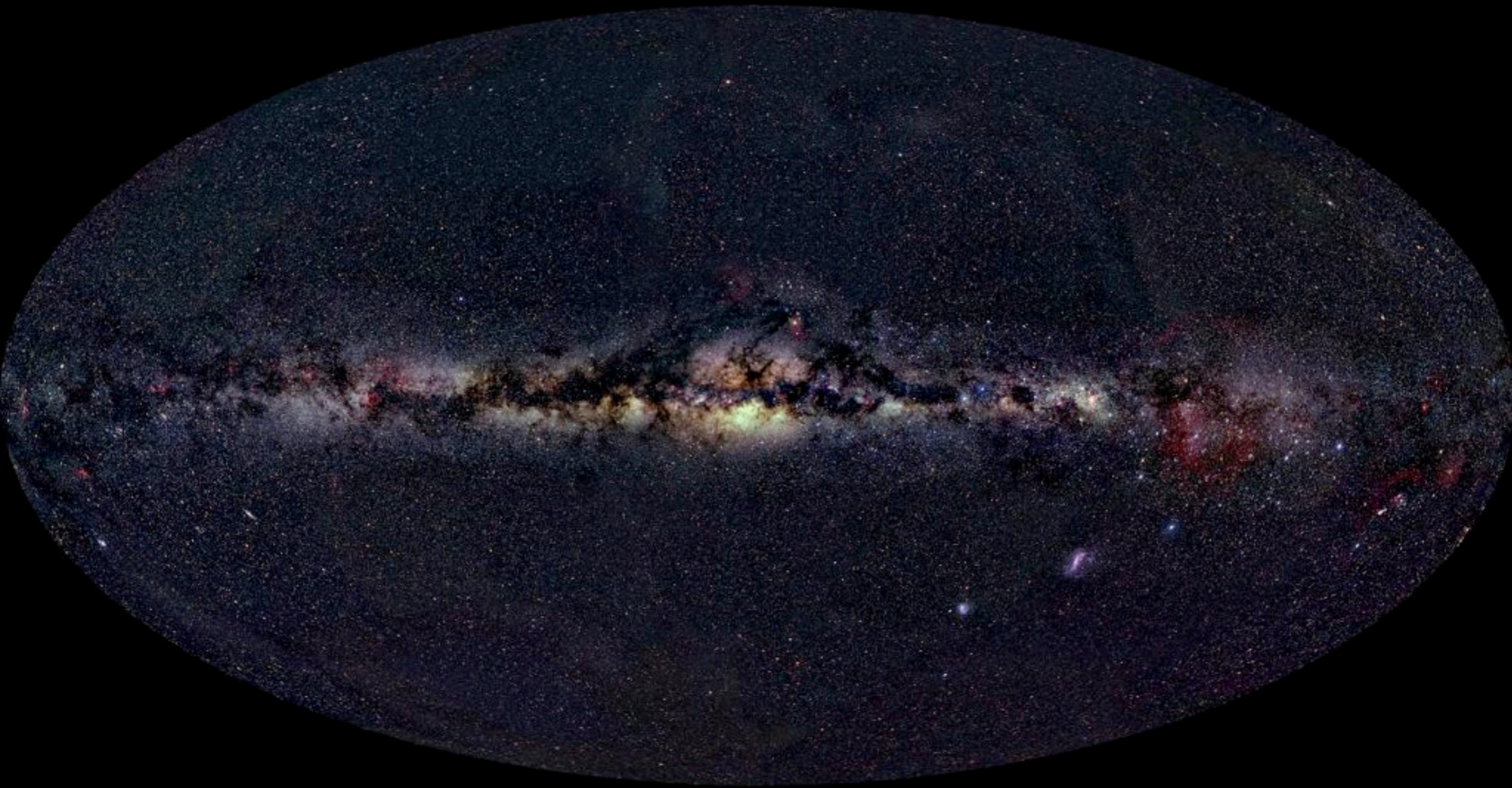
emission from resolved subhalos (SubSm+SubSub)



The background is a deep space image featuring a dense field of stars. A prominent spiral galaxy is visible, centered in the frame, with its bright core and swirling arms. The text is overlaid in a bold, red, italicized font, centered over the galaxy's core.

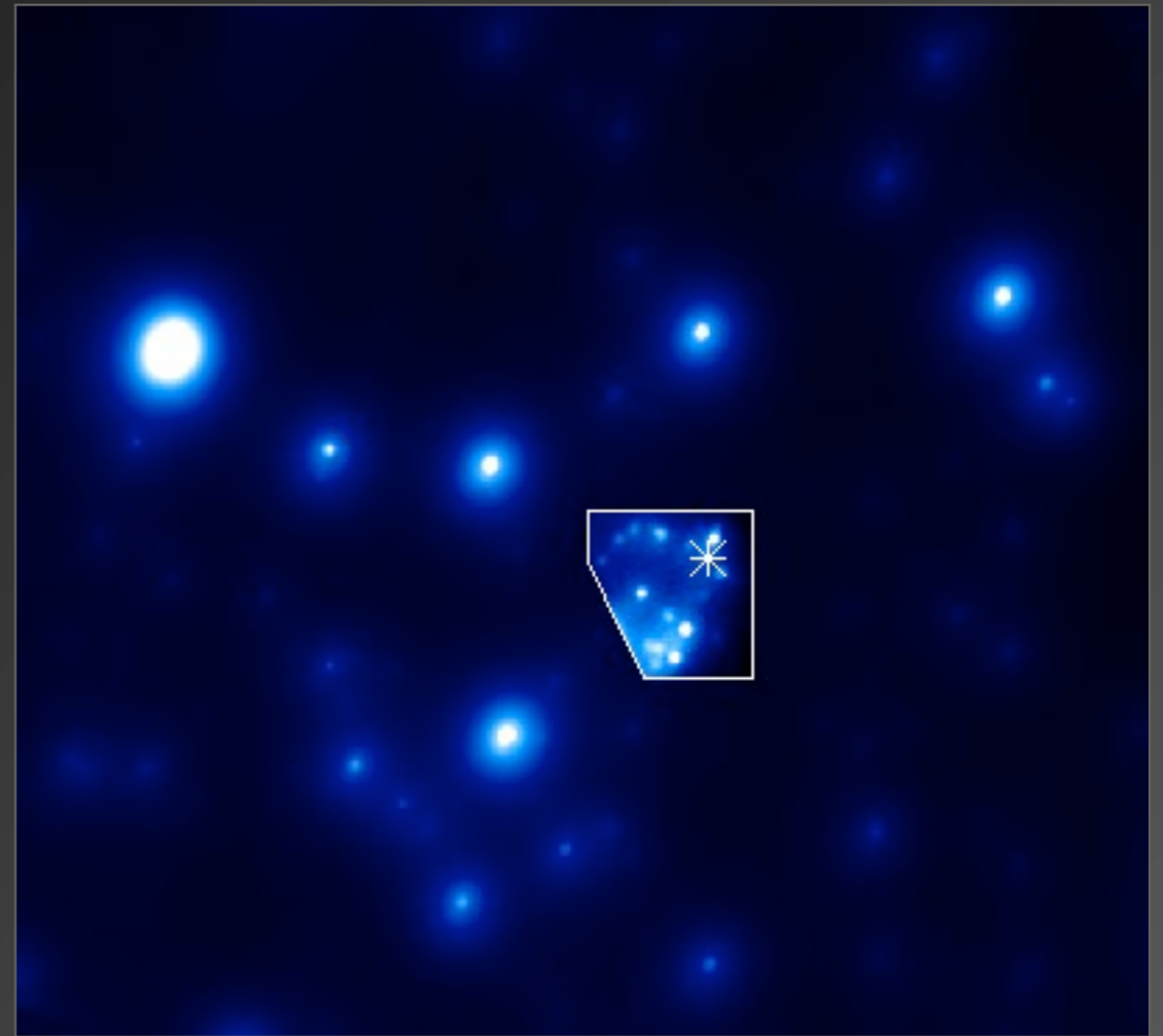
*DARK MATTER
ANNIHILATION AT
THE GALACTIC
CENTER?*

The Milky Way in the Sky



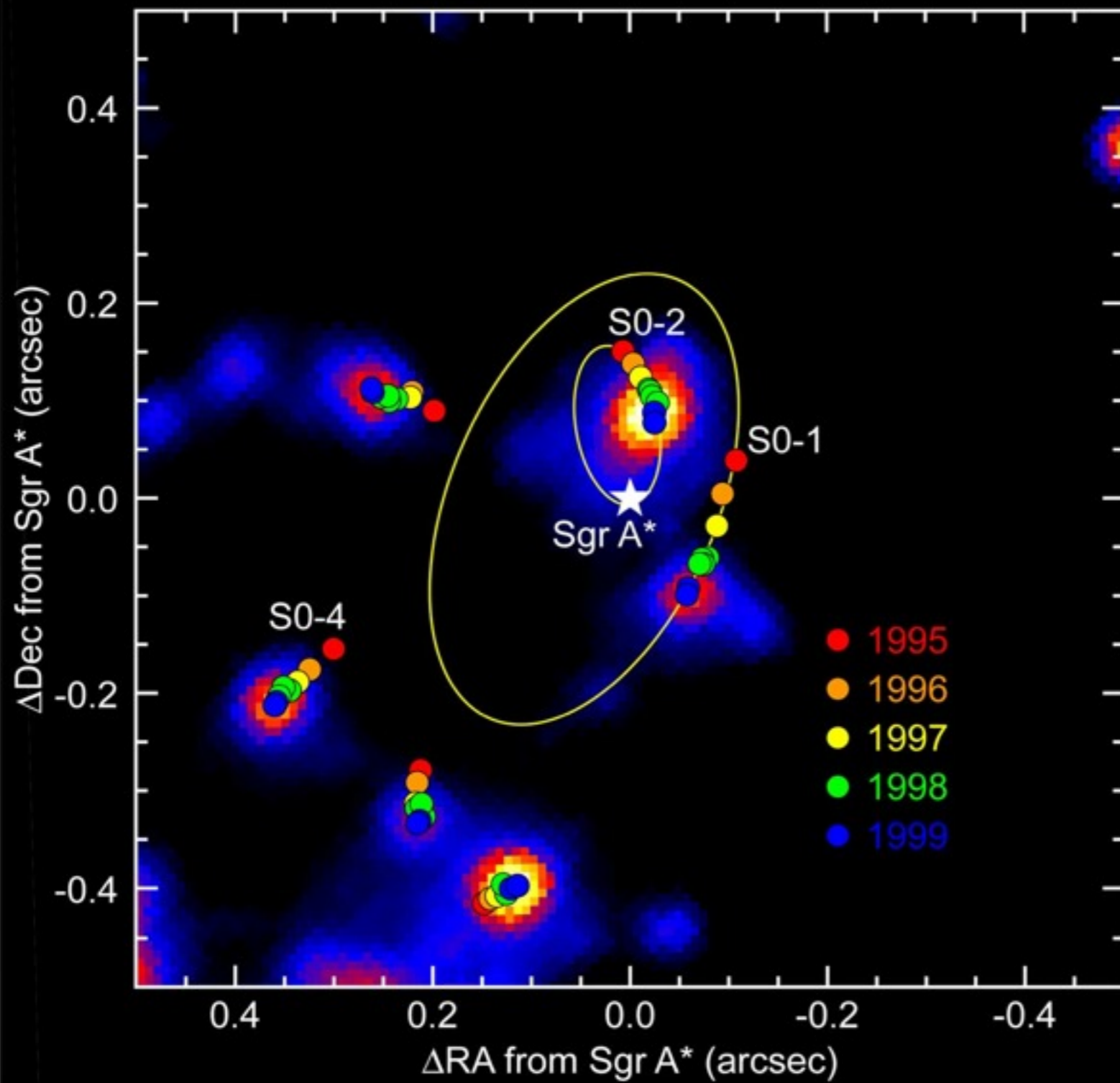
There's a supermassive black hole at the center of our galaxy...

- Modern large telescopes can track individual stars at galactic center
 - Need infrared (to penetrate dust).
 - Need very good resolution (use adaptive optics).
- and have been observing for past 10 years, with improving resolution...



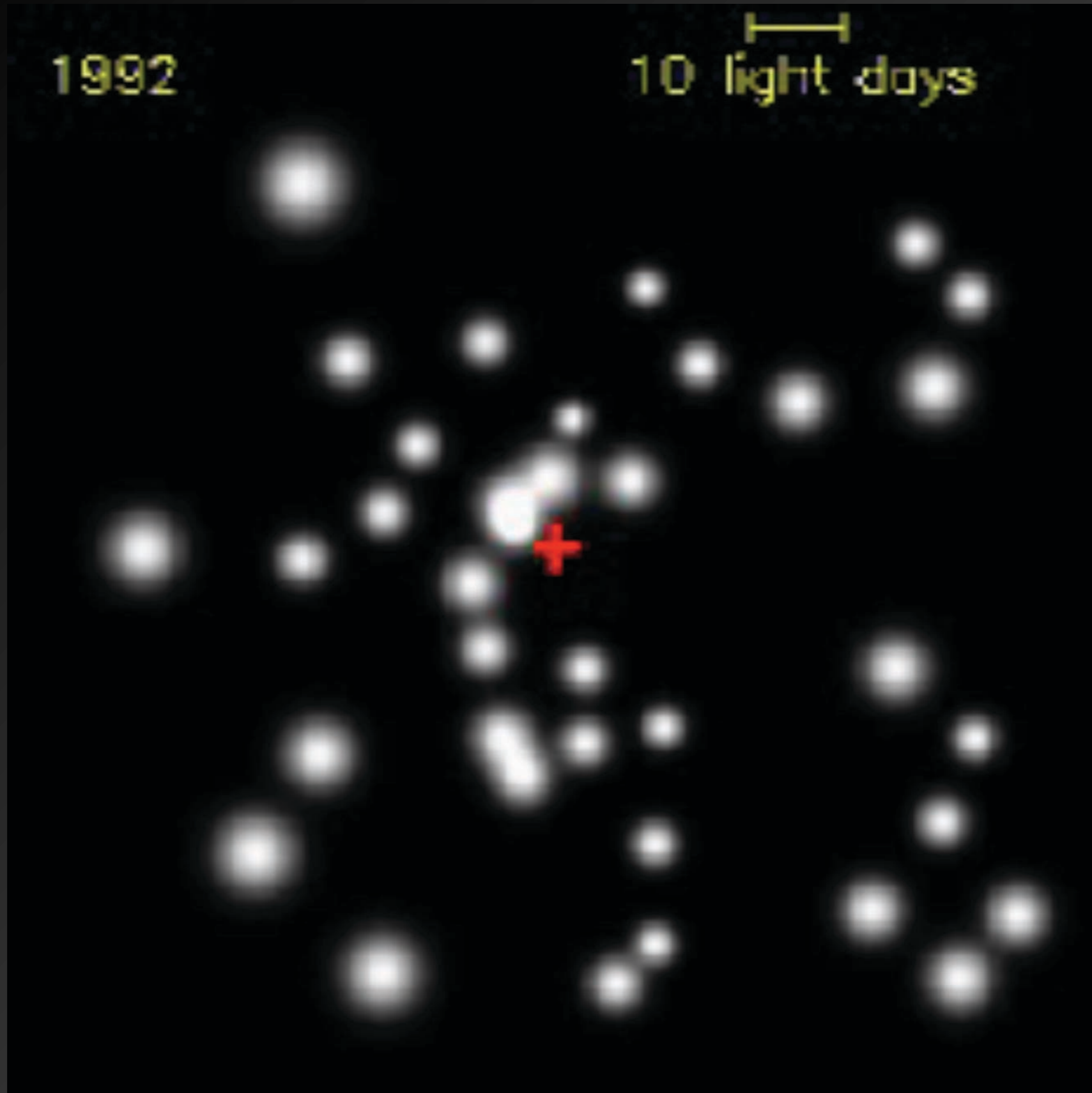
Keck, 2 μm

Ghez, et al.



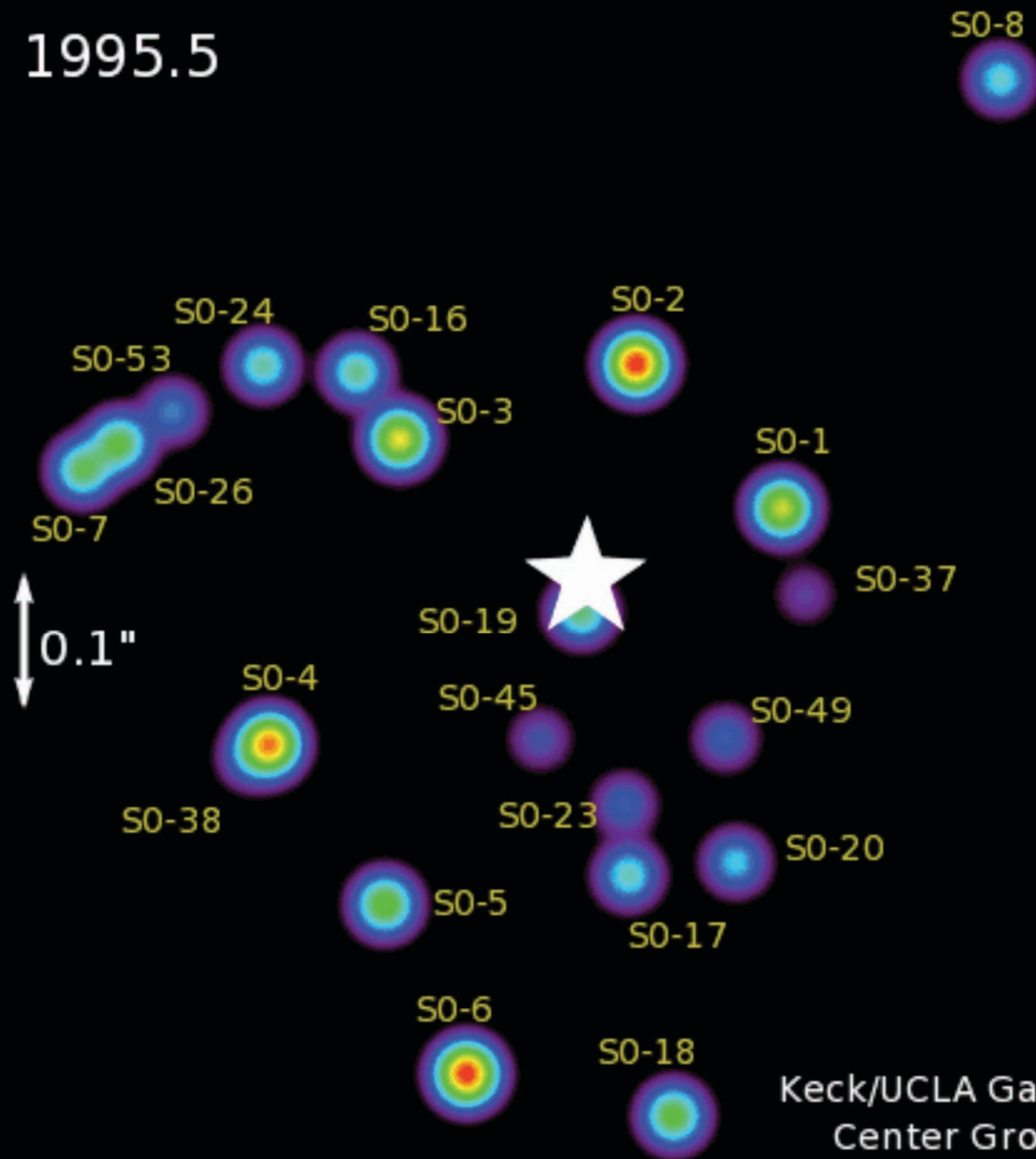
*Motions of stars
consistent with
large, dark mass
located at Sgr
A*...*

Ghez, et al.

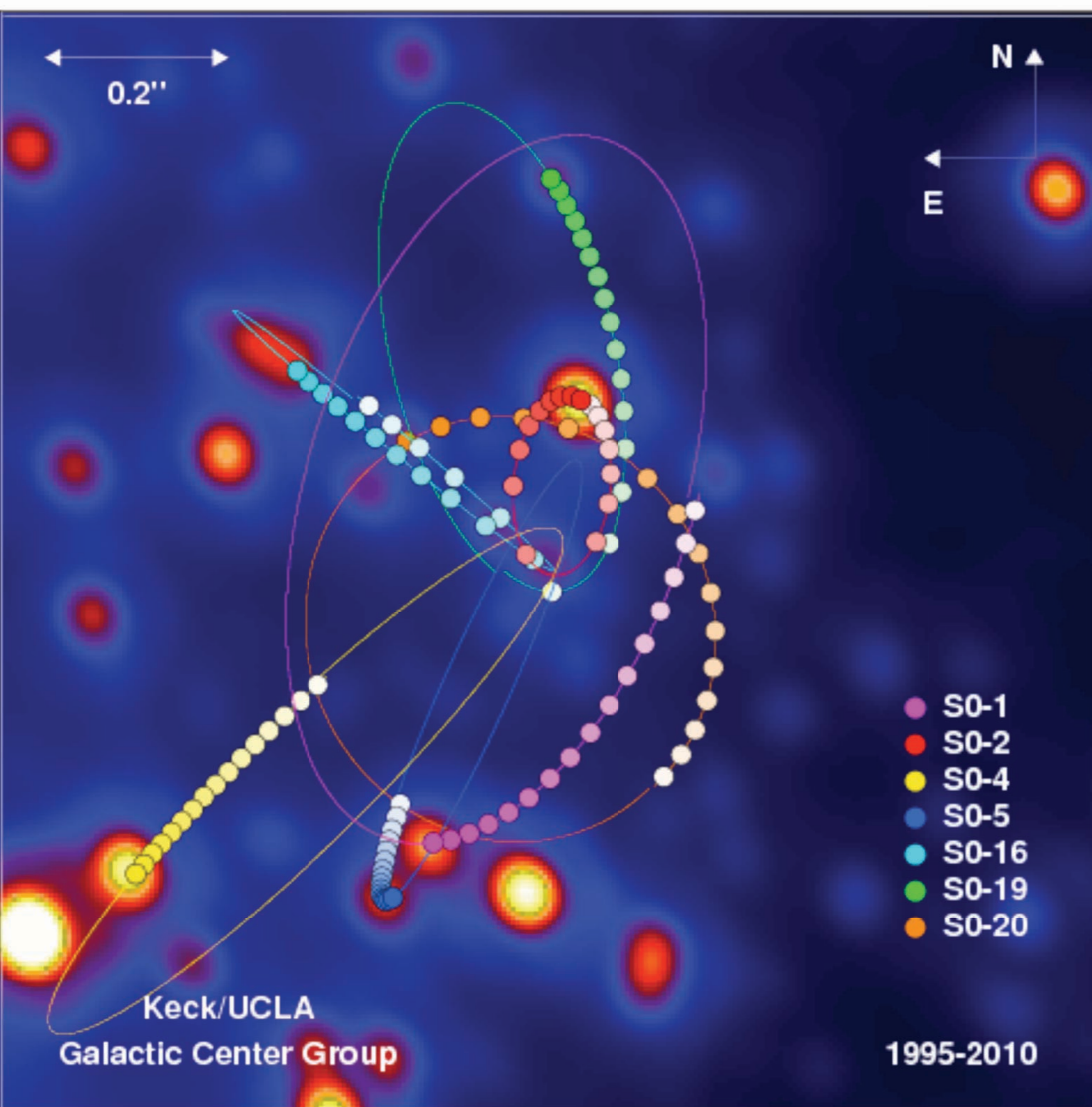


Schödel, Genzel, et al. 2004

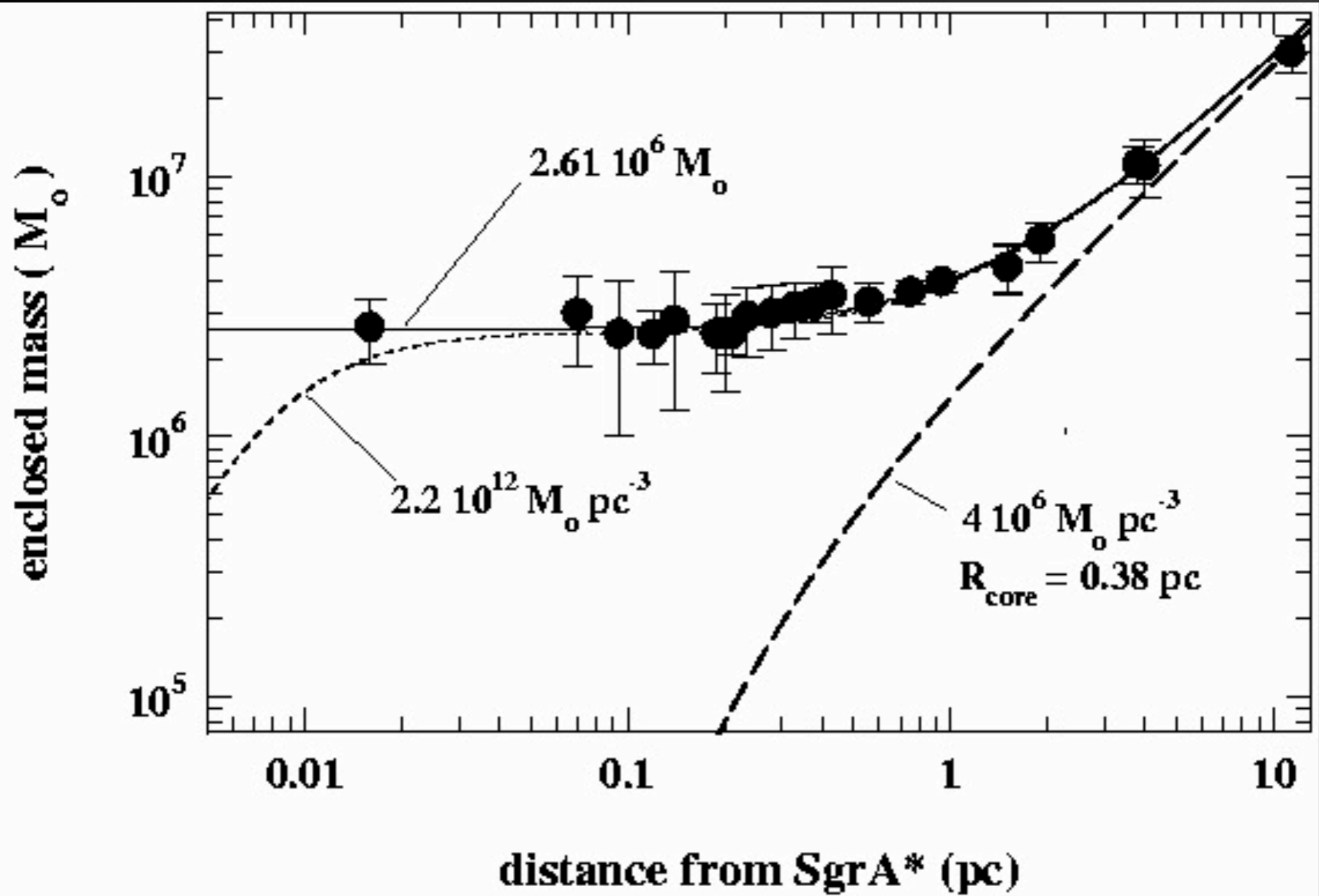
1995.5



Keck/UCLA Galactic
Center Group



A 2.2 micron animation of the stellar orbits in the central parsec. Images taken from the years 1995 through 2010 are used to track specific stars orbiting the proposed black hole at the center of the Galaxy. These orbits, and a simple application of Kepler's Laws, provide the best evidence yet for a supermassive black hole, which has a mass of 4 million times the mass of the Sun. Especially important are the stars S0-2, which has an orbital period of only 15.78 years, and S0-16, which comes a mere 90 astronomical units from the black hole.



Schödel et al. 2003

- The central object at the center of the Milky Way is...
 - Very dark – but now seen to flare in X-rays and IR.
 - Very massive (~3 million solar masses).
 - Must be very compact (star S0-2 gets within 17 light hours of the center).
- Currently the best case for any supermassive black hole.

γ rays from WIMP annihilation at the Galactic Center

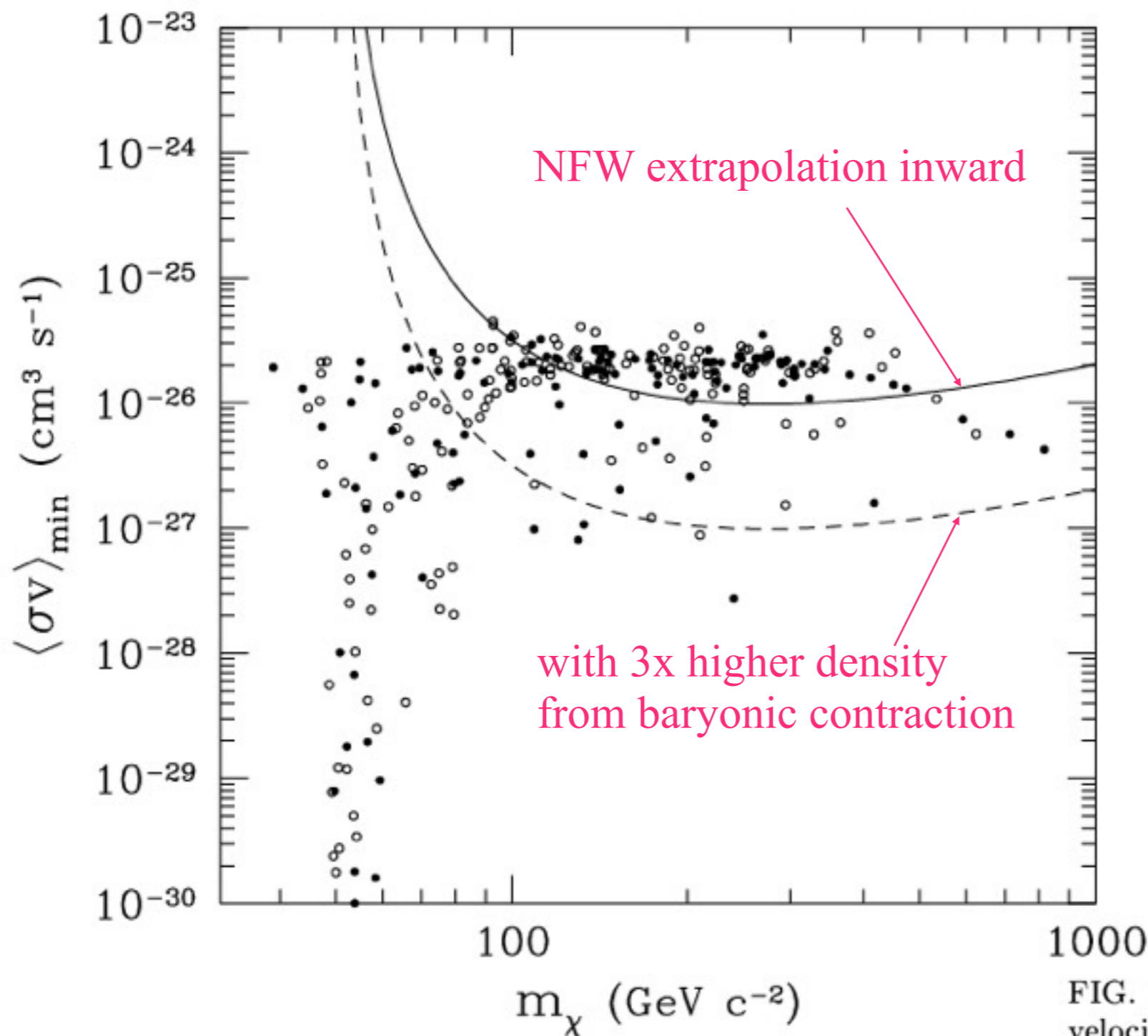


FIG. 1: Minimum detectable annihilation cross section times velocity as a function of WIMP mass. The filled circles correspond to SUSY model WIMPs with $\Omega_\chi h^2 = 0.11 \pm 0.01$ [32] and the open circles correspond to SUSY models with $\Omega_\chi h^2$ between 1σ and 2σ away from the central value.

Scattering of WIMPs by star cluster around central supermassive black hole predicts WIMP density

$$\rho(r) \propto r^{-3/2}$$

in central pc. The annihilation rate $\propto \rho^2$ so signal is modestly enhanced and centrally peaked.

Scattering off stars sets a universal profile.— The above considerations assumed that the phase-space density of dark matter particles is conserved. However, in addition to the supermassive black hole, the Galactic center harbors a compact cluster of stars, with density at least $\rho_* = 8 \times 10^8 M_\odot \text{pc}^{-3}$ in the inner 0.004 pc [18]. These stars frequently scatter dark matter particles and cause the distribution function to evolve towards an equilibrium solution. Both stars and dark matter experience two-body relaxation.

The idealized problem of a stellar distribution around a massive black hole in star clusters has been considered in the past (cf. [19] for a review). Stars driven inward towards the black hole by two-body relaxation try to reach thermal equilibrium with the stars in the core, but are unable to do so because of tidal disruption or capture by the black hole. Unlike core collapse in self-gravitating star clusters, however, the density of inner stars does not grow toward infinity. A steady-state solution is possible where the energy released by removal of the most bound stars is transported outward by diffusion. Because there is no special scale in the problem, the quasi-equilibrium distribution function is a power-law of energy, $f(E) \propto |E|^p$ and the density is a power-law of radius, $\rho \propto r^{-3/2-p}$ [20, 21]. The solution is unique and independent of the initial conditions.

The evolution of the dark matter distribution $f(E, t)$ in a two-component system of dark matter particles of mass m_χ and stars of mass m_* can be described by a collisional equation in the Fokker-Planck form:

$$\frac{\partial q}{\partial E} \frac{\partial f}{\partial t} = A \frac{\partial}{\partial E} \left[\frac{m_\chi}{m_*} f \int_E^\infty f_* \frac{\partial q_*}{\partial E_*} dE_* + \frac{\partial f}{\partial E} \left\{ \int_E^\infty f_* q_* dE_* + q \int_{-\infty}^E f_* dE_* \right\} \right],$$

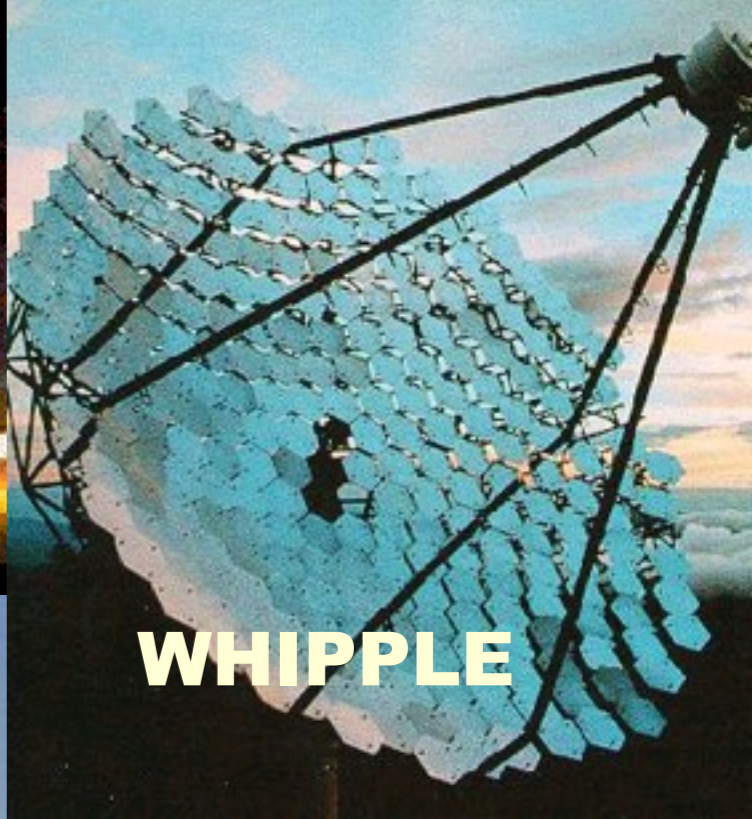
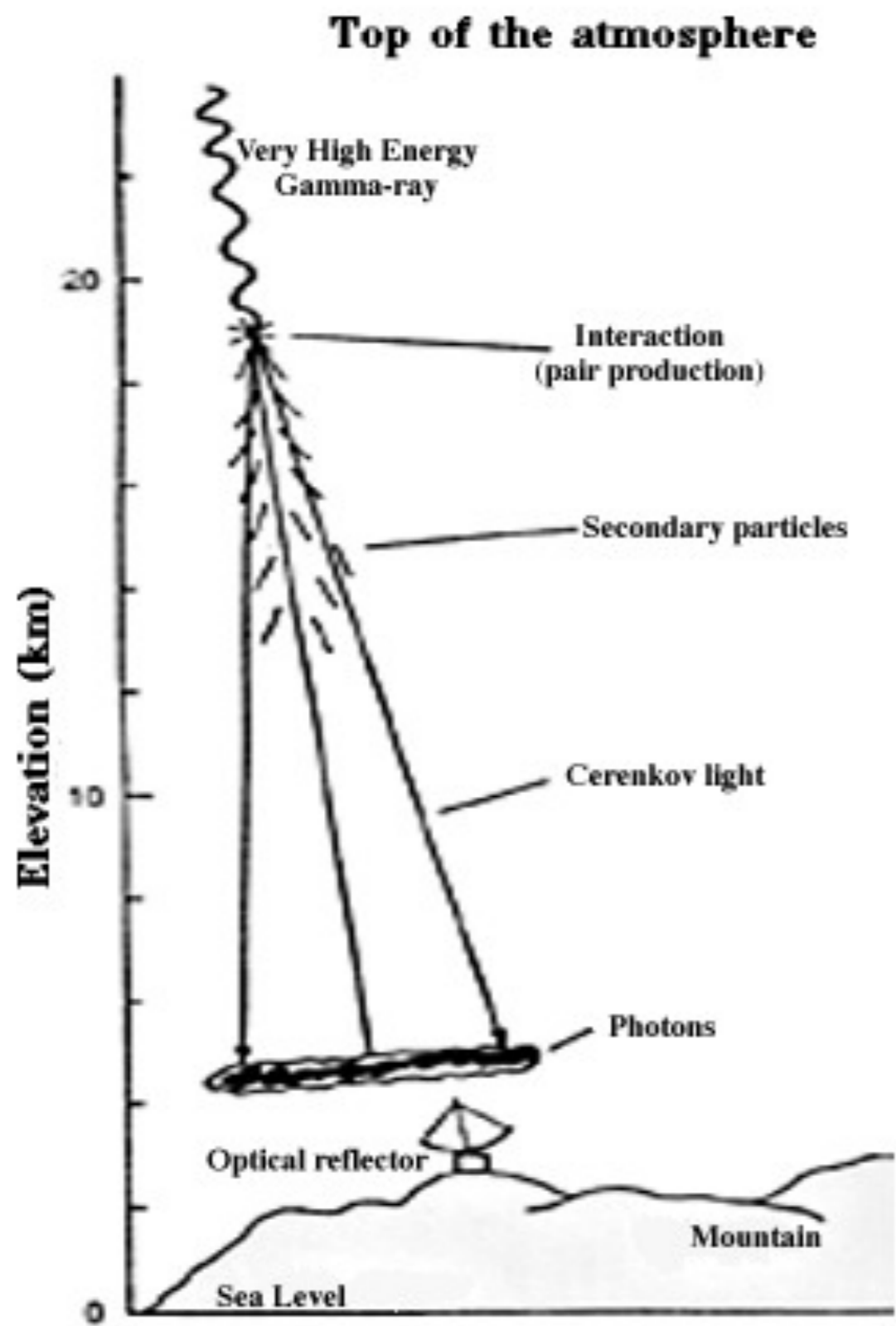
where $E = v^2/2 - GM_{\text{bh}}/r$ is the energy within the sphere of influence of the black hole, $q(E) = (2^{3/2}/3)\pi^3 G^3 M_{\text{bh}}^3 E^{-3/2}$, $A \equiv 16\pi^2 G^2 m_*^2 \ln \Lambda$, and $\ln \Lambda = \ln M_{\text{bh}}/m_* \approx 15$ is the standard Coulomb logarithm. The equilibrium distribution function of stars is $f_*(E_*, t) \propto |E_*|^{1/4}$, i.e. $p = 1/4$. For dark matter particles, however, the first term in the square brackets vanishes since the particle mass is negligible compared to stellar mass. An equilibrium solution with no energy flux requires $\partial f/\partial E = 0$, or $p = 0$. The corresponding density profile is $\rho_{\text{dm}} \propto r^{-3/2}$.

Implications for dark matter searches.— The dark matter density in the central region of the Galaxy is thus given by

$$\rho_{\text{dm}}(r) = \begin{cases} \rho_0 (r/r_{\text{bh}})^{-3/2} & L < r \leq r_{\text{bh}} , \\ \rho_0 (r/r_{\text{bh}})^{-\alpha} & r_{\text{bh}} \leq r , \end{cases}$$

where $L \approx 10^{-3}$ pc, and we expect that $0 < \alpha < 1.5$.

Early Atmospheric Čerenkov Telescopes



New Ground and Space Based Telescopes

High Energy Stereoscopic System

H.E.S.S.



CANGAROO III



VERITAS



MAGIC

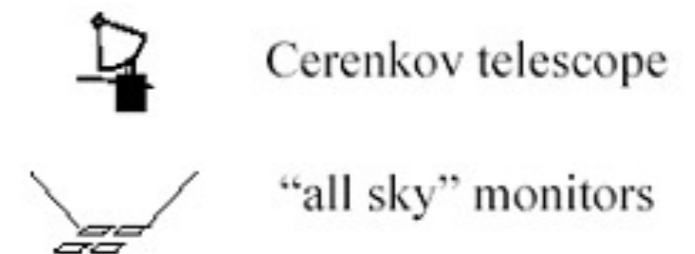
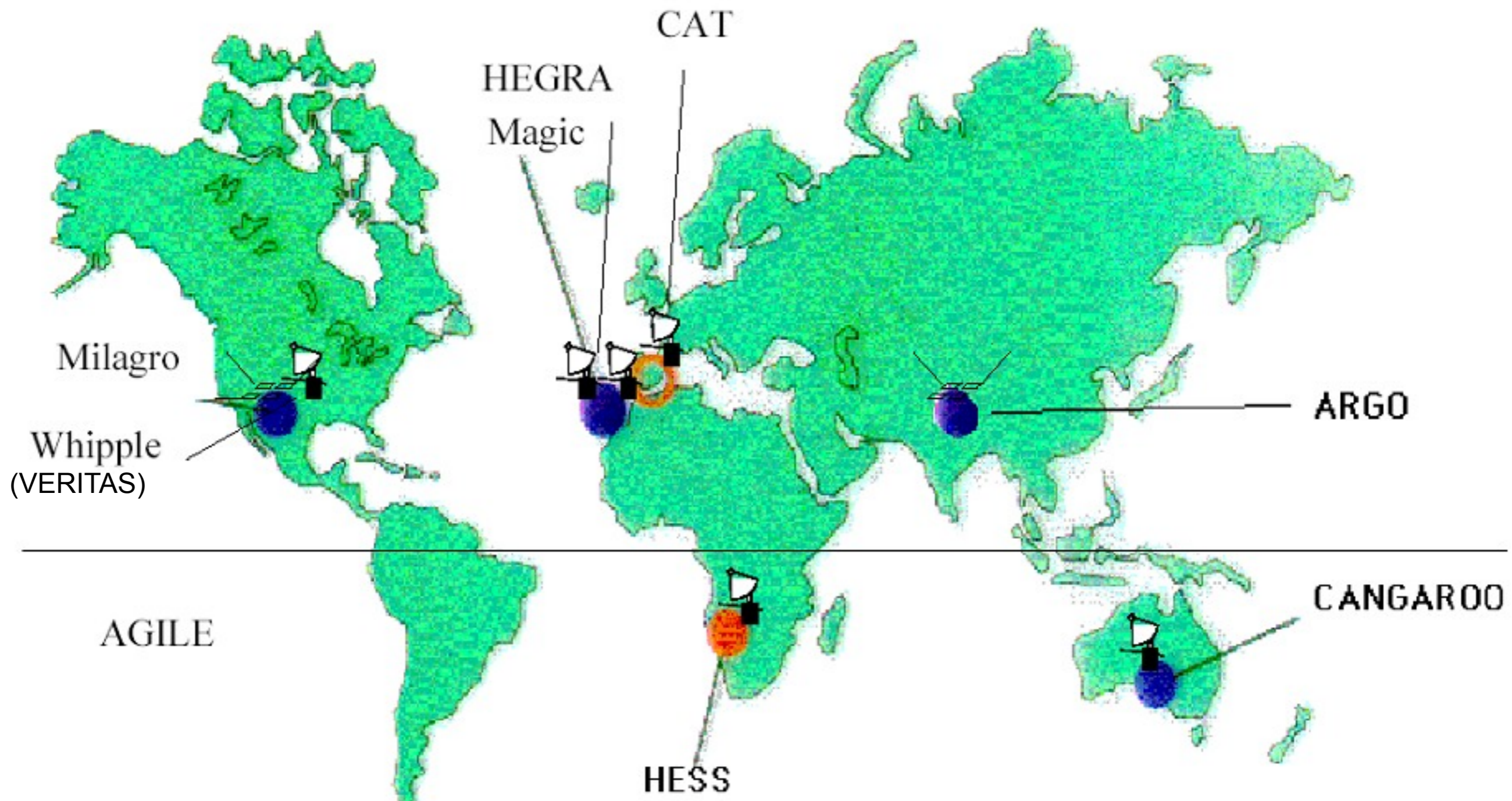


GLAST

Exploring Nature's Highest Energy Processes with the Gamma-ray Large Area Space Telescope



Ground-based Gamma Ray Telescopes 2



Results from H.E.S.S. on MWy Center

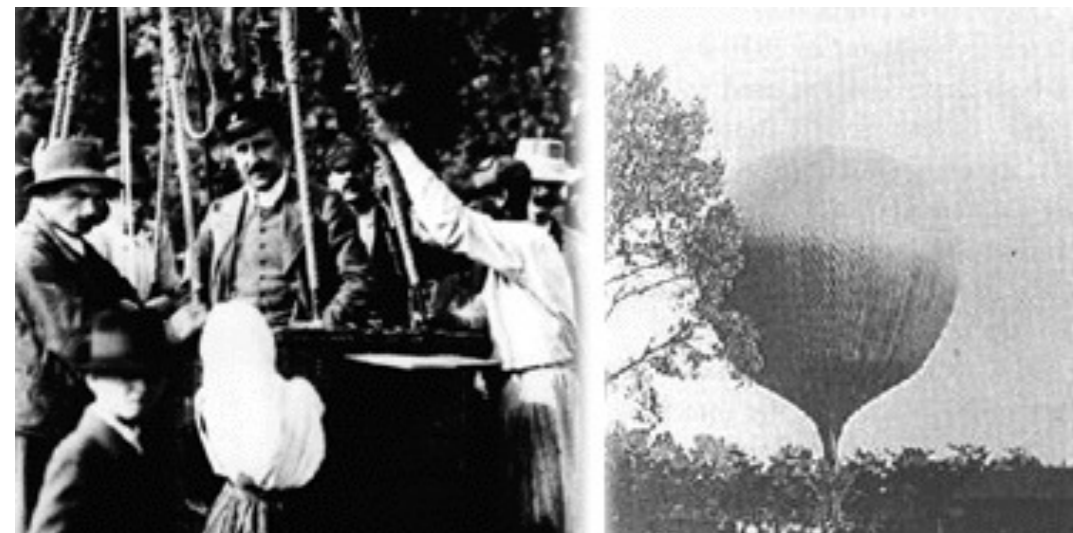
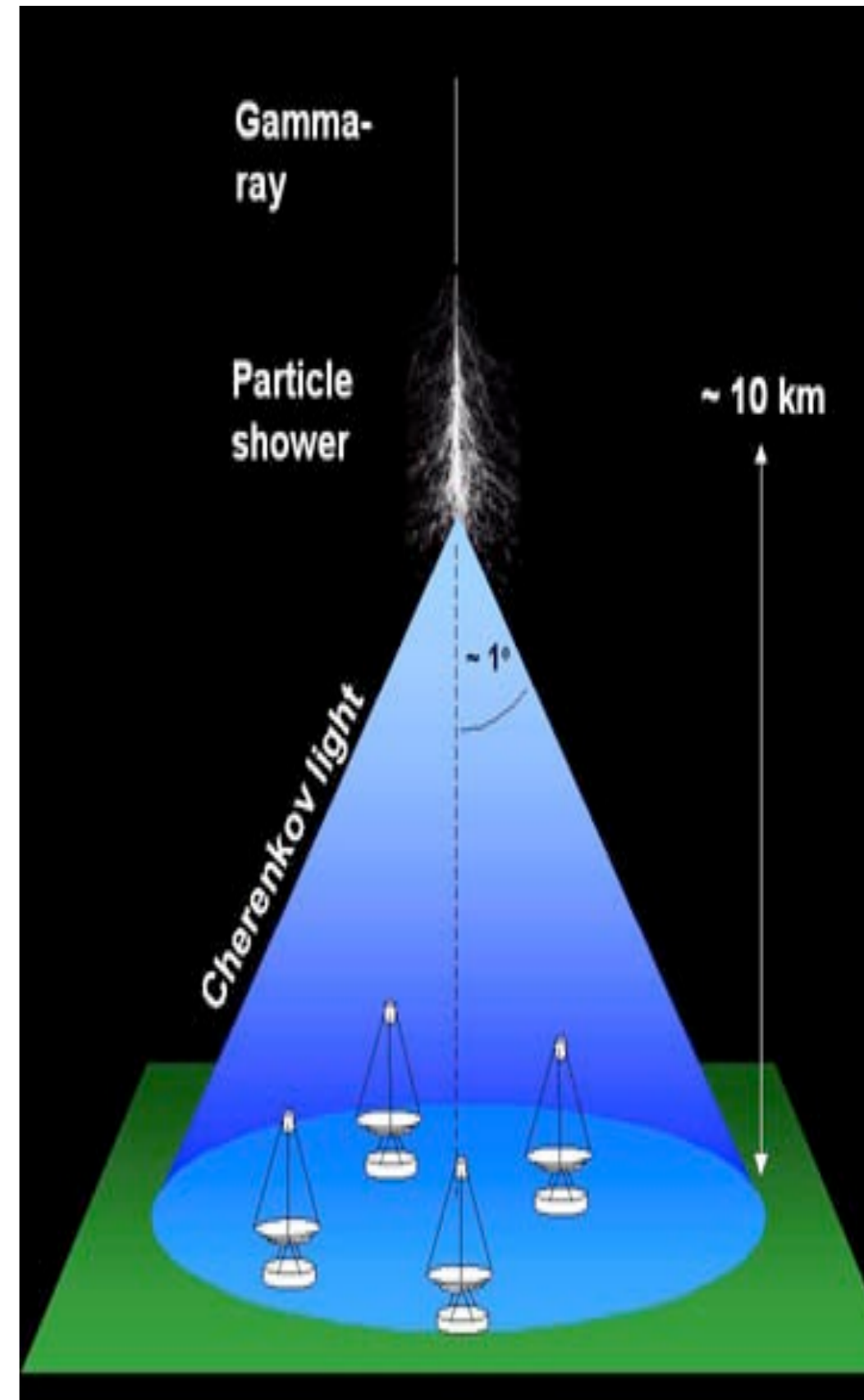


H.E.S.S.: High Energy Stereoscopic System

- Array 4 telescopes, diameter ~ 12 m
- Field of view $\sim 5^\circ$
- Angular resolution (single photon): $\sim 6'$
(with hard cuts): $\sim 4'$
- Energy resolution $\sim 15\%$
- Location: Namibia, 1800 m asl
Coord.: $23^\circ 16' S$, $16^\circ 30' E$

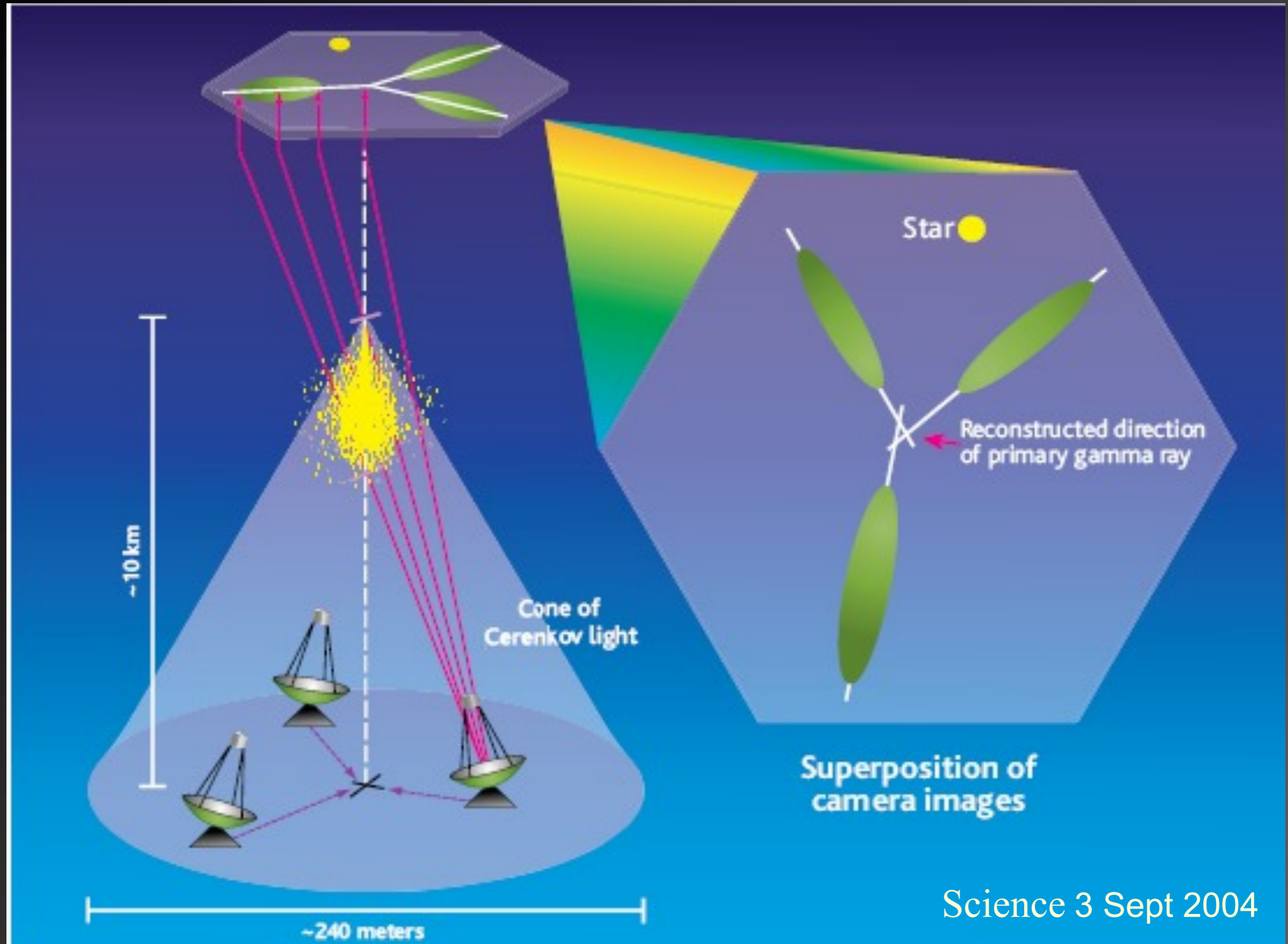
Energy Threshold (pre - post cuts):

0° :	(105 GeV, 125 GeV)
20° :	(115 GeV, 145 GeV)
45° :	(265 GeV, 305 GeV)
60° :	(785 GeV, 925 GeV)



Victor Hess
1912 balloon
flight to 6 km:
"cosmic ray"
intensity
increased with
altitude

H.E.S.S.: High Energy Stereoscopic System



Very high energy gamma rays from the direction of Sagittarius A*

F. Aharonian¹, A.G. Akhperjanian¹, K.-M. Aye², A.R. Bazer-Bachi³, M. Beilicke⁴, W. Benbow¹, D. Berge¹, P. Berghaus⁵, K. Bemböhr^{1,6}, O. Bolz¹, C. Boisson⁷, C. Borgmeier⁶, F. Breitling⁶, A.M. Brown², J. Bussons Gordo⁸, P.M. Chadwick², V.R. Chitnis⁹ *, L.-M. Chounet¹⁰, R. Cornils⁴, L. Costamante¹, B. Degrange¹⁰, A. Djannati-Atai⁵, L.O'C. Drury¹¹, T. Ergin⁶, P. Espigat⁵, F. Feinstein⁸, P. Fleury¹⁰, G. Fontaine¹⁰, S. Funk¹, Y. Gallant⁸, B. Giebels¹⁰, S. Gillessen¹, P. Goret¹², J. Guy⁹, C. Hadjichristidis², M. Hauser¹³, G. Heinzlmann⁴, G. Henri¹⁵, G. Hermann¹, J. Hinton¹, W. Hofmann¹, M. Holleran¹⁴, D. Horns¹, O.C. de Jager¹⁴, I. Jung^{1,13}, B. Khélifi¹, Nu. Komin⁶, A. Konopelko^{1,6}, I.J. Latham², R. Le Gallou², M. Lemoine¹⁰, A. Lemièrè⁵, N. Leroy¹⁰, T. Lohse⁶, A. Marcowith³, C. Masterson¹, T.J.L. McComb², M. de Naurois⁹, S.J. Nolan², A. Noutsos², K.J. Orford², J.L. Osborne², M. Ouchrif⁹, M. Panter¹, G. Pelletier¹⁵, S. Pita⁵, M. Pohl^{16**}, G. Pühlhofer^{1,13}, M. Punch⁵, B.C. Raubenheimer¹⁴, M. Raue⁴, J. Raux⁹, S.M. Rayner², I. Redondo^{10***}, A. Reimer¹⁶, O. Reimer¹⁶, J. Ripken⁴, M. Rivoal⁹, L. Rob¹⁷, L. Rolland⁹, G. Rowell¹, V. Sahakian¹⁸, L. Sauge¹⁵, S. Schlenker⁶, R. Schlickeiser¹⁶, C. Schuster¹⁶, U. Schwanke⁶, M. Siewert¹⁶, H. Sol⁷, R. Steenkamp¹⁹, C. Stegmann⁶, J.-P. Tavernet⁹, C.G. Théoret⁵, M. Tluczykont¹⁰, D.J. van der Walt¹⁴, G. Vasileiadis⁸, P. Vincent⁹, B. Visser¹⁴, H. Völk¹, and S.J. Wagner¹³

A&A Letters, **425L**, 13 (October 2004)

Abstract.

We report the detection of a point-like source of very high energy (VHE) γ -rays coincident within $1'$ of Sgr A*, obtained with the H.E.S.S. array of Cherenkov telescopes. The γ -rays exhibit a power-law energy spectrum with a spectral index of $-2.2 \pm 0.09 \pm 0.15$ and a flux above the 165 GeV threshold of $(1.82 \pm 0.22) \cdot 10^{-7} \text{ m}^{-2} \text{ s}^{-1}$. The measured flux and spectrum differ substantially from recent results reported by the CANGAROO and Whipple collaborations, which could be interpreted as time variability of the source.

See also Dieter Horns' talk at Gamma2004, astro-ph/0408192, Phys Lett B;
and HESS contributions to ICRC29 (2005) by Hinton, Ripkin, Rolland

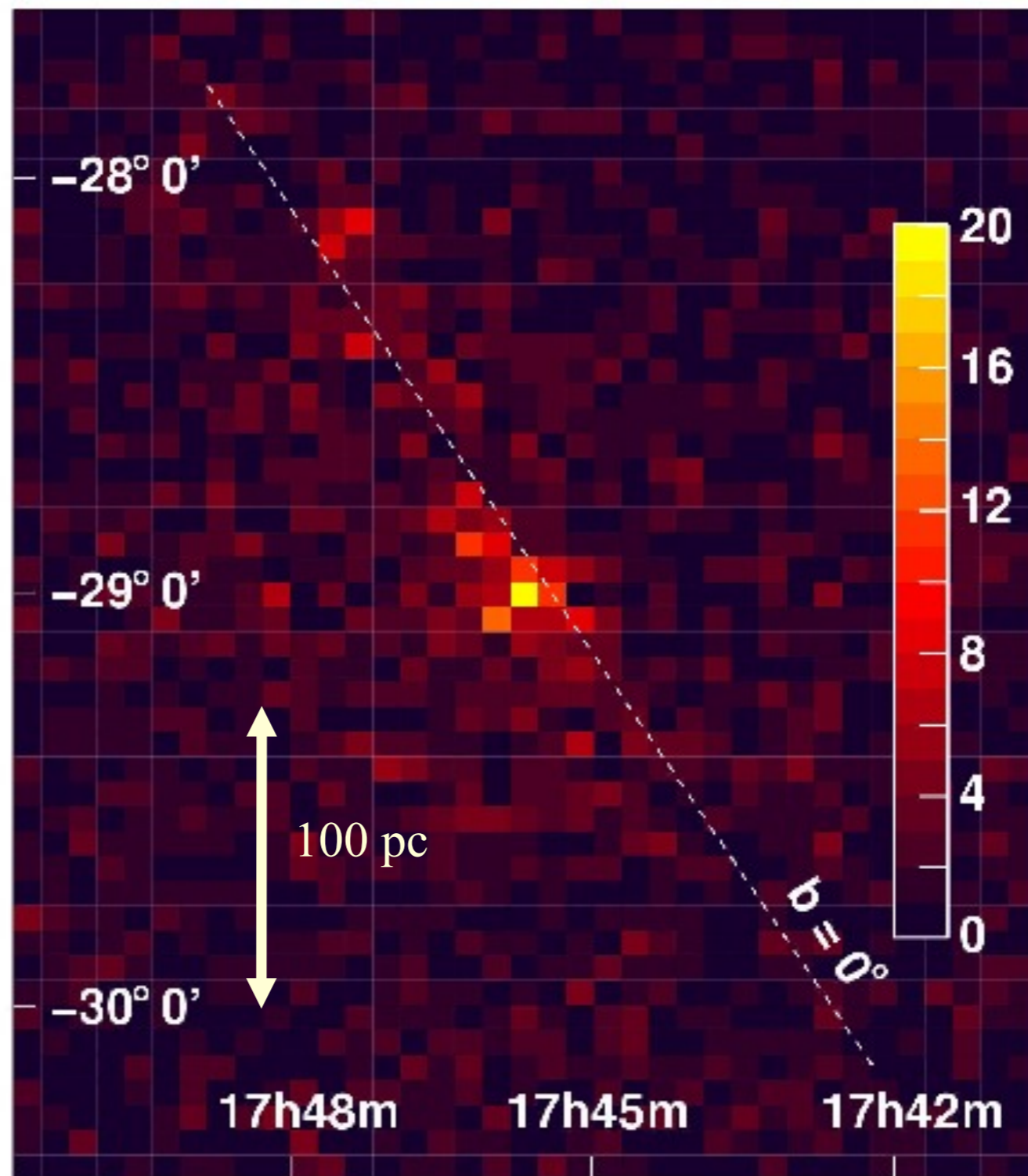


Fig. 1. Angular distribution of γ -ray candidates for a 3° field of view centred on Sgr A*. Both data sets ('June/July' and 'July/August') are combined, employing tight cuts to reduce the level of background. The significance of the feature extending along the Galactic Plane is under investigation.

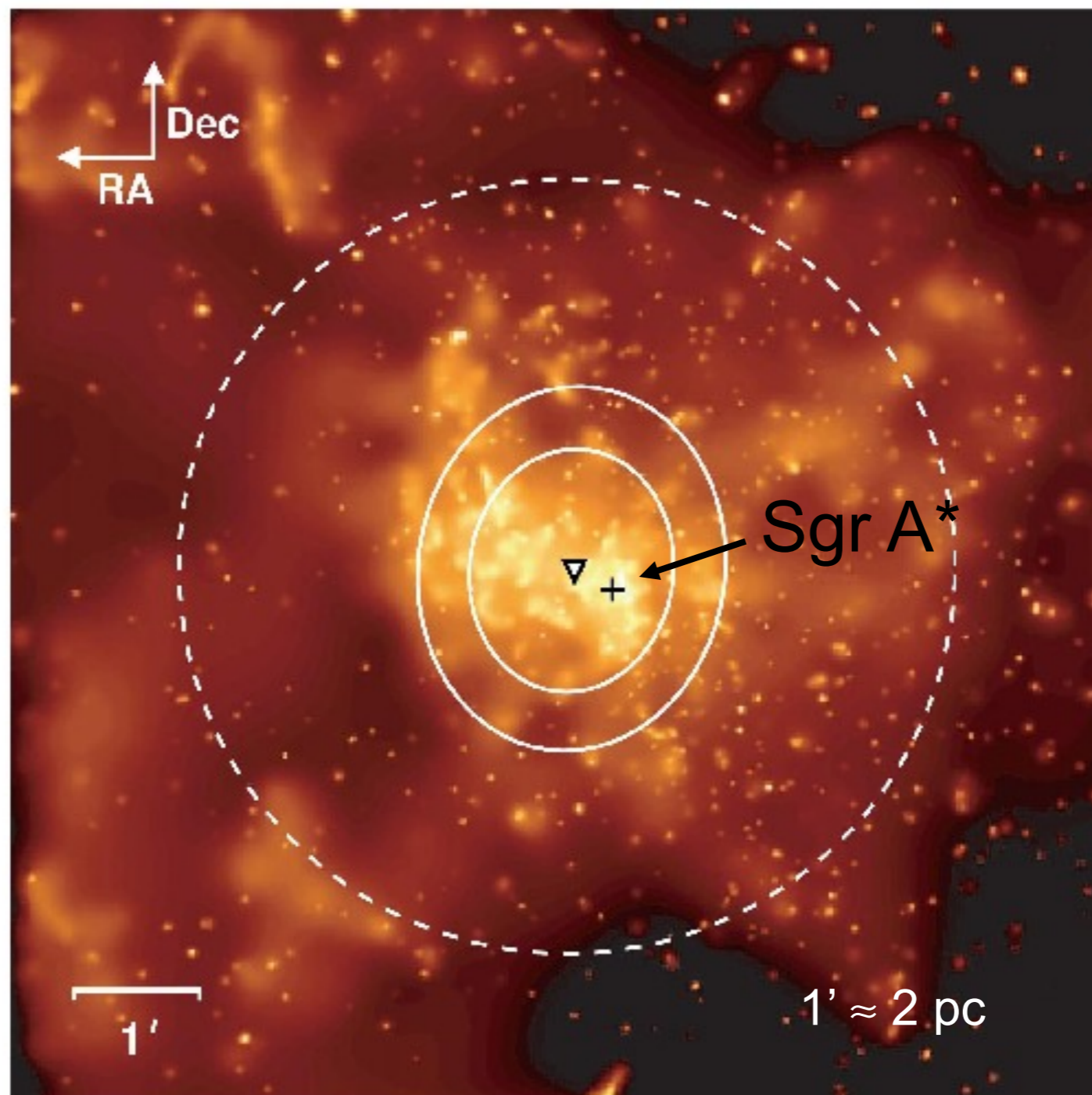
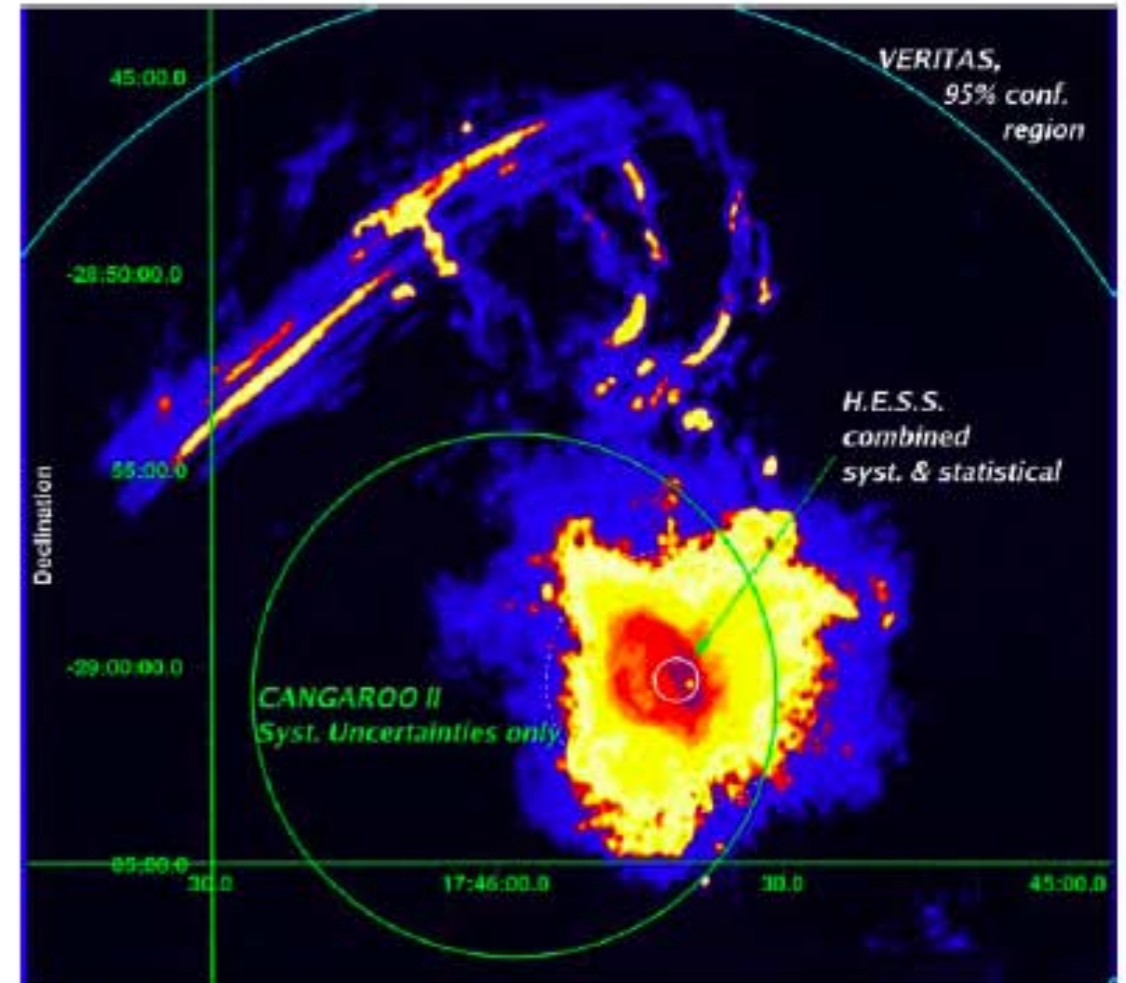
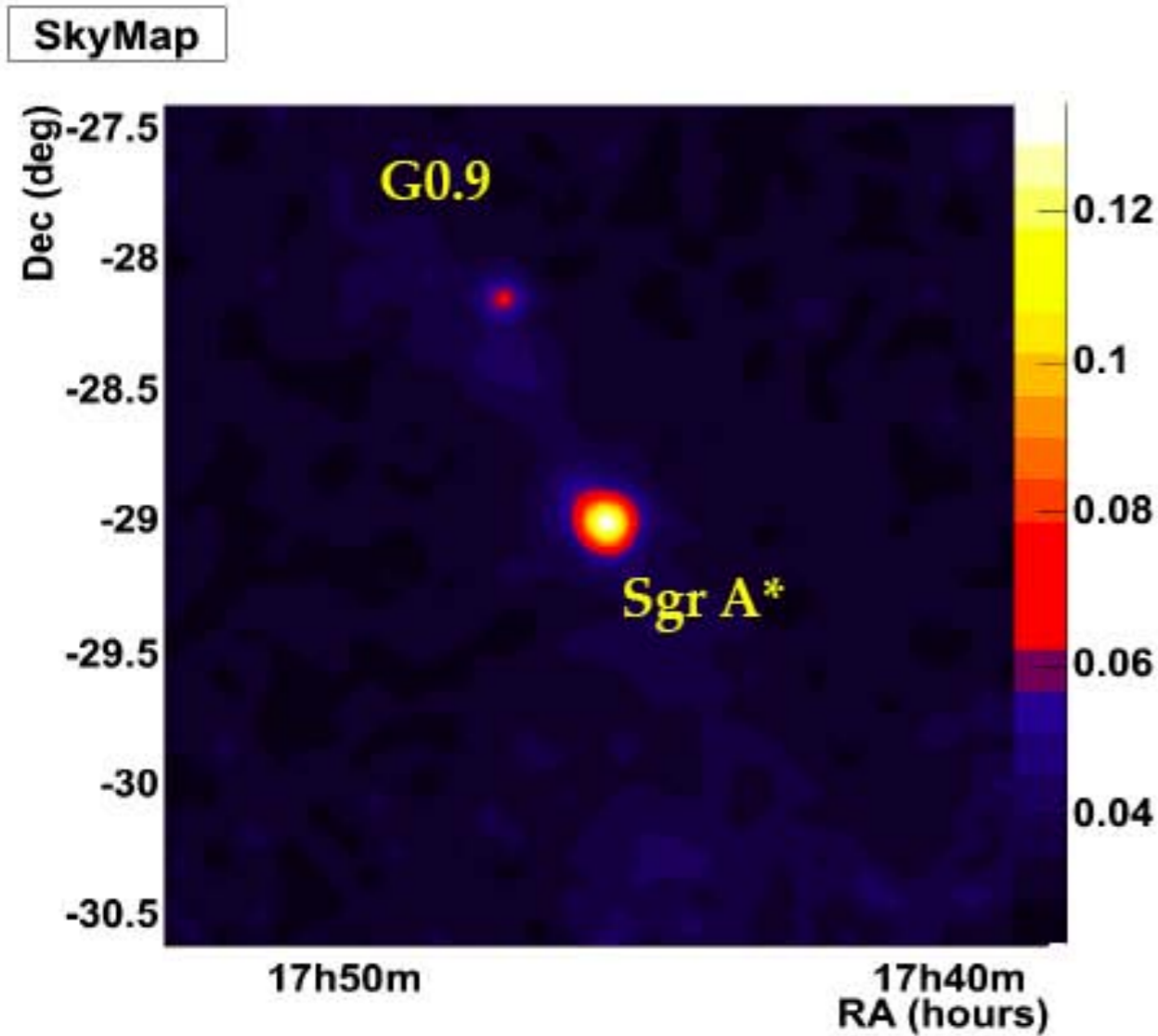
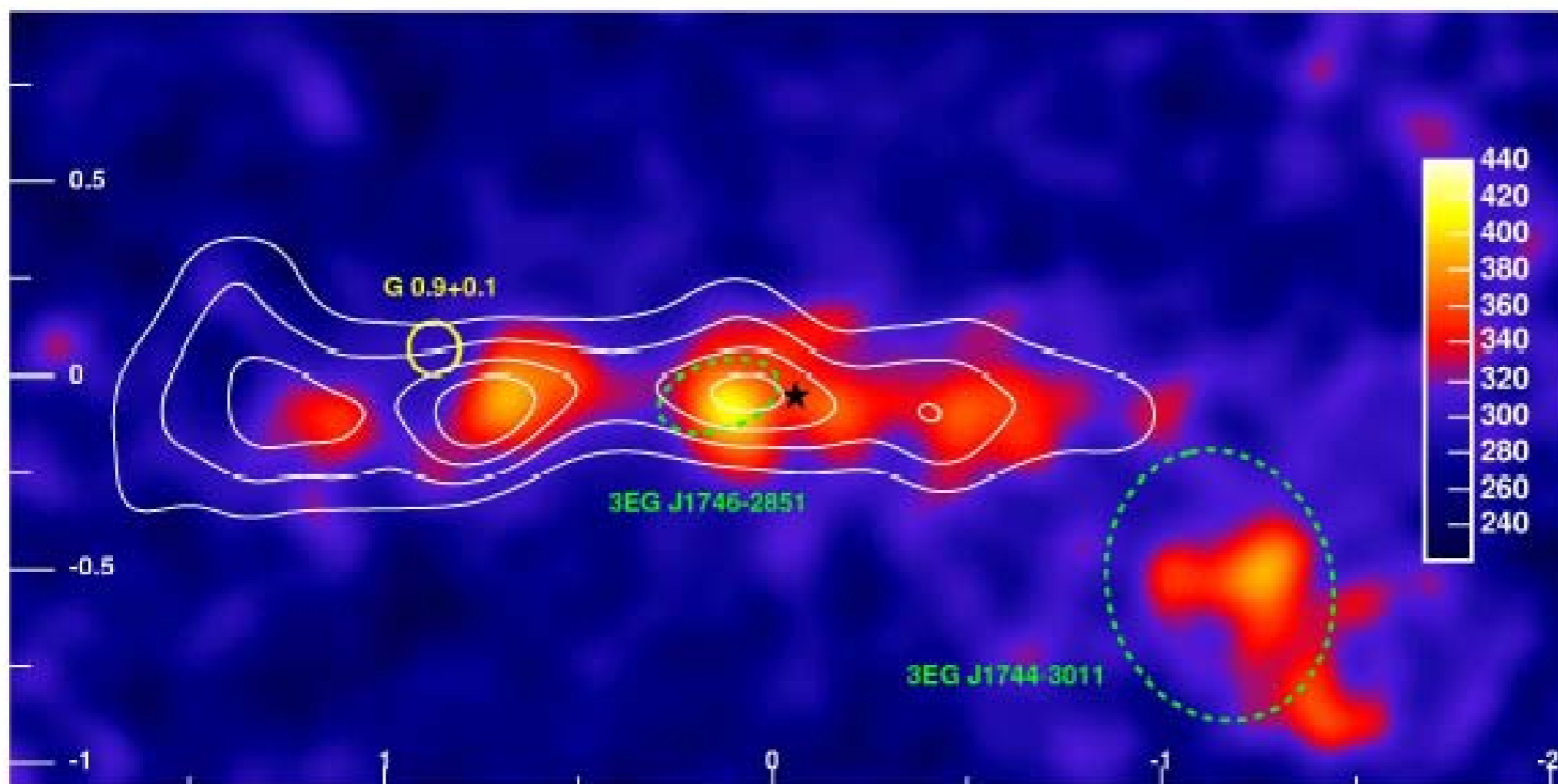
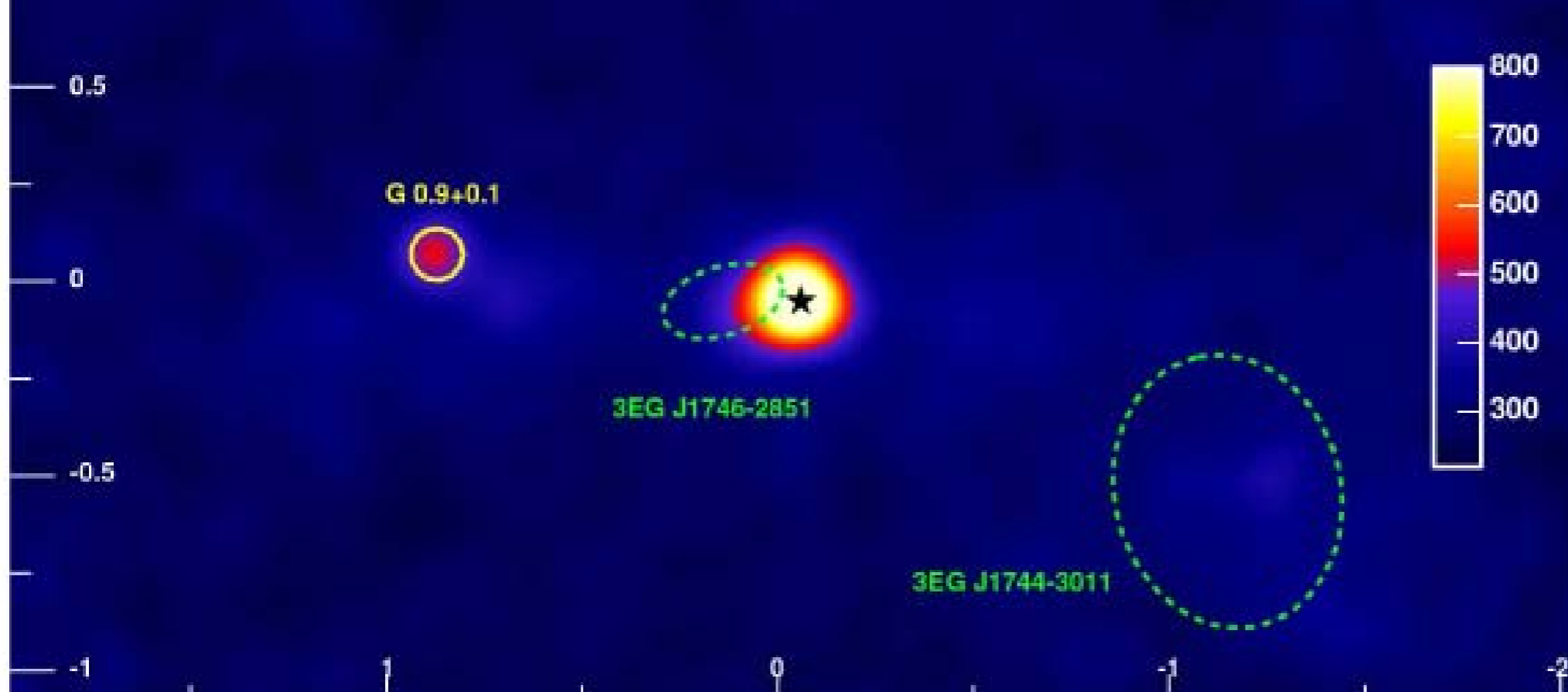


Fig. 2. Centre of gravity of the VHE signal (triangle), superimposed on a 8.5' by 8.5' Chandra X-ray map (Munro et al. 2003) of the GC. The location of Sgr A* is indicated by a cross. The contour lines indicate the 68% and 95% confidence regions for the source position, taking into account systematic pointing errors of 20". The white dashed line gives the 95% confidence level upper limit on the rms source size. The resolution for individual VHE photons - as opposed to the precision for the centre of the VHE signal - is 5.8' (50% containment radius).

Felix Aharonian's talk at Texas @ Stanford December 2004



it extended source - size less than 3' (7 pc)
if point-like source – position within 1' around Sgr A*



Discovery of Very-High-Energy Gamma-Rays from the Galactic Centre Ridge

Authors: The H.E.S.S.

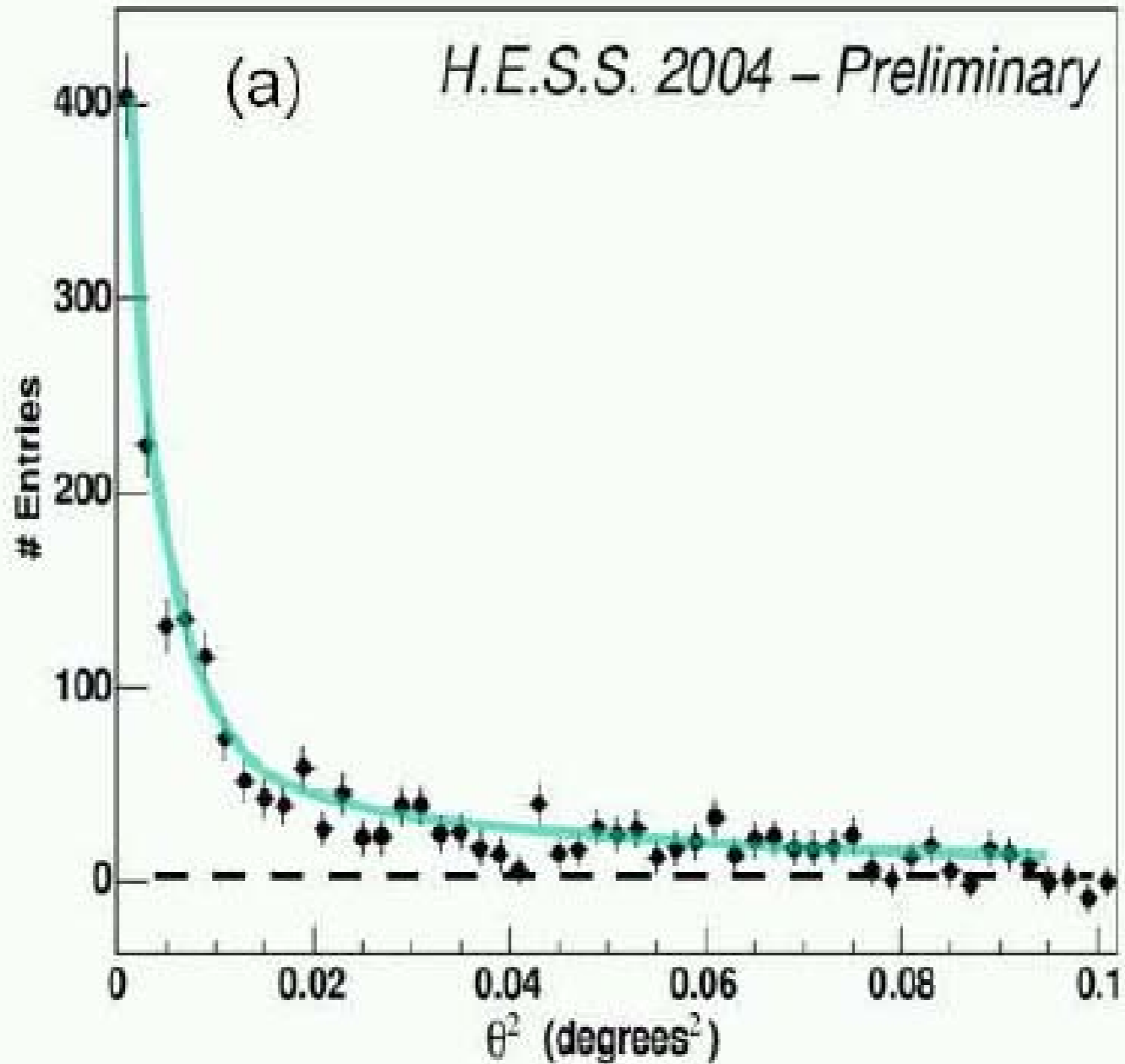
Collaboration: F. A. Aharonian, et al Nature

Journal-ref: Nature 439 (2006) 695

Felix Aharonian's talk at Texas @ Stanford

TeV Gamma-rays from central <10 pc region of GC

- Annihilation of DM ? *mass of DM particles > 12 TeV ?*
- Sgr A* : $3 \cdot 10^6 M_{\odot}$ BH ? *somewhat speculative but possible*
- SNR Sgr A East ? *why not ?*
- Plerionic (IC) source(s) *why not ?*
- Interaction of CRs with dense molecular gas (clouds) ? *easily*

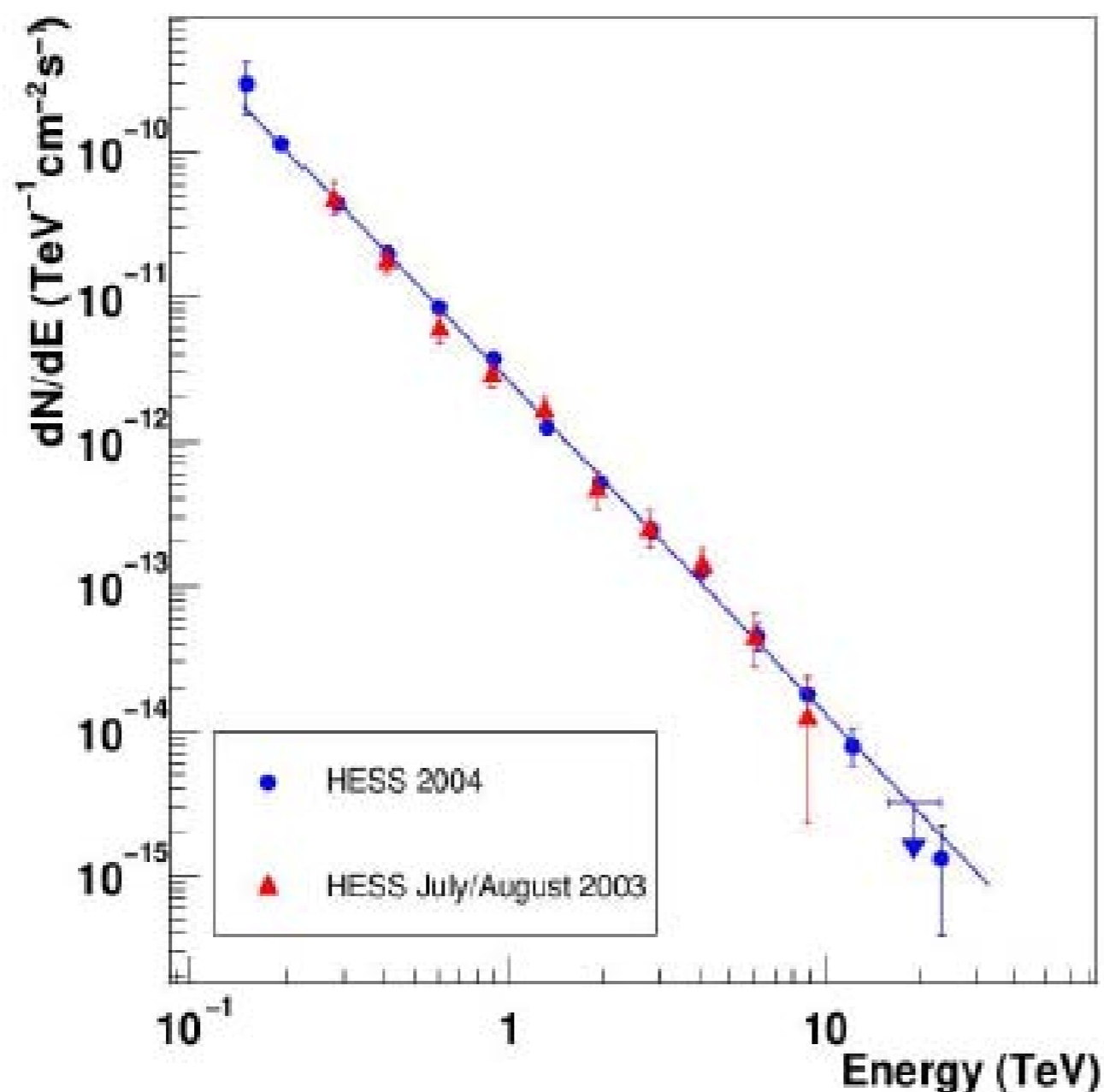


Angular distribution of the gamma-ray emission from the Sgr A source.

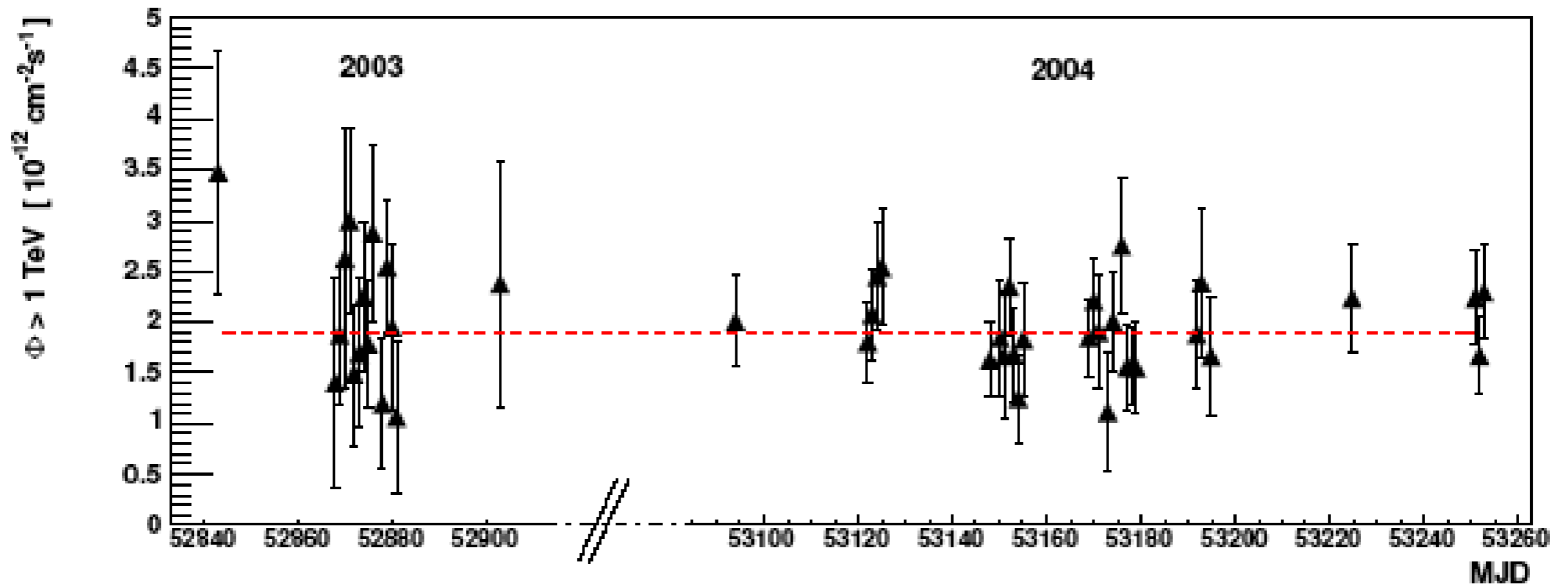
Spectrum and variability of the VHE Galactic Centre source observed with H.E.S.S.

L. Rolland^a and J. Hinton^b for the H.E.S.S. collaboration

The High Energy Stereoscopic System (H.E.S.S.) is an array of four imaging air-Cherenkov telescopes located in Namibia, in the Southern hemisphere. We report the detection of a source of very high energy γ -rays in the direction of the Galactic Centre in observations made in 2003 and 2004. The unprecedented sensitivity of H.E.S.S. enables to strongly constrain the VHE spectrum and variability.



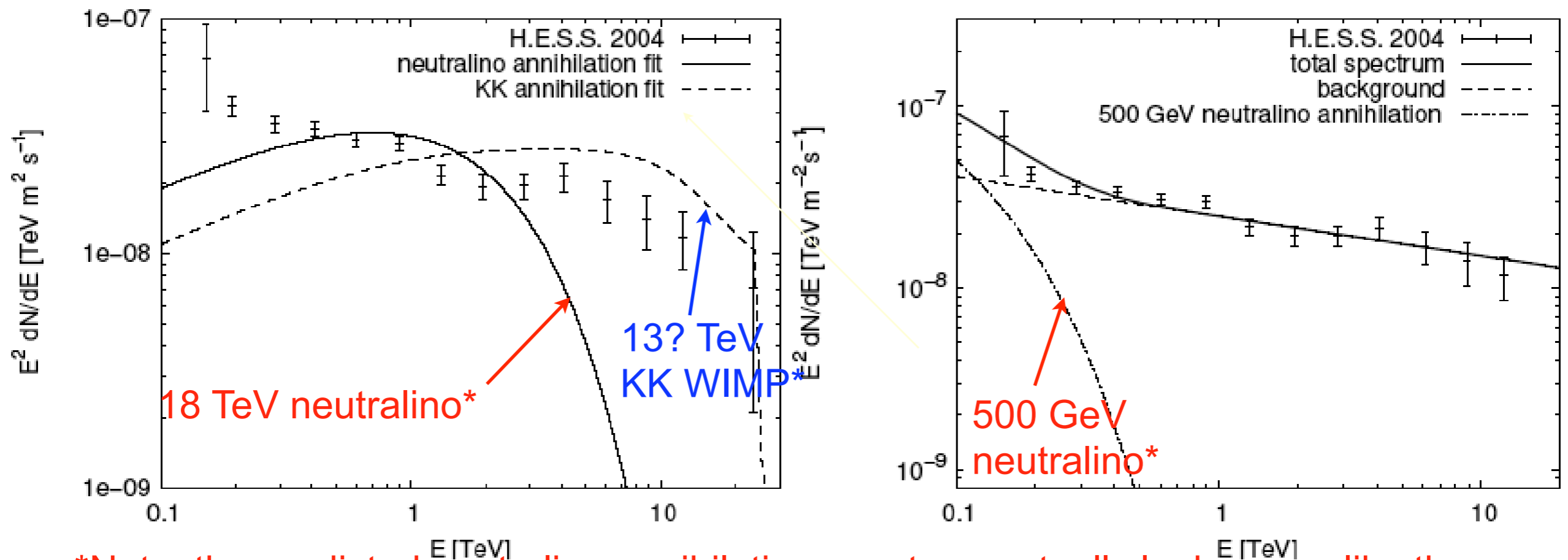
Differential energy spectrum from the direction of the Galactic Center measured in 2003 (two telescopes) and 2004 (four telescopes).



Galactic Centre source light curves. The integral nightly average flux above 1 TeV is given as function of time in modified Julian Days for both 2003 and 2004 observations. The Galactic Centre source flux is consistent with a constant flux at all probed time scales.

Dark matter annihilation as possible origin of the very high energy γ -radiation from the Galactic center measured by H.E.S.S.

J. Ripken^a, D. Horns^b, L. Rolland^c, J. Hinton^d on behalf of the H.E.S.S. collaboration



*Note: the predicted neutralino annihilation spectrum actually looks more like the observed one -- see Bergstrom et al. PRL 95 (2005) 241301

Figure 1. Left: Spectral energy distribution of the γ -radiation from Sgr A* as measured by H.E.S.S. together with fits of annihilation radiation only (hypothesis 1). The used neutralino annihilation spectrum is from [9] and the KK annihilation spectrum from [10]. For the $B^{(1)}$ such high masses are larger than anticipated. Right: Again the measured Sgr A* spectral energy distribution together with a power law plus an annihilation spectrum of a 500 GeV neutralino (hypothesis 2).

* 10 TeV KK annihilation spectrum is from Bergstrom et al. PRL 94 (2005) 131301

Gamma Rays from Kaluza-Klein Dark Matter

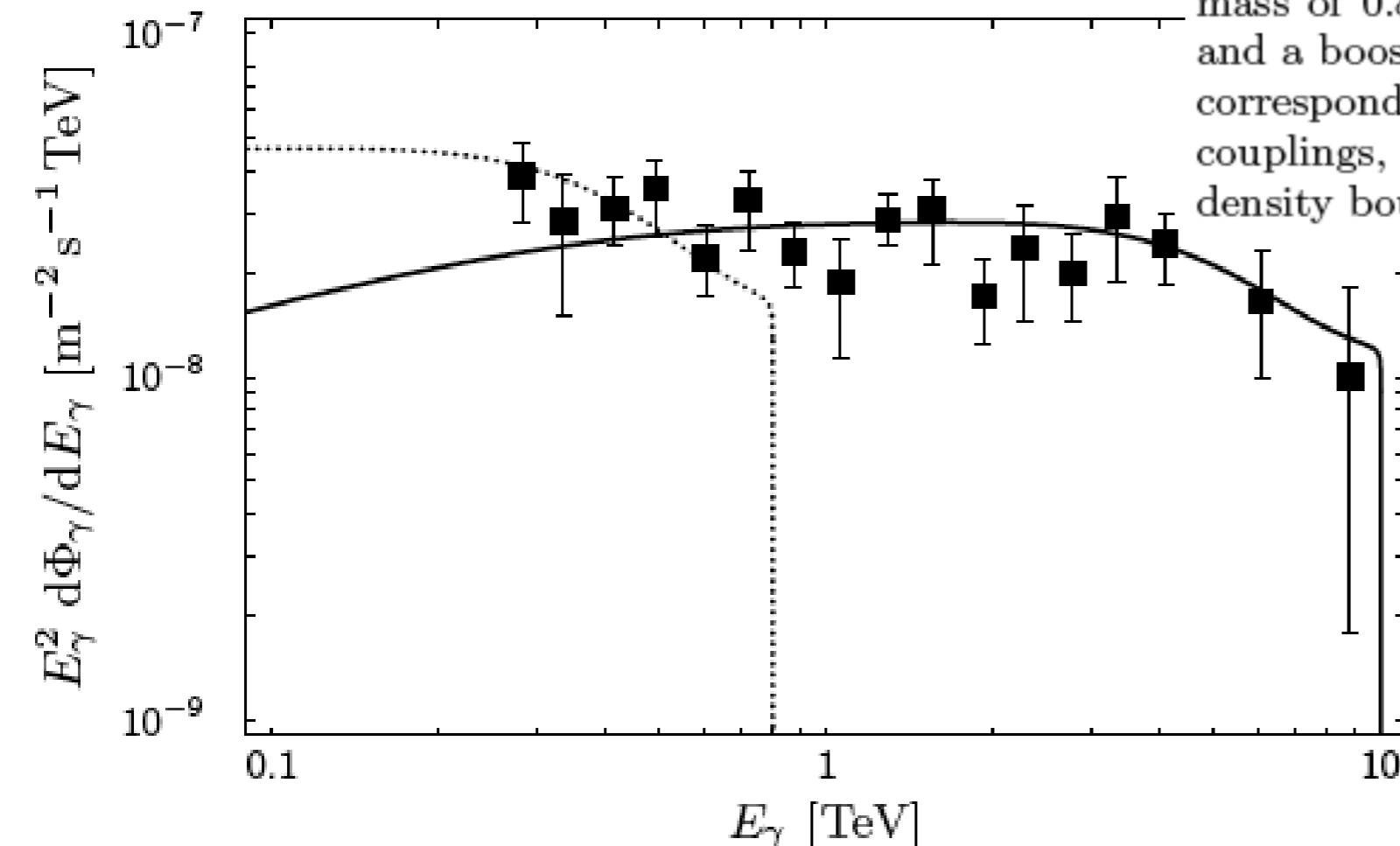
Phys.Rev.Lett. 94 (2005) 131301

Lars Bergström,^{*} Torsten Bringmann,[†] Martin Eriksson,[‡] and Michael Gustafsson[§]

Department of Physics, Stockholm University, AlbaNova University Center, SE - 106 91 Stockholm, Sweden

A TeV gamma-ray signal from the direction of the Galactic center (GC) has been detected by the H.E.S.S. experiment. Here, we investigate whether Kaluza-Klein (KK) dark matter annihilations near the GC can be the explanation. Including the contributions from internal bremsstrahlung as well as subsequent decays of quarks and τ leptons, we find a very flat gamma-ray spectrum which drops abruptly at the dark matter particle mass. For a KK mass of about 1 TeV, this gives a good fit to the H.E.S.S. data below 1 TeV. A similar model, with gauge coupling roughly three times as large and a particle mass of about 10 TeV, would give both the correct relic density and a photon spectrum that fits the complete range of data.

FIG. 3: The H.E.S.S. data [3] compared to the gamma-ray flux from a region of 10^{-5} sr encompassing the GC, for a $B^{(1)}$ mass of 0.8 TeV, a 5% mass splitting at the first KK level, and a boost factor b around 200 (dashed line). The solid line corresponds to a hypothetical 10 TeV WIMP with similar couplings, a total annihilation rate given by the WMAP relic density bound, and a boost factor around 1000.



Gamma Rays from Heavy Neutralino Dark Matter

Phys.Rev.Lett. 95 (2005) 241301

Lars Bergström,^{*} Torsten Bringmann,[†] Martin Eriksson,[‡] and Michael Gustafsson[§]

Department of Physics, Stockholm University, AlbaNova University Center, SE - 106 91 Stockholm, Sweden

We consider the gamma-ray spectrum from neutralino dark matter annihilations and show that internal bremsstrahlung of W pair final states gives a previously neglected source of photons at energies near the mass of the neutralino. For masses larger than about 1 TeV, and for present day detector resolutions, this results in a characteristic signal that may dominate not only over the continuous spectrum from W fragmentation, but also over the $\gamma\gamma$ and γZ line signals which are known to give large rates for heavy neutralinos. Observational prospects thus seem promising.

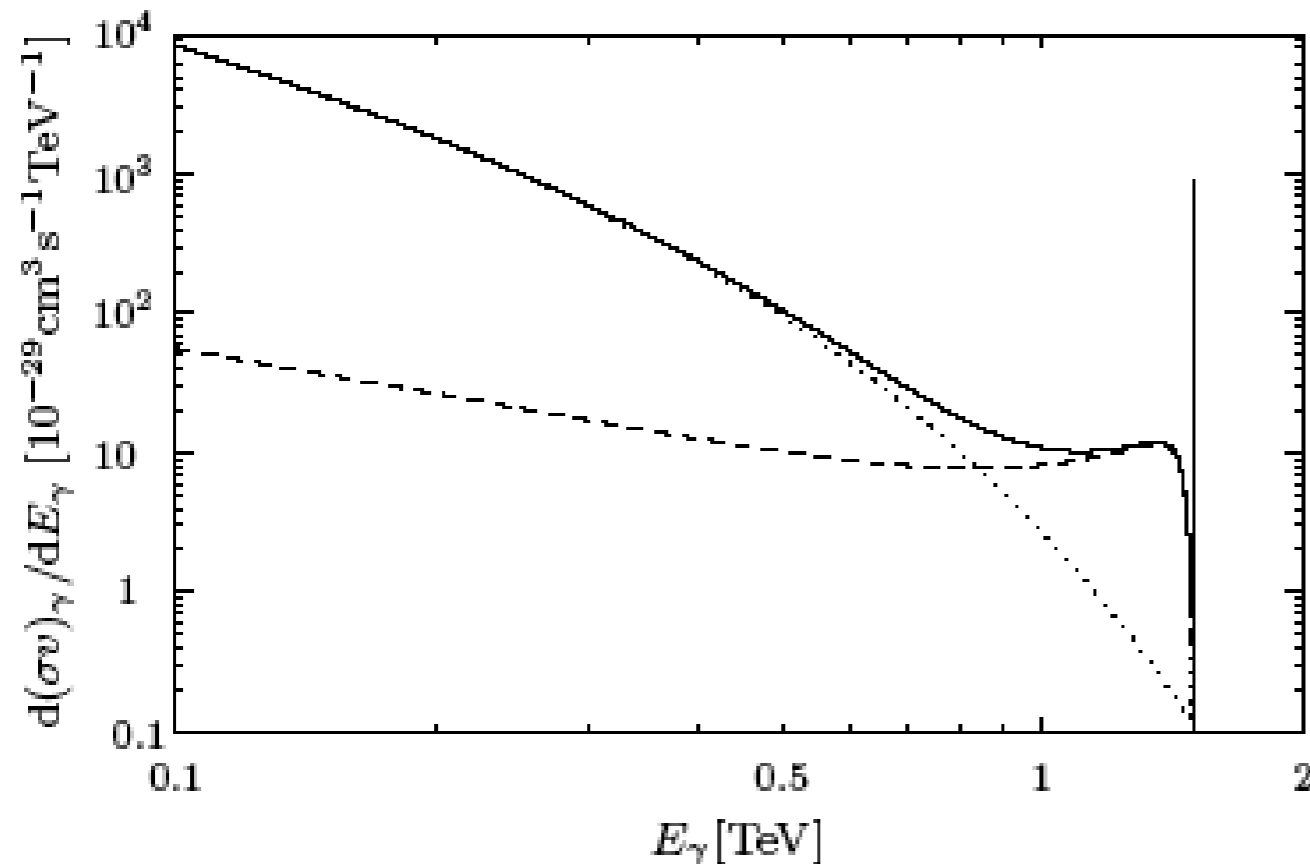


FIG. 3: The total differential photon distribution from $\chi\chi$ annihilations (solid line) for the MSSM model of Table I. Also shown separately is the contribution from radiative processes $\chi\chi \rightarrow W^+W^-\gamma$ (dashed), and the W fragmentation together with the $\chi\chi \rightarrow \gamma\gamma, Z\gamma$ lines (dotted).

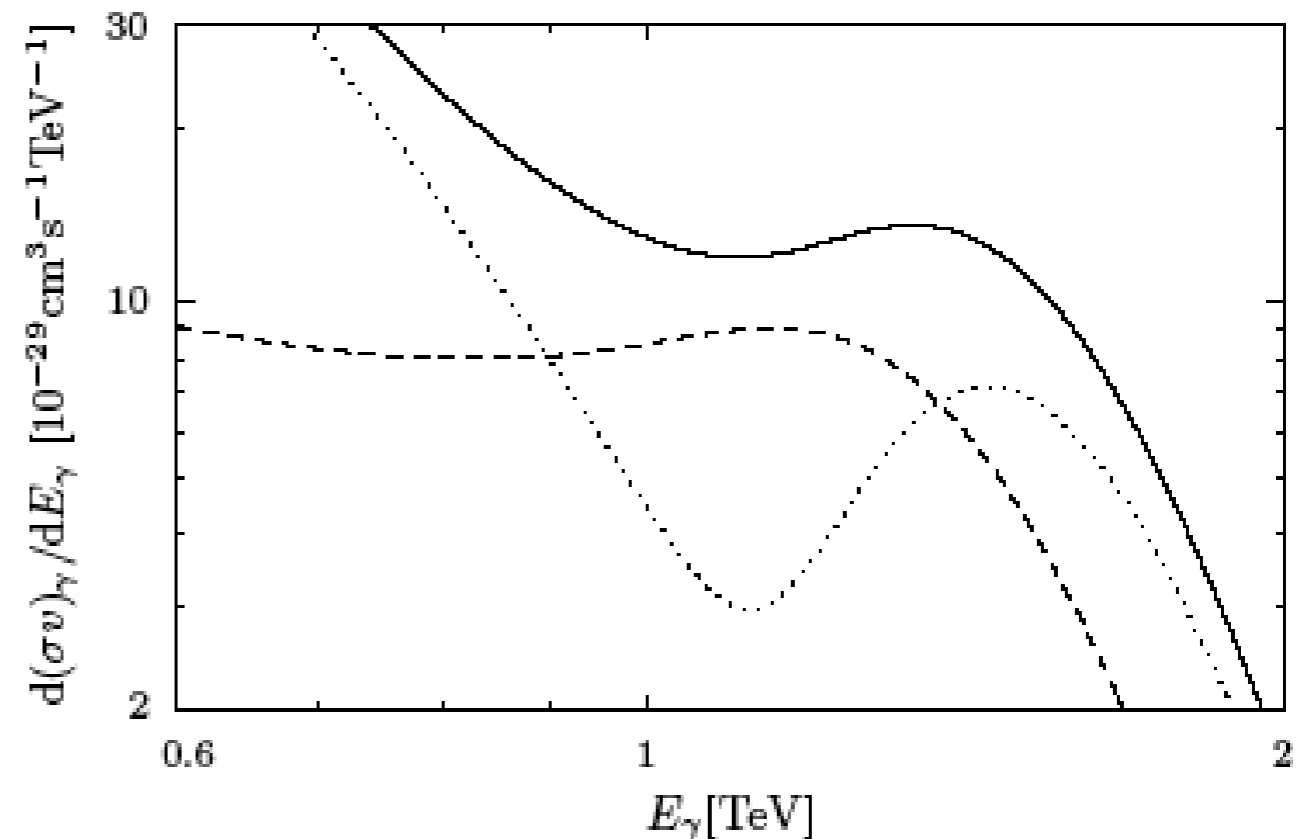


FIG. 4: The same spectra as in Fig. 3, as seen by a detector with an energy resolution of 15 percent.

Comments

- The H.E.S.S. galactic center signal could possibly be explained by a SN remnant, or by emission associated with accretion by the SMBH or dark matter annihilation near it, or a combination of sources
- A SN remnant is an extended source expected to produce a power-law energy spectrum offset from the SMBH, accretion is expected to be variable, while DM annihilation should produce a cuspy angular distribution with an energy spectrum cut off near the WIMP mass
- No time variability has been seen by H.E.S.S.

Comments, con'd

- The power law spectrum observed to ~ 12 TeV requires $M_{\text{WIMP}} > 30$ TeV -- can a SUSY WIMP that massive be consistent with unitarity and $\Omega_m \approx 0.25$? UCSC grad student Rudy Gilmore answers NO for usual SUSY neutralinos, but he is investigating whether WIMP annihilation through an s-channel Higgs could work
- The angular resolution of the 4-telescope H.E.S.S. array may allow determination of the angular distributions; MAGIC and VERITAS may also help measure the high energy spectrum and see if there is a roll-off

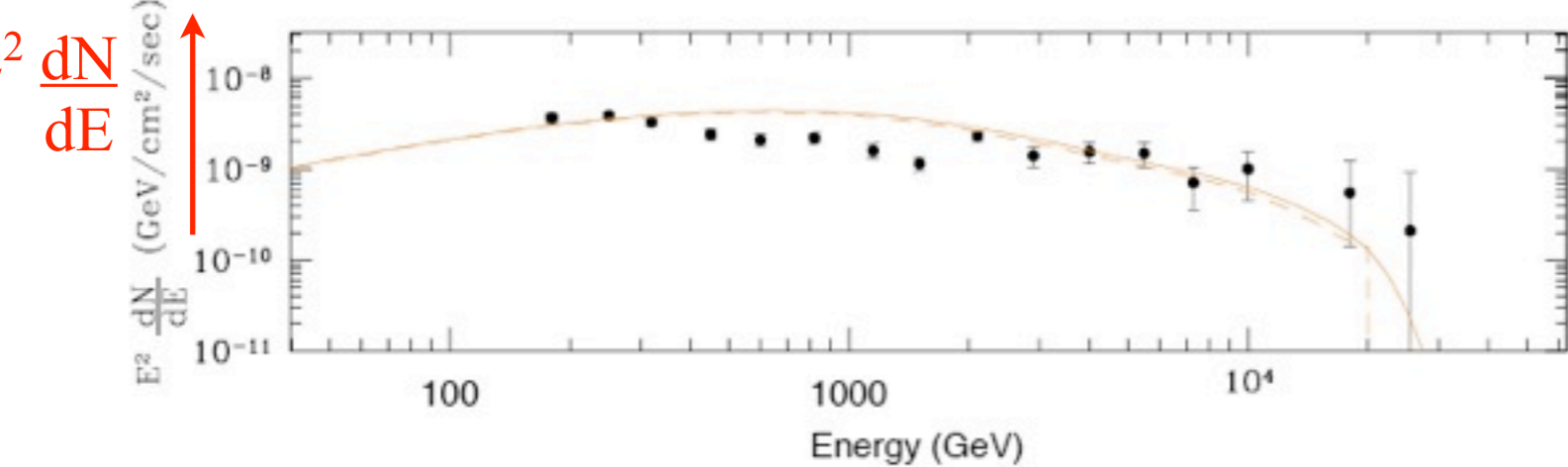
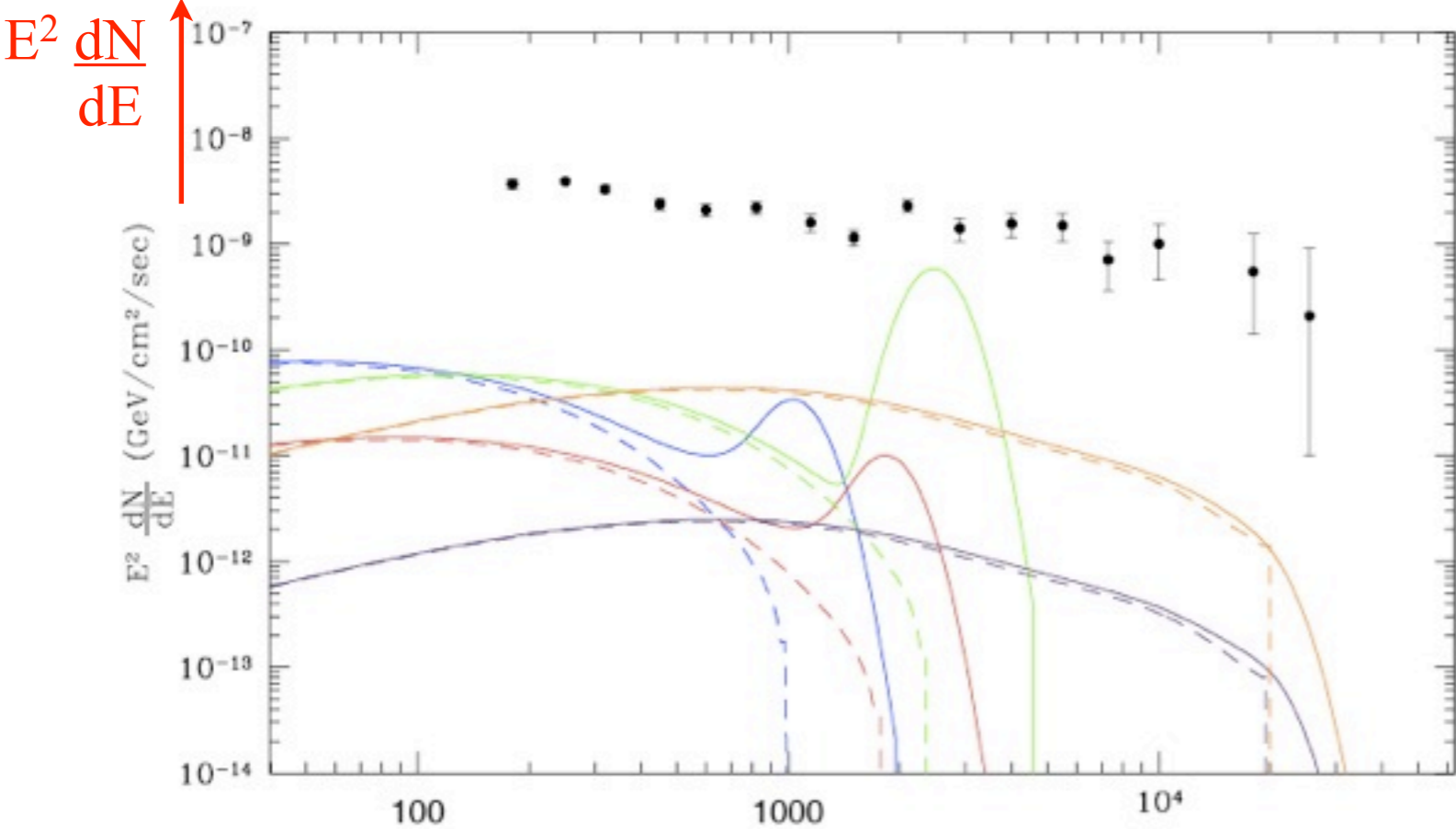
Rudy C. Gilmore, Mass Limits on Neutralino Dark Matter (

Phys.Rev.D76:043520 (2007)

Abstract: We set an upper limit on the mass of a supersymmetric neutralino dark matter particle using the [MicrOMEGAS](#) and [DarkSUSY](#) software packages and the most recent constraints on relic density from combined WMAP and SDSS data. We explore several different possible scenarios within the MSSM, including coannihilation with charginos and sfermions and annihilation through a massive Higgs resonance, using low energy mass inputs. We find that no coannihilation scenario is consistent with dark matter in observed abundance with a mass greater than 2.5 TeV for a wino-type particle or 1.8 TeV for a Higgsino-type. Contrived scenarios involving Higgs resonances with finely-tuned mass parameters can allow masses as high as 34 TeV. The resulting gamma-ray energy distribution is not in agreement with the recent multi-TeV gamma ray spectrum observed by H.E.S.S. originating from the center of the Milky Way. Our results are relevant only for dark matter densities resulting from a thermal origin.

Rudy C. Gilmore, Mass Limits on Neutralino Dark Matter

SUSY DM maximum mass is too low, spectrum shape is wrong, to account for Sag A* gamma rays



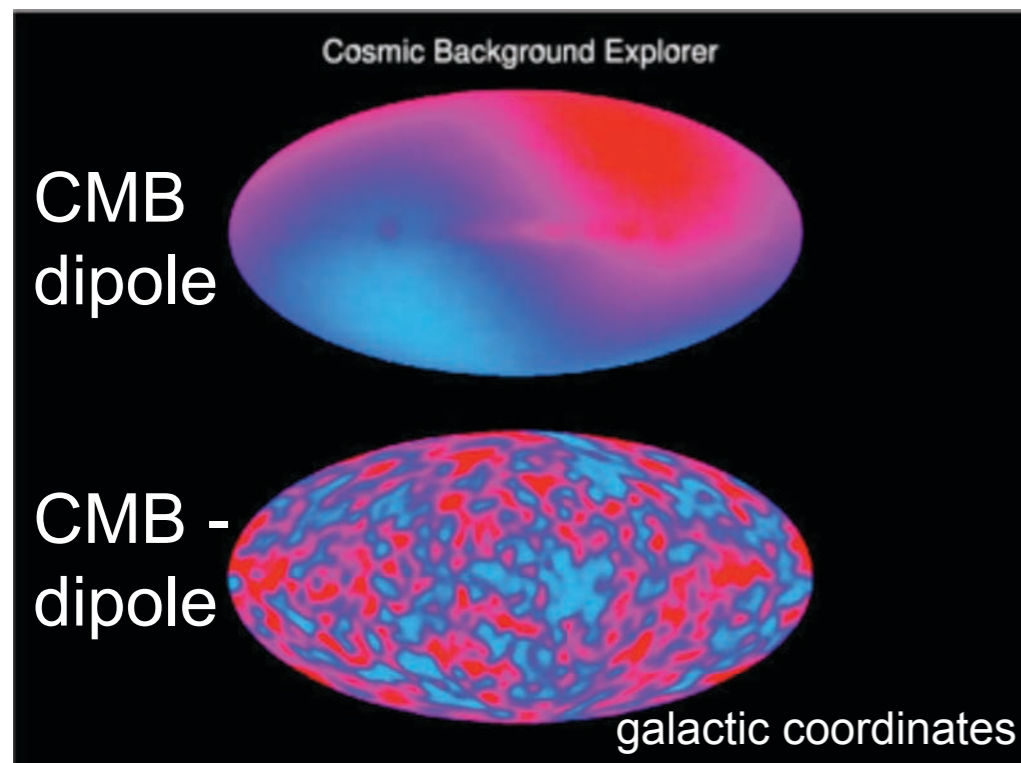
In the upper plot, we summarize our findings by showing the resulting local gamma-ray flux from the galactic center in several annihilation scenarios using the halo model of [12] with fiducial normalization (no baryonic compression), and compare to the latest observations of the H.E.S.S. experiment (black data points, [30]). The dashed lines show the true continuous distribution, while the solid lines show the total (continuous plus discrete) emission spectra as seen by a detector with an energy resolution of 15 percent. The blue line is a 1 TeV Higgsino, coannihilating with a nearly degenerate chargino and second Higgsino. The red line shows the same model with coannihilation from a 3rd generation squark, at a mass of 1.8 TeV. The green line is a 2.4 TeV wino. The purple and orange lines are both a mixed type neutralino annihilating through a heavy Higgs resonance. The orange model has been optimized by fine tuning of the resonance, so that the cross section and resulting flux are maximized, while the purple line shows a more typical model. The lower plot demonstrates an attempt to fit a Higgs resonance model to the H.E.S.S. data. A factor 10 density boost is applied, resulting in a 10^2 increase in flux above the fiducial value.

Cosmic Microwave Background

Early History

Although Penzias and Wilson discovered the CMB in 1965, Weinberg (p. 104) points out that Adams and McKellar had shown that the rotational spectra of cyanogen (CN) molecules observed in 1941 suggested that the background temperature is about 3K.

The COBE FIRAS measurements showed that the spectrum is that of thermal radiation with $T = 2.73\text{K}$.



The CMB dipole anisotropy was discovered by Paul Henry (1971) and Edward Conklin (1972), and confirmed by Conklin and Wilkinson (1977) and Smoot, Gorenstein, and Muller (1977) -- see <http://www.astro.ucla.edu/~wright/CMB-dipole-history.html>

The upper panel of the figure shows the CMB dipole anisotropy in the COBE data. It is usually subtracted when the temperature anisotropy map is displayed (lower panel).

CMB Temperature Anisotropy

Sachs & Wolfe (1967, ApJ, 147, 73) showed that on large angular scales the temperature anisotropy is $\Delta T/T = \varphi/3c^2$. White & Hu give a pedagogical derivation in <http://background.uchicago.edu/~whu/Papers/sw.pdf>

PERTURBATIONS OF A COSMOLOGICAL MODEL AND ANGULAR VARIATIONS OF THE MICROWAVE BACKGROUND

R. K. SACHS AND A. M. WOLFE

Relativity Center, The University of Texas, Austin, Texas

Received May 13, 1966

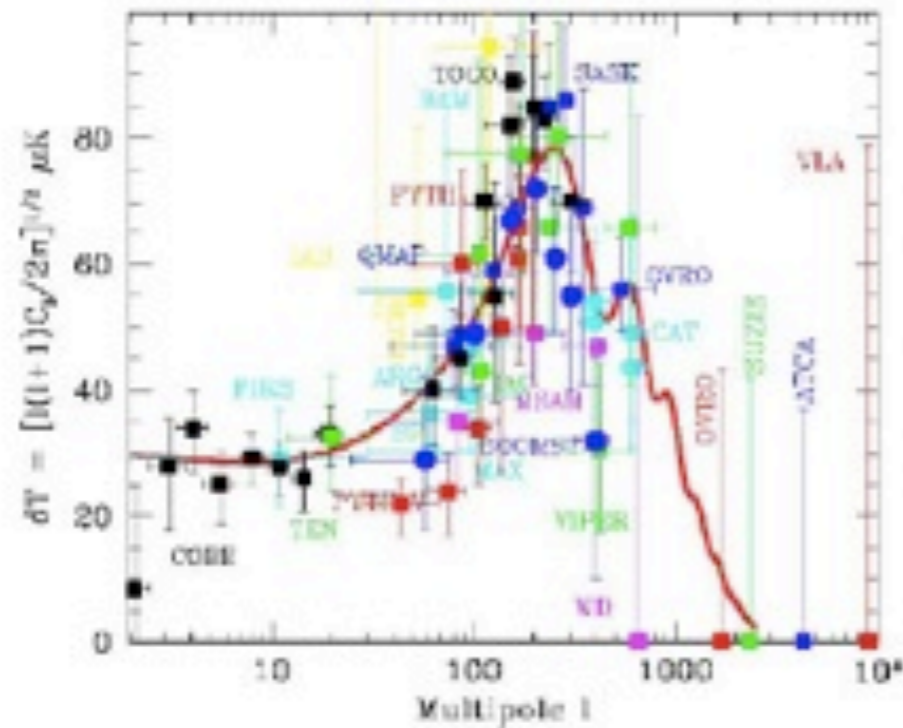
ABSTRACT

We consider general-relativistic, spatially homogeneous, and isotropic $k = 0$ cosmological models with either pressure zero or pressure one-third the energy density. The equations for general linearized perturbations away from these models are explicitly integrated to obtain density fluctuations, rotational perturbations, and gravitational waves. The equations for light rays in the perturbed models are integrated. The models are used to estimate the anisotropy of the microwave radiation, assuming this radiation is cosmological. It is estimated that density fluctuations now of order 10 per cent with characteristic lengths now of order 1000 Mpc would cause anisotropies of order 1 per cent in the observed microwave temperature due to the gravitational redshift and other general-relativistic effects. The $p = 0$ models are compared in detail with corresponding Newtonian models. The perturbed Newtonian models do not contain gravitational waves, but the density perturbations and rotational perturbations are surprisingly similar.

This was first convincingly seen by the COBE DMR experiment, reported by George Smoot on April 27, 1992. Their result $\Delta T/T = 10^{-5}$ had been predicted by the CDM model (Blumenthal, Faber, Primack, & Rees 1984). The search then began for smaller-angular-scale CMB anisotropies.



Shown at DM2000:

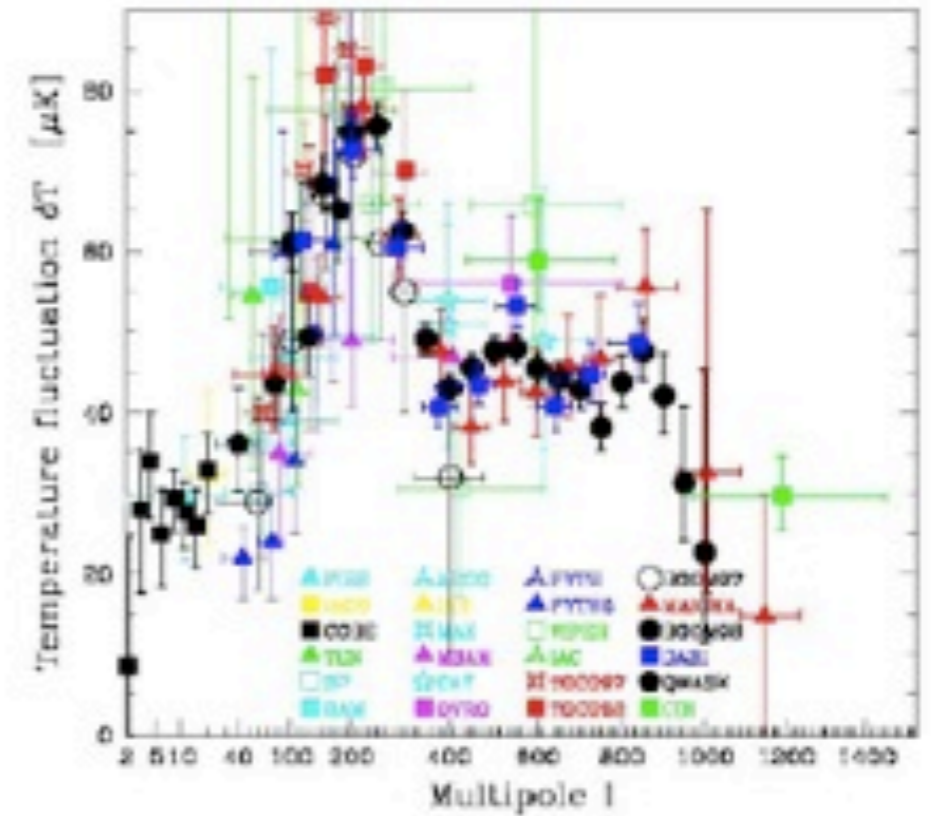


Max Tegmark
Dept. of Physics, MIT
tegmark@mit.edu
DM2000
February 28, 2000

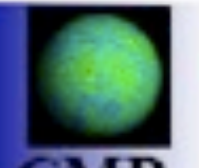
Max Tegmark



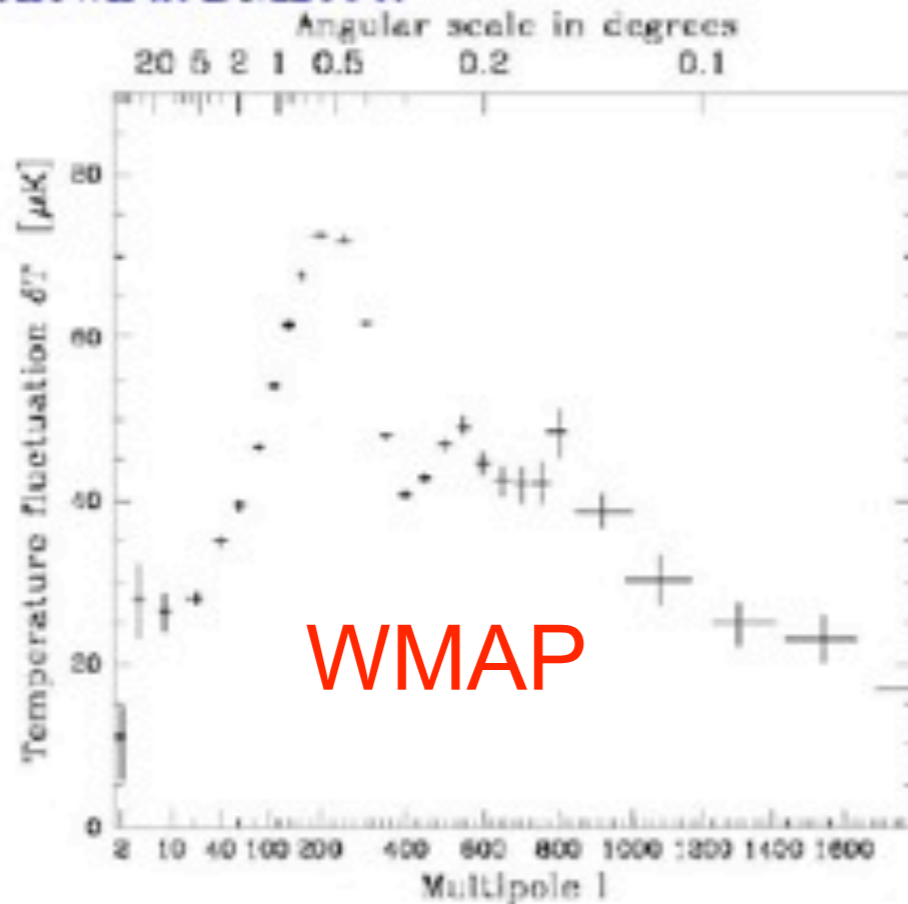
Shown at DM2002:



Max Tegmark
Dept. of Physics, MIT
tegmark@mit.edu
DM2002
February 28, 2000

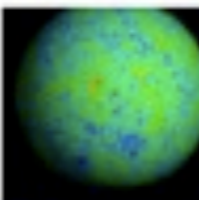


Shown at DM2004:

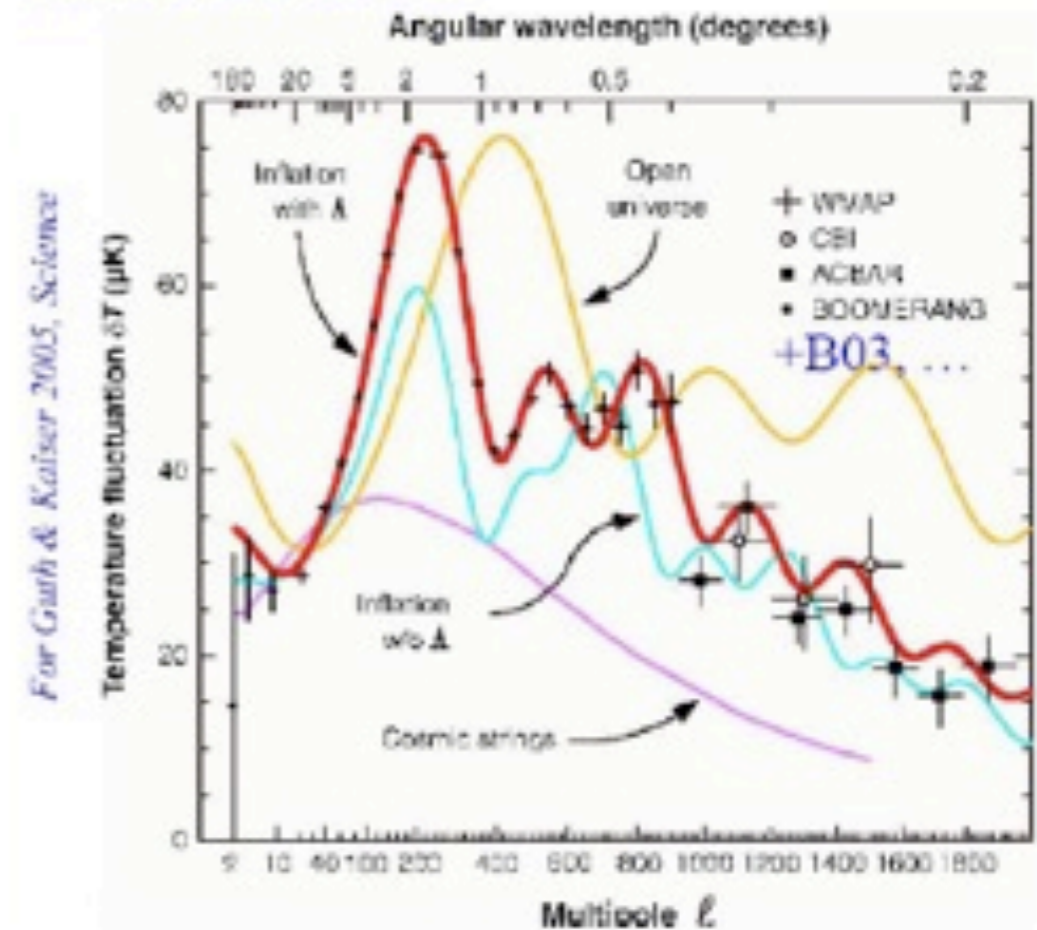


Max Tegmark
Dept. of Physics, MIT
tegmark@mit.edu
DM2004
February 28, 2004

WMAP



Shown at DM2006:



Max Tegmark
Dept. of Physics, MIT
tegmark@mit.edu
DM2006
February 28, 2006

For Guth & Kaiser 2005, Science

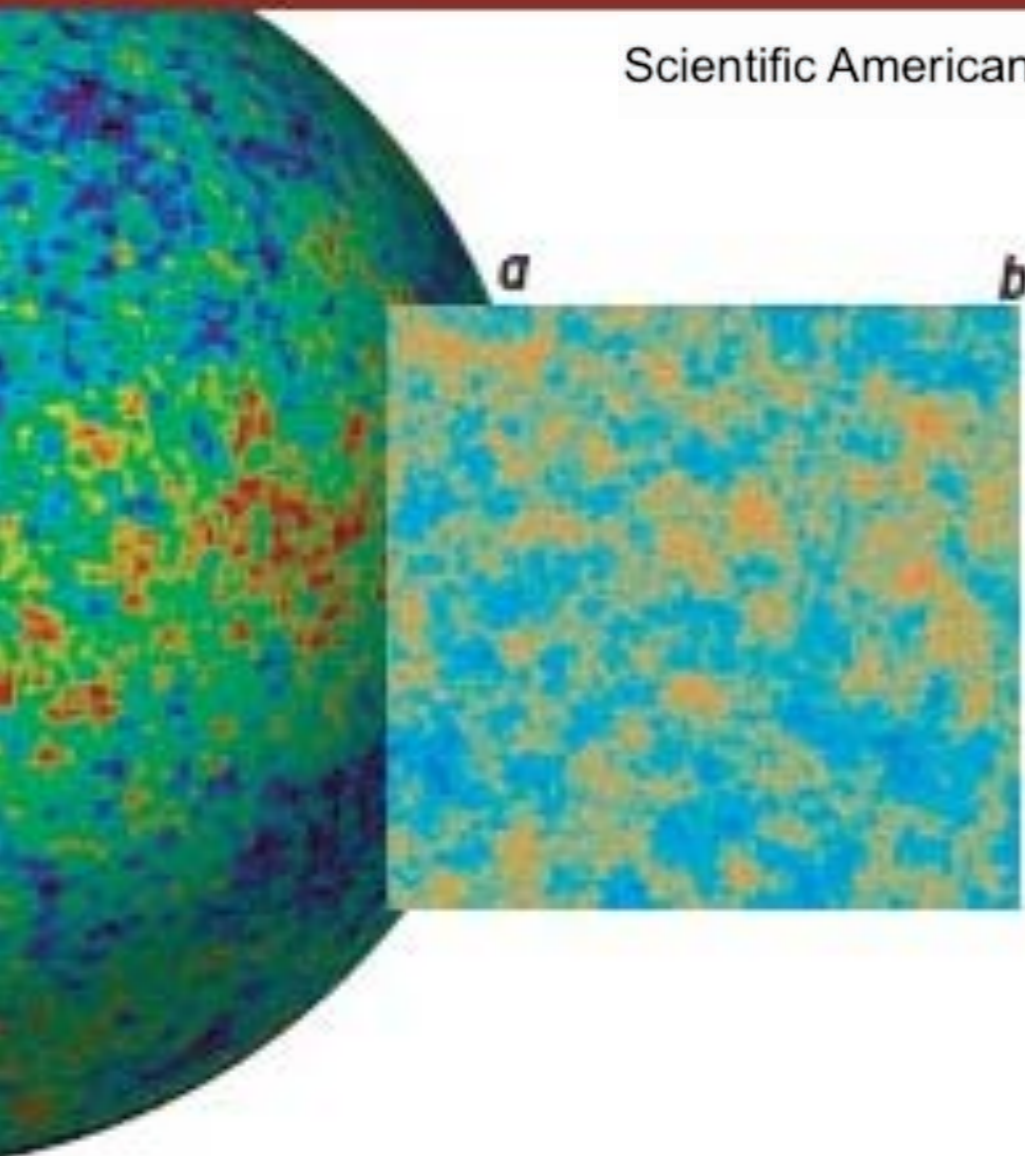
THE POWER SPECTRUM

THE COSMIC SYMPHONY

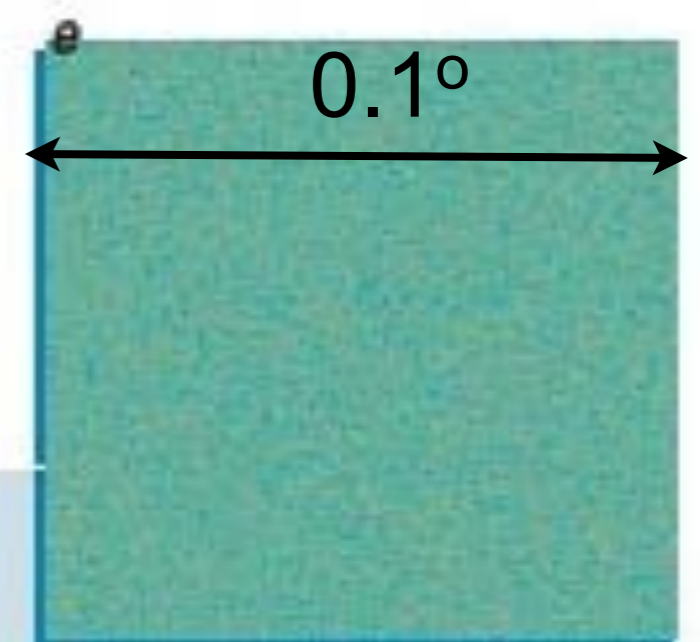
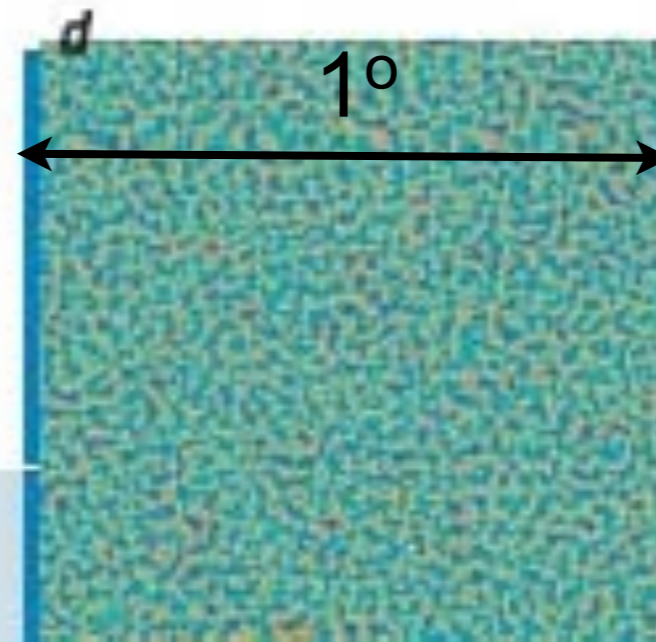
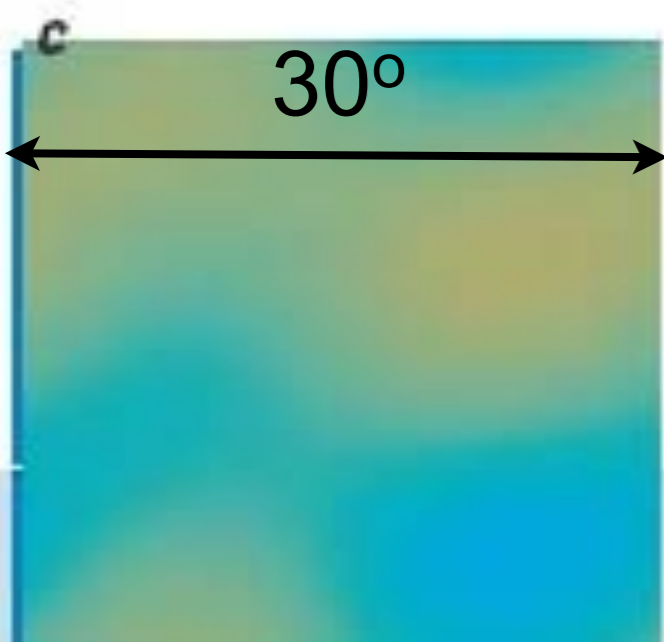
By Wayne Hu and Martin White

Scientific American

February 2004



OBSERVATIONS OF THE CMB provide a map of temperature variations across the whole sky [a]. When researchers analyze portions of that map [b], they use band filters to show how the temperature of the radiation varies at different scales. The variations are barely noticeable at large scales corresponding to regions that stretch about 30 degrees across the sky [c] and at small scales corresponding to regions about a tenth of a degree across [e]. But the temperature differences are quite distinct for regions about one degree across [d]. This first peak in the power spectrum [graph at bottom] reveals the compressions and rarefactions caused by the fundamental wave of the early universe; the subsequent peaks show the effects of the overtones.

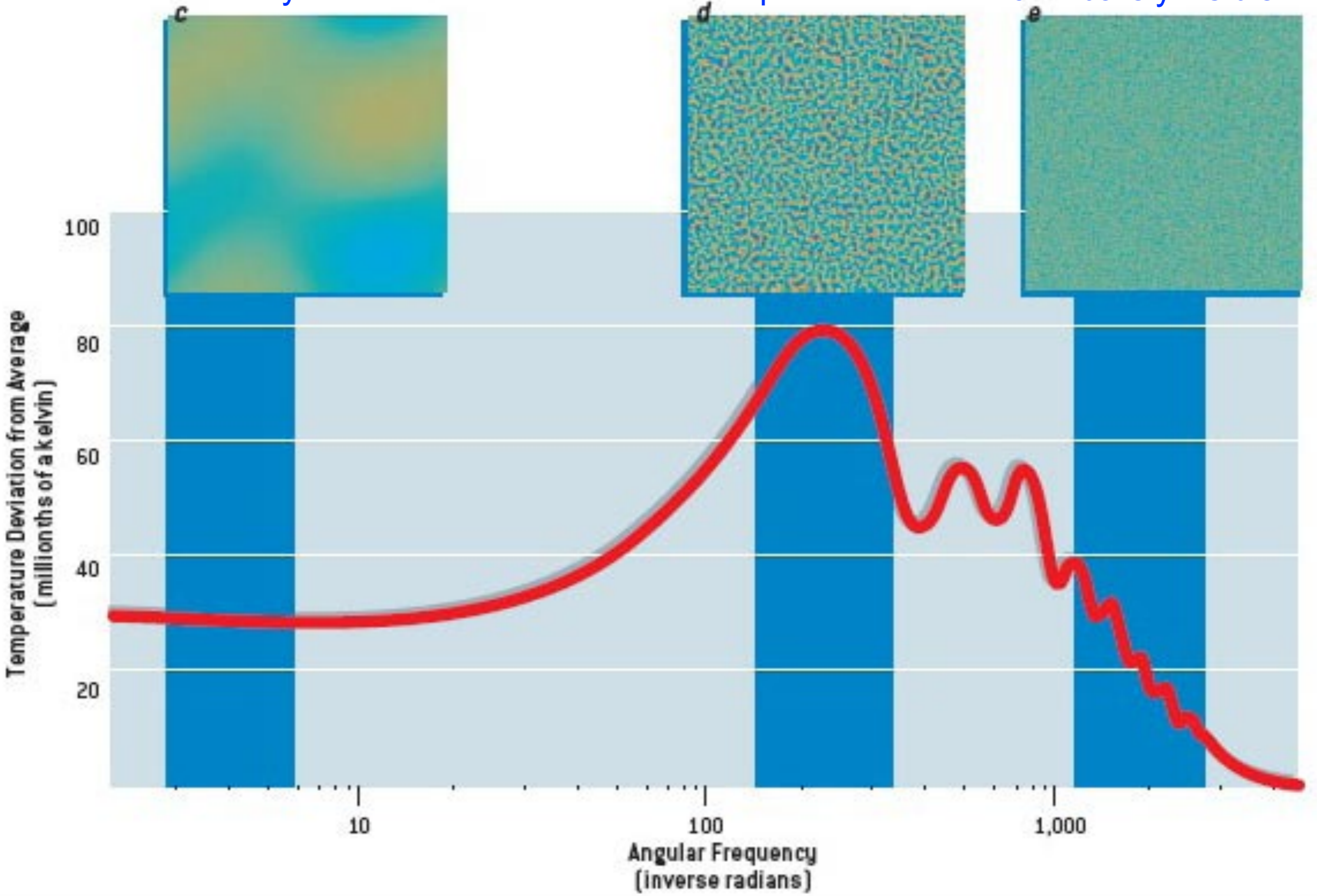


Angular Thermal Variations

30° barely visible

1° prominent

0.1° barely visible



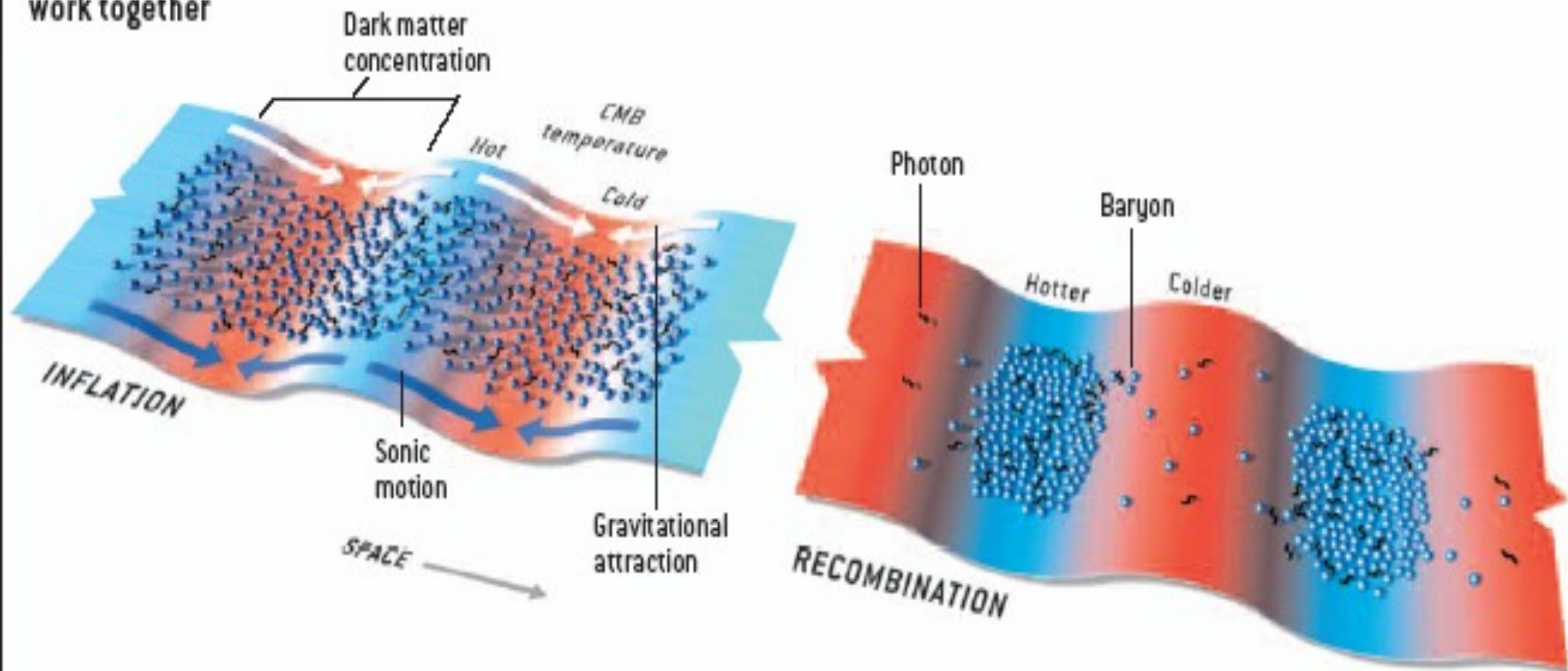
GRAVITATIONAL MODULATION

INFLUENCE OF DARK MATTER modulates the acoustic signals in the CMB. After inflation, denser regions of dark matter that have the same scale as the fundamental wave (represented as troughs in this potential-energy diagram) pull in baryons and photons by gravitational attraction. (The troughs are shown in

red because gravity also reduces the temperature of any escaping photons.) By the time of recombination, about 380,000 years later, gravity and sonic motion have worked together to raise the radiation temperature in the troughs (blue) and lower the temperature at the peaks (red).

FIRST PEAK

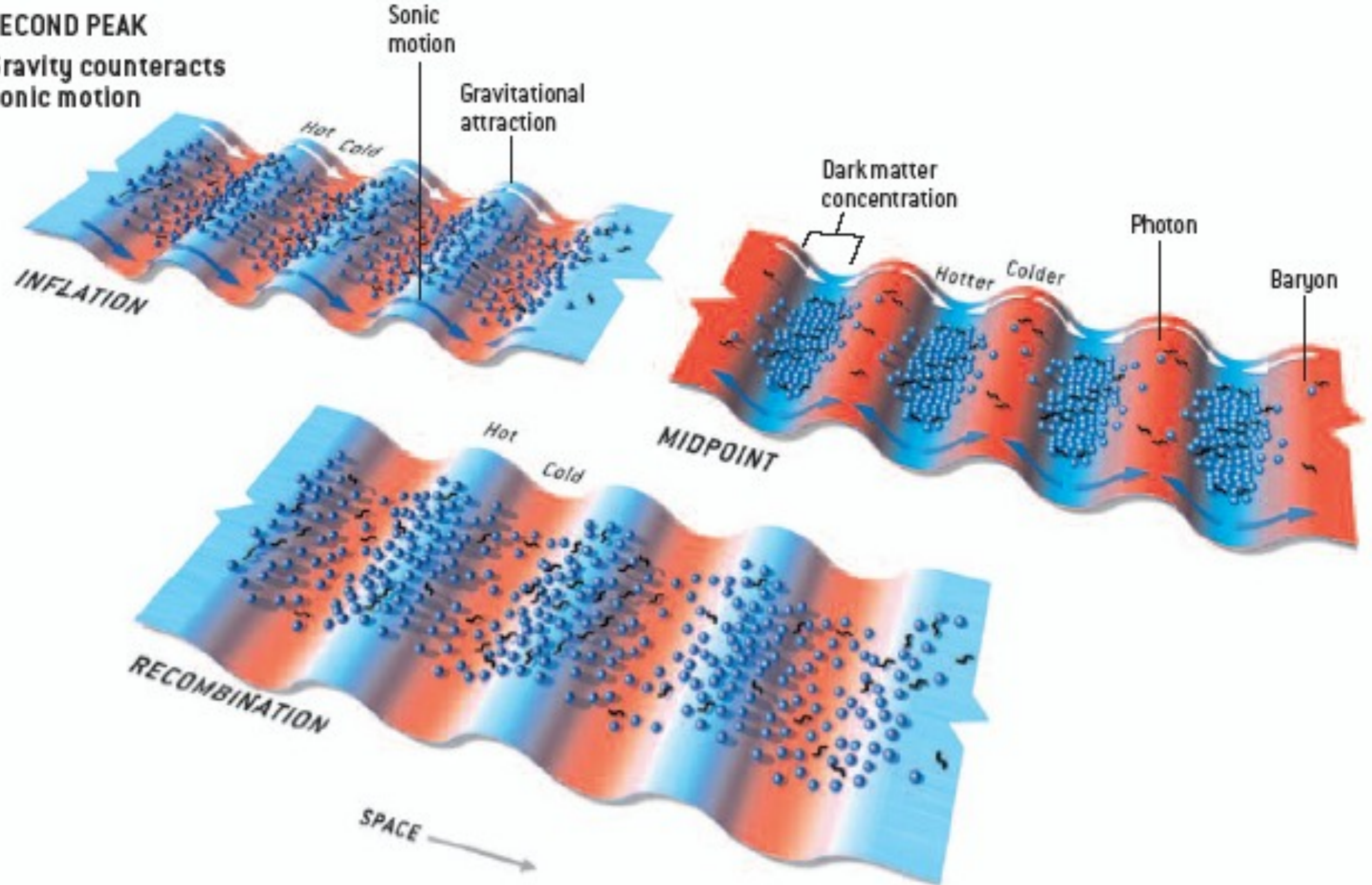
Gravity and sonic motion work together



AT SMALLER SCALES, gravity and acoustic pressure sometimes end up at odds. Dark matter clumps corresponding to a second-peak wave maximize radiation temperature in the troughs long before recombination. After this midpoint, gas pressure pushes

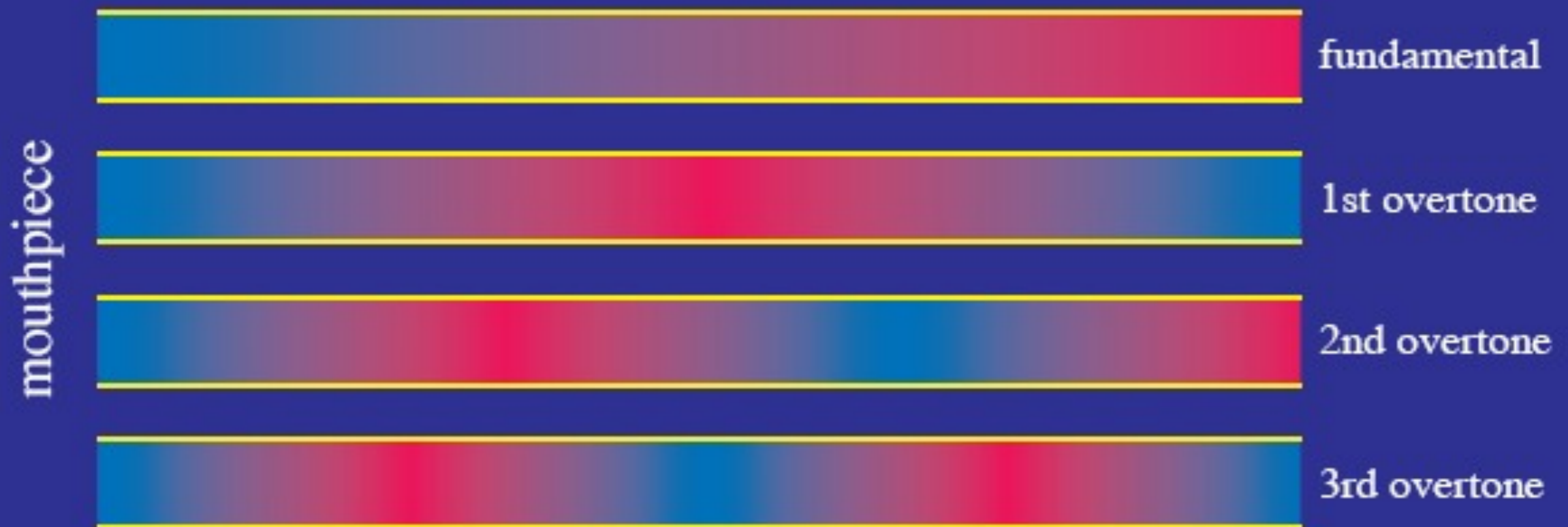
baryons and photons out of the troughs (*blue arrows*) while gravity tries to pull them back in (*white arrows*). This tug-of-war decreases the temperature differences, which explains why the second peak in the power spectrum is lower than the first.

SECOND PEAK
Gravity counteracts sonic motion



Piper at the Gates of Dawn

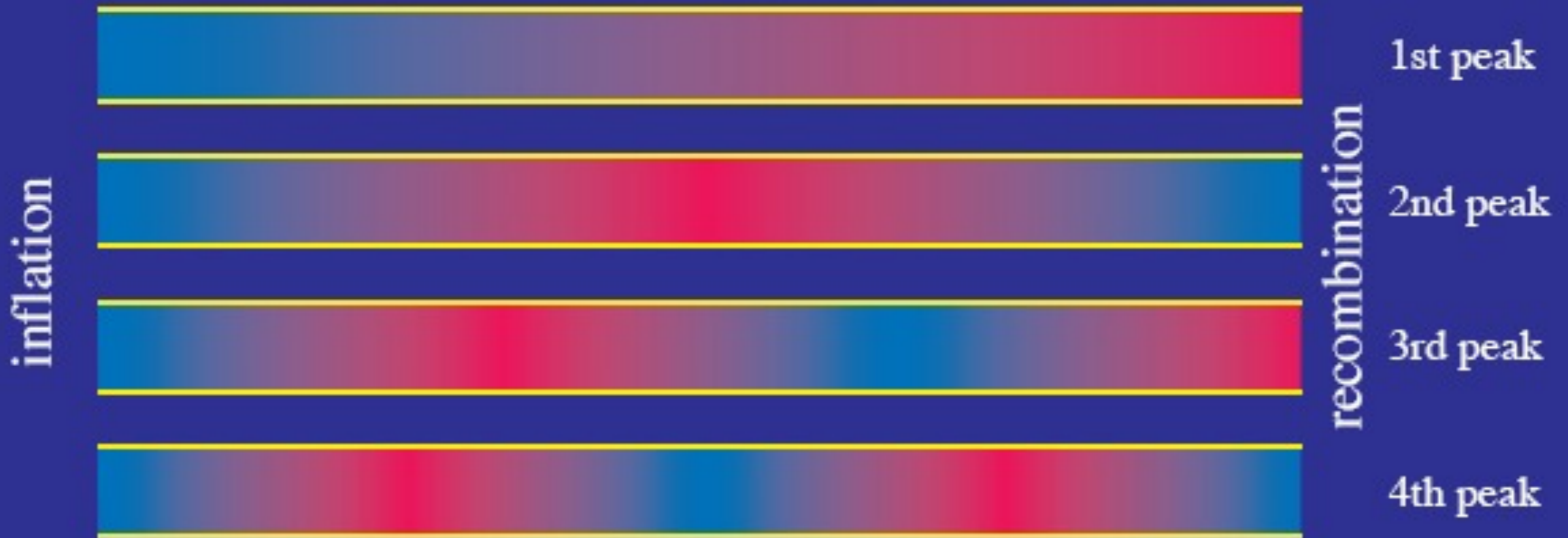
- Blow into a **flute** or an **open pipe**
- **Spectrum** of sound contains a **fundamental frequency** and **harmonic overtones**



This and the next several slides are from a talk by Wayne Hu; see <http://background.uchicago.edu/~whu/beginners/introduction.html>

Piper at the Gates of Dawn

- **Inflation** is the source of sound waves at the **beginning of time**
- Sound waves are frozen at **recombination**, yielding a **harmonic spectrum** of frequencies that reach **maximum displacement**



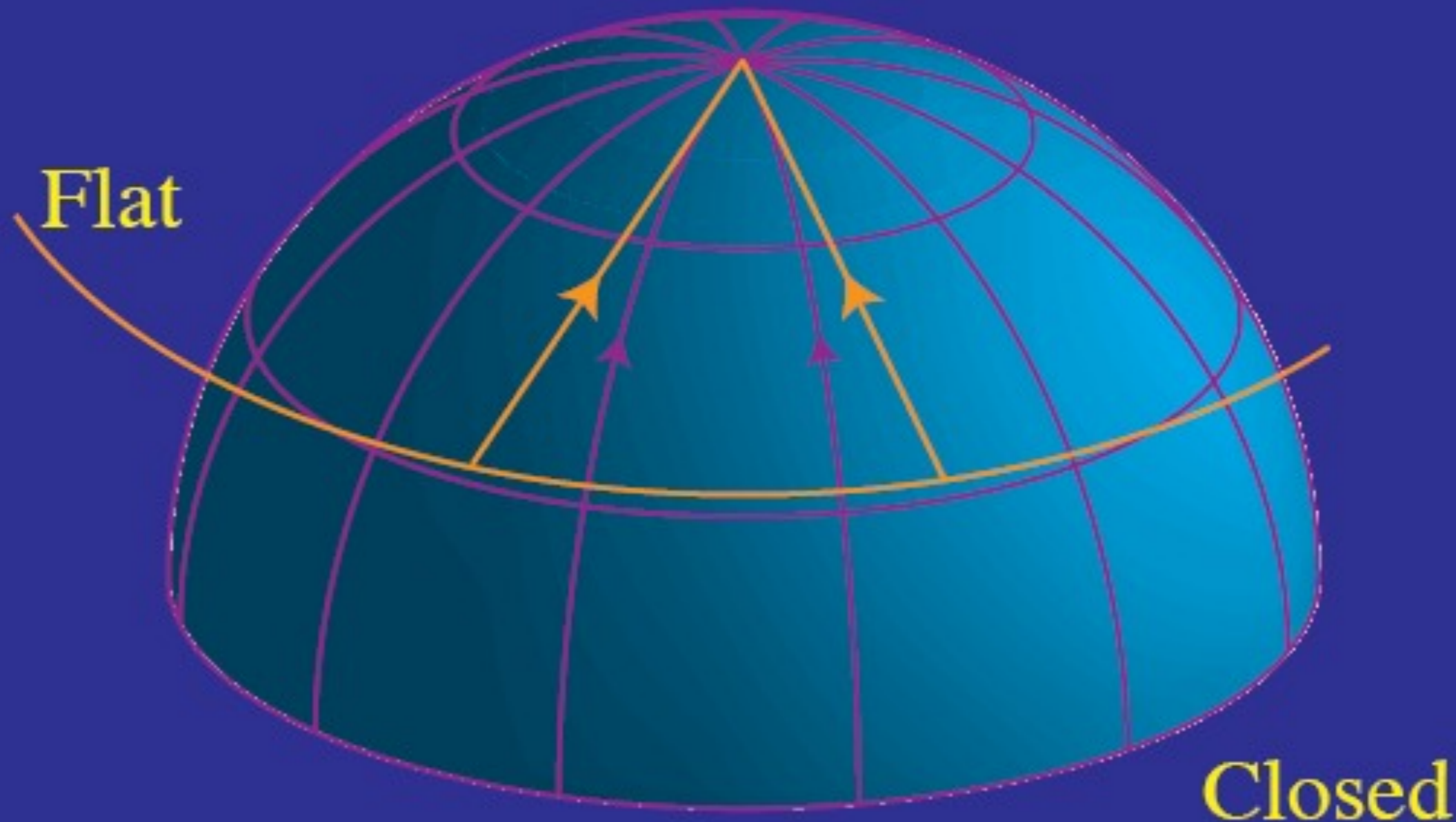
See also Annual Rev. Astron. and Astrophys. 2002
Cosmic Microwave Background Anisotropies
by **Wayne Hu** and **Scott Dodelson**

Harmonic Signature

- Much like a **musical instrument**, identify construction through the pattern of **overtones** on the **fundamental** frequency
- **Without inflation**, fluctuations must be generated at **intermediate times**
- Like **drilling holes** in the pipe and blowing in **random places**, **harmonic** structure of peaks **destroyed**
- **Observed** frequency **spectrum** consistent with **inflationary origin**
- Detailed examination of the **overtones**, reveals the **composition** of the universe
- But first...

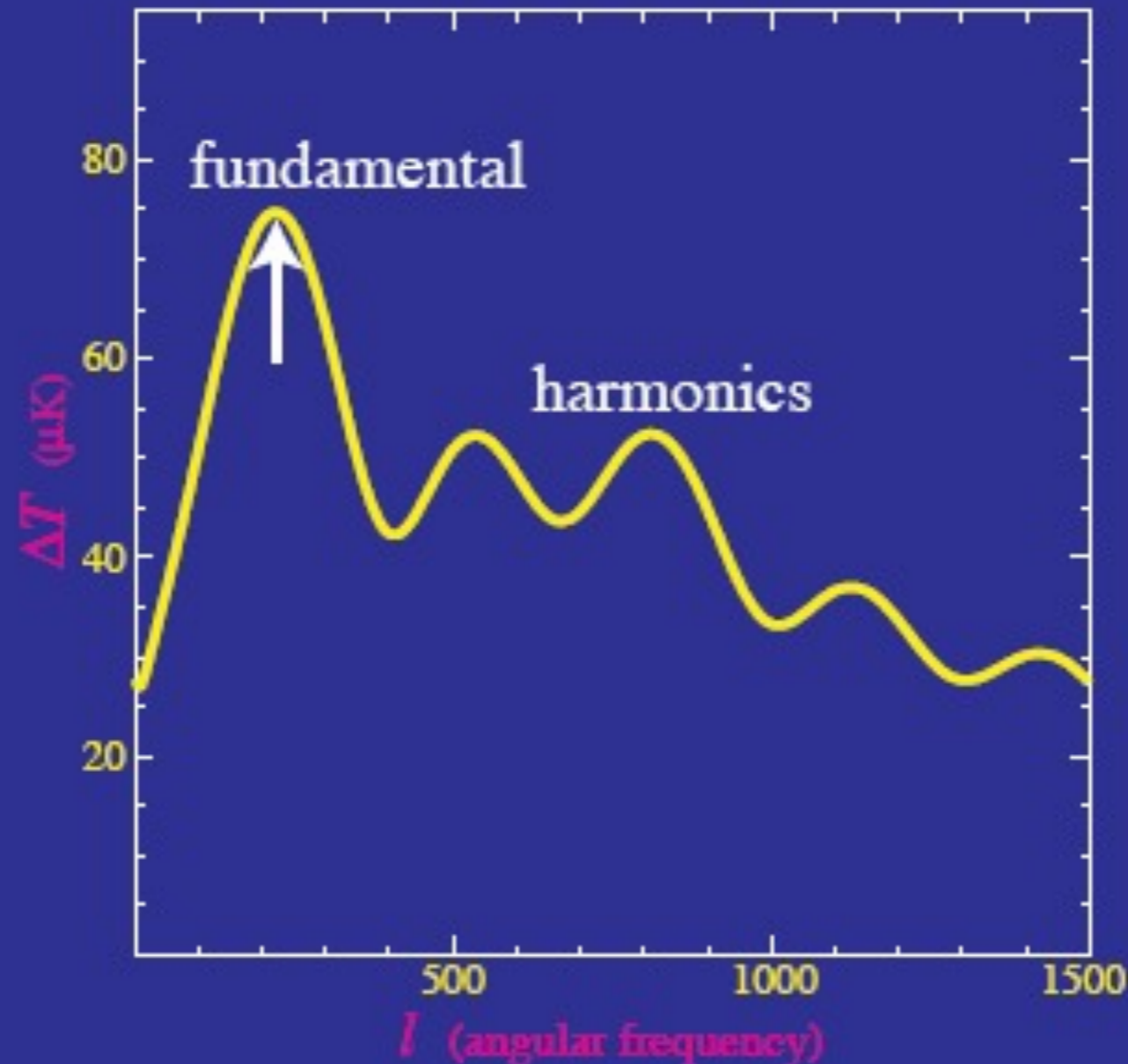
Fundamental: Weighing the Universe

- Measuring the **angular extent** of the **fundamental wavelength** (spot size) yields the **curvature** - universe is spatially **flat**
- Einstein says **matter-energy density** curves space: universe is at the **critical density**



Sound Spectrum

- Spectrum of sound shows harmonics at integer ratios of the fundamental
- Other models that generate structure causally at intermediate times would **not have** these harmonics



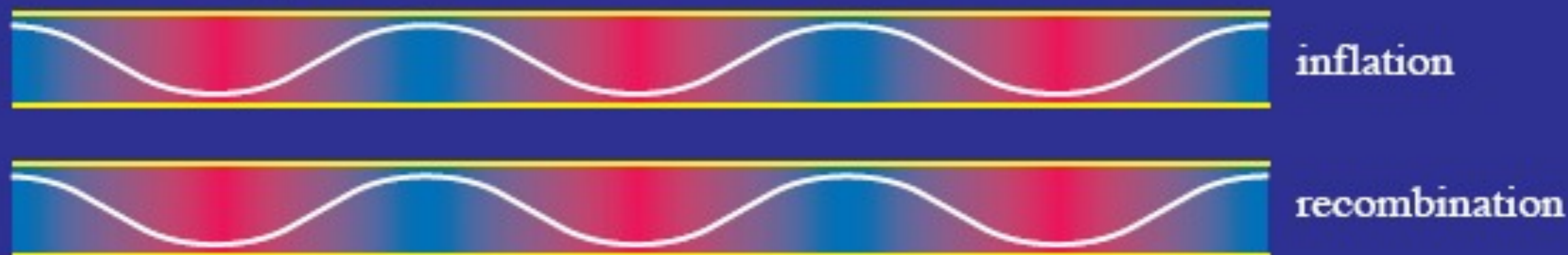
Harmonics: Ordinary Matter

- Competition between **gravity** and **pressure** depends on **phase** of oscillation
- At the **fundamental** (and **odd frequency multiples**) **gravity assists** sonic motion; at **second peak** (and **even multiples**) **gravity fights** sonic motion

Fundamental

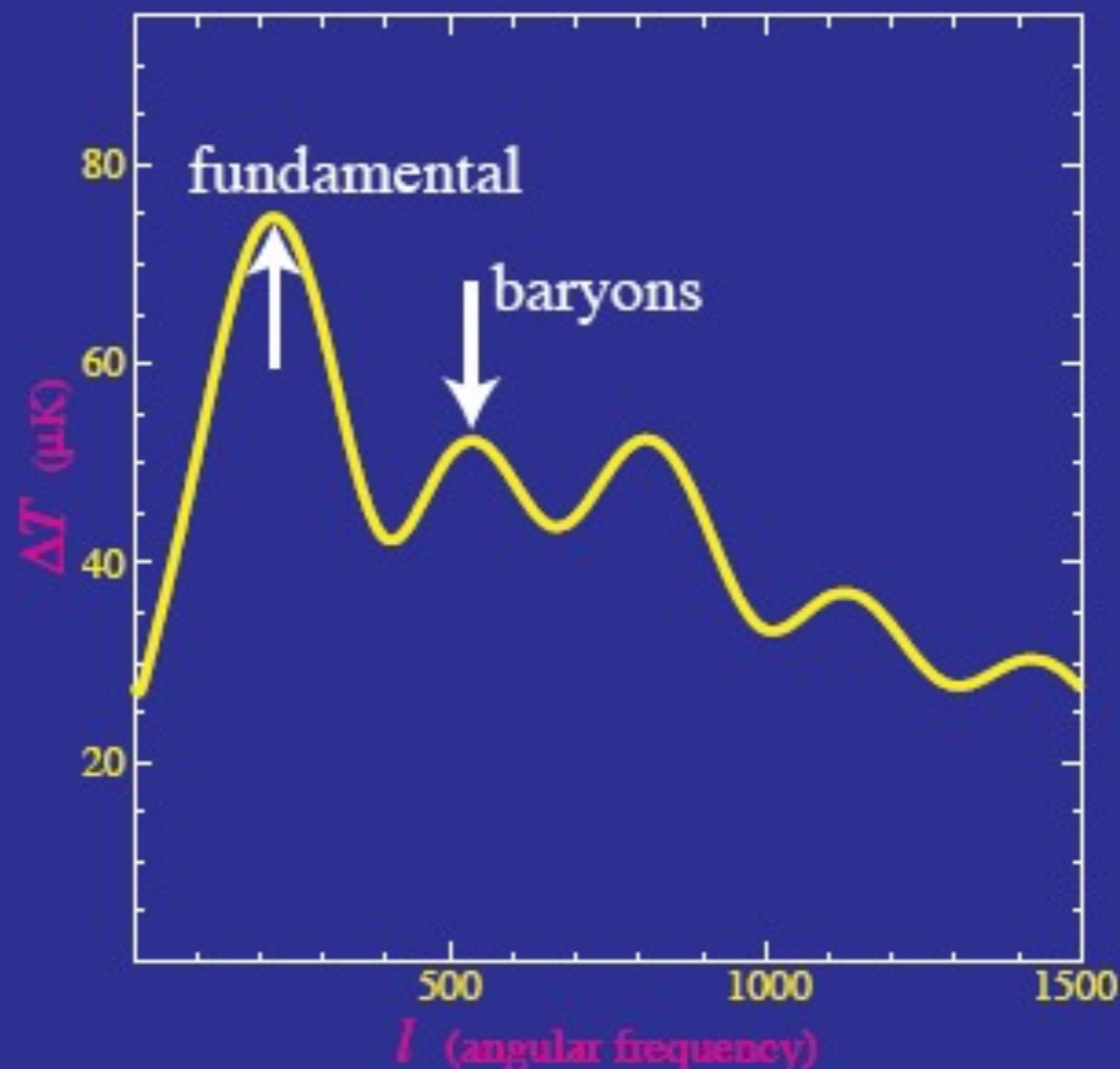


2nd Peak



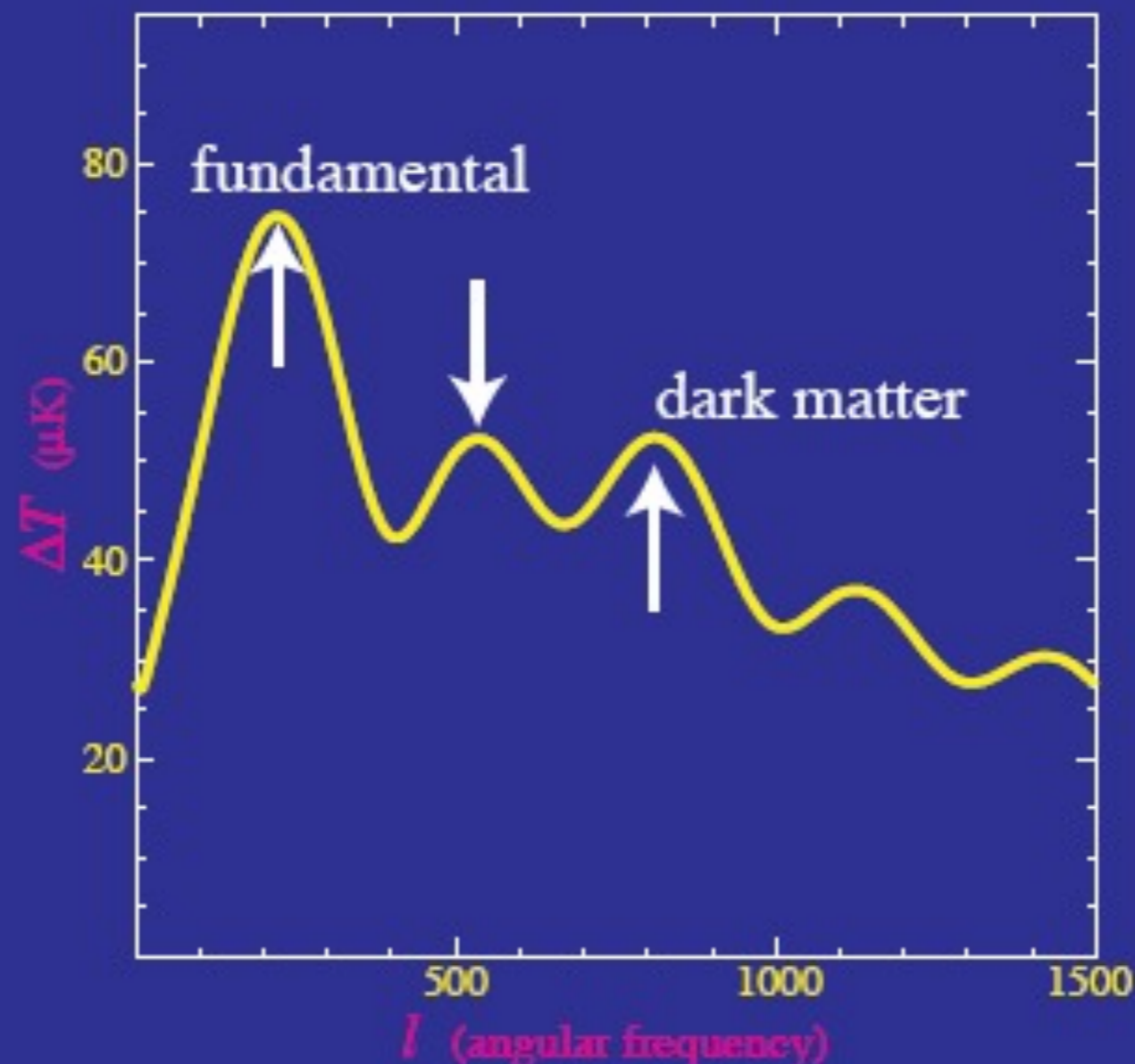
Ordinary Matter

- A **low second peak** indicates **baryon** or **ordinary matter** density **comparable** to **photon** density
- Ordinary matter consists of **$\sim 5\%$** of the critical density today



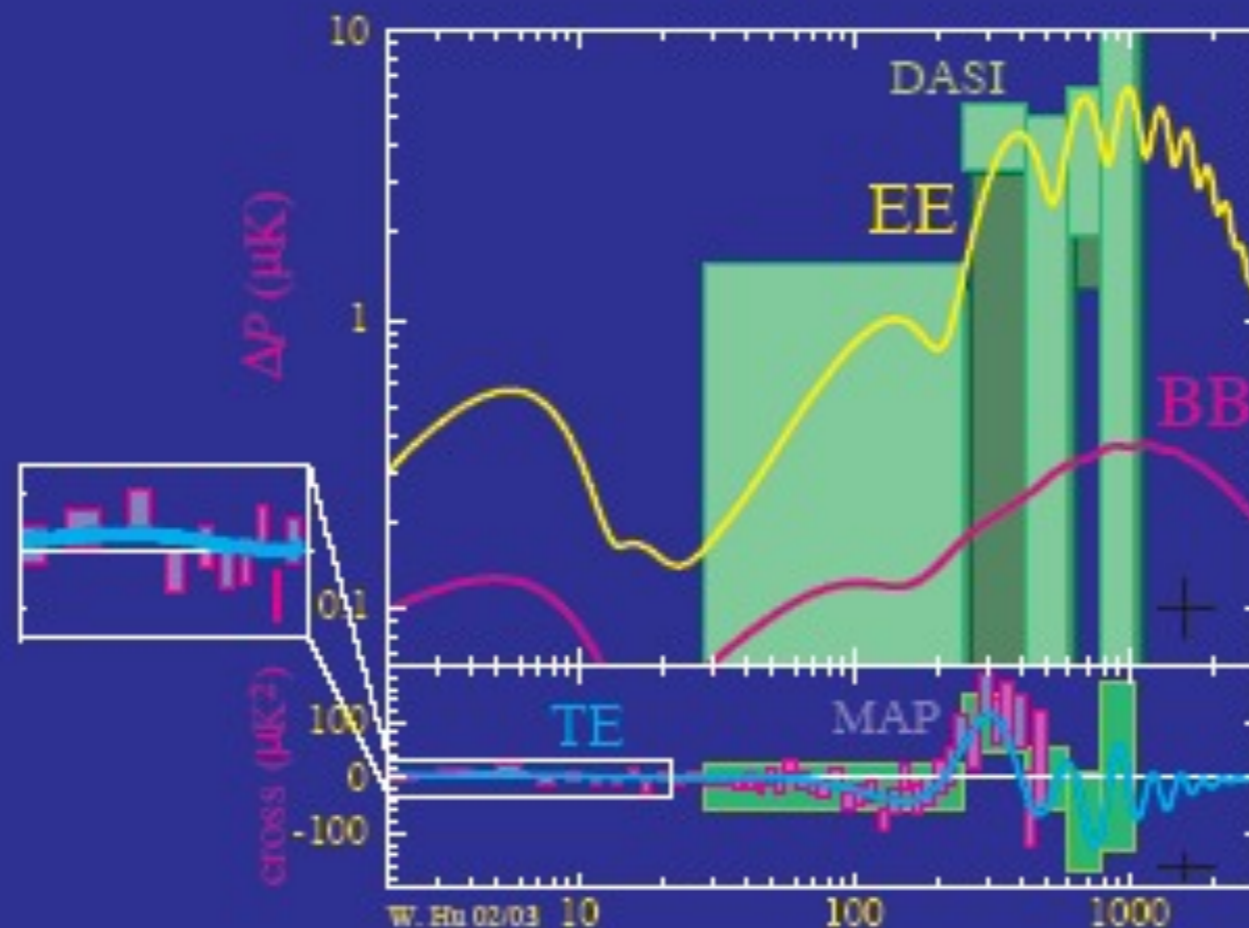
Dark Matter

- A third peak comparable to second peak indicates a dark matter density $\sim 5x$ that of ordinary matter
- Dark matter $\sim 25\%$ of the critical density



Predictive Power

- Model predicts the precise form of the damping of sound waves: observed ✓
- Model predicts that associated with the damping, the CMB becomes polarized: observed ✓
- Model predicts that temperature fluctuations correlated with local structure due to the dark energy: observed ✓



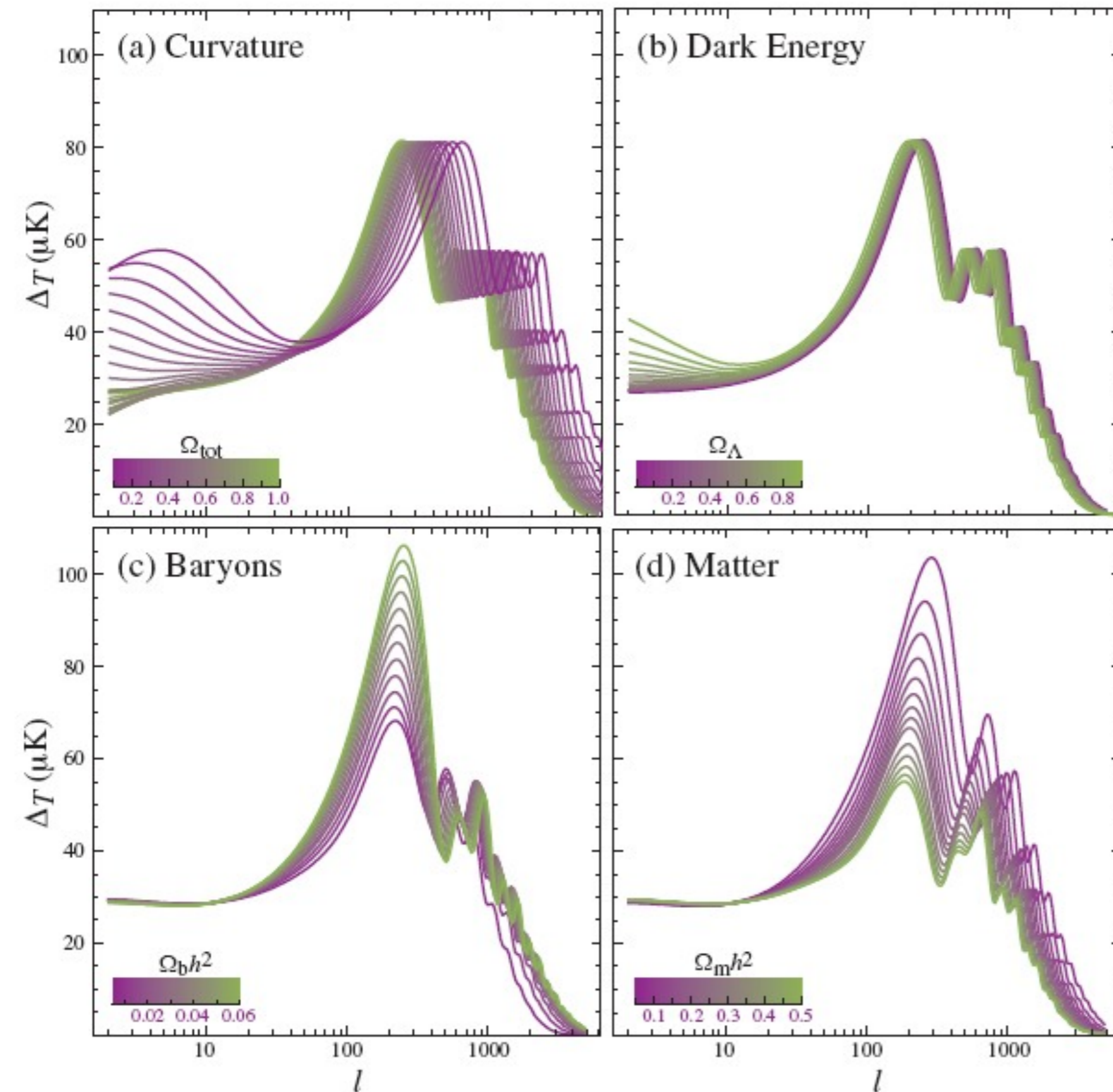


Plate 4: Sensitivity of the acoustic temperature spectrum to four fundamental cosmological parameters (a) the curvature as quantified by Ω_{tot} (b) the dark energy as quantified by the cosmological constant Ω_{Λ} ($w_{\Lambda} = -1$) (c) the physical baryon density $\Omega_b h^2$ (d) the physical matter density $\Omega_m h^2$, all varied around a fiducial model of $\Omega_{\text{tot}} = 1$, $\Omega_{\Lambda} = 0.65$, $\Omega_b h^2 = 0.02$, $\Omega_m h^2 = 0.147$, $n = 1$, $z_{\text{ri}} = 0$, $E_i = 0$.

Annu. Rev. Astron. and
Astrophys. 2002
Cosmic Microwave Background
Anisotropies by **Wayne Hu** and
Scott Dodelson

For animation of the effects of changes in cosmological parameters on the CMB angular power spectrum and the matter power spectrum, plus links to many CMB websites, see Max Tegmark's and Wayne Hu's websites:

<http://space.mit.edu/home/tegmark/>

<http://background.uchicago.edu/~whu/physics/physics.html>

WMAP 5-year data and papers are at <http://lambda.gsfc.nasa.gov/>

G. Hinshaw et al. ApJS, 180, 225 (2009)

Five-Year Wilkinson Microwave Anisotropy Probe (WMAP¹) Observations:
Data Processing, Sky Maps, & Basic Results

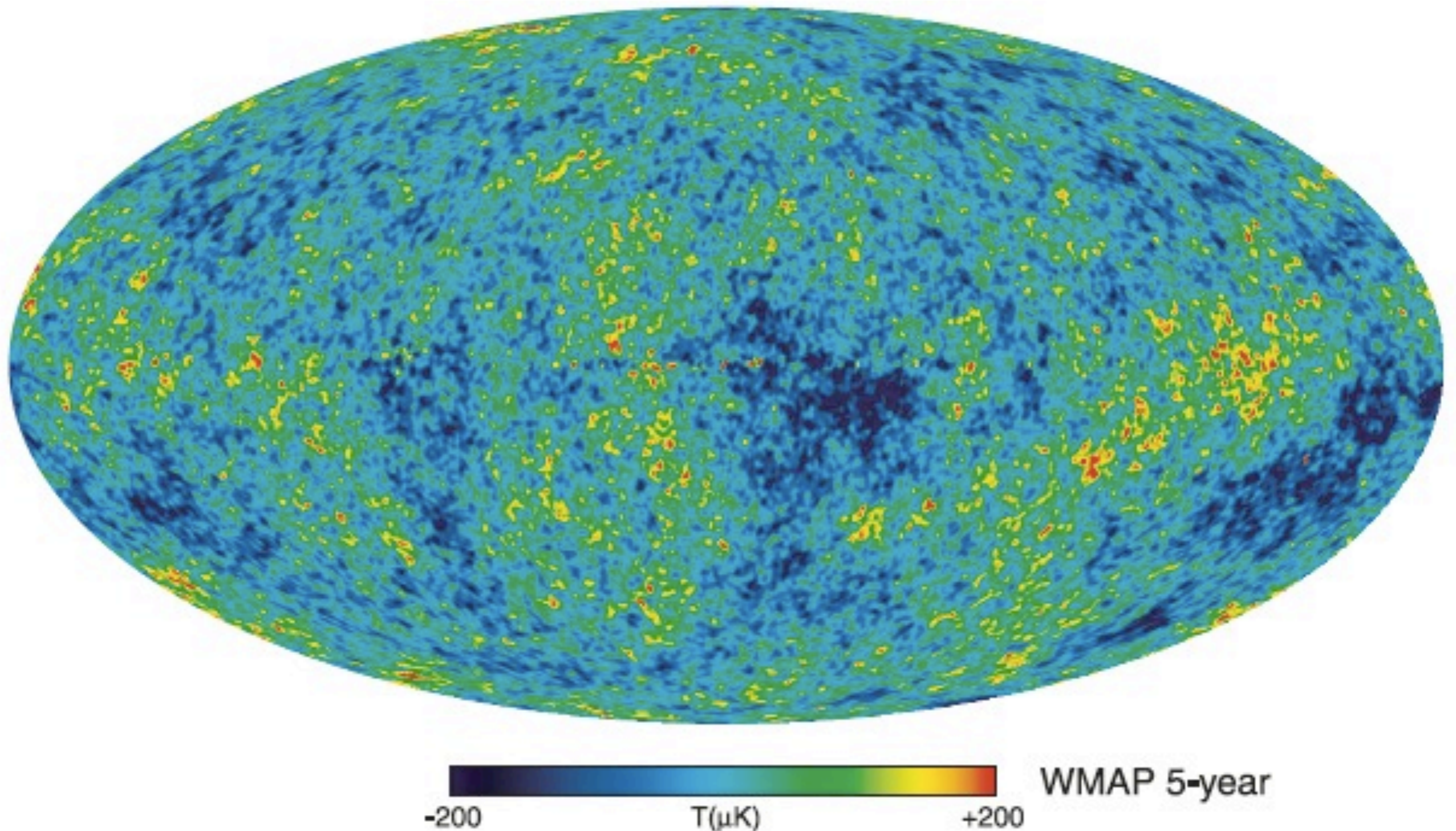


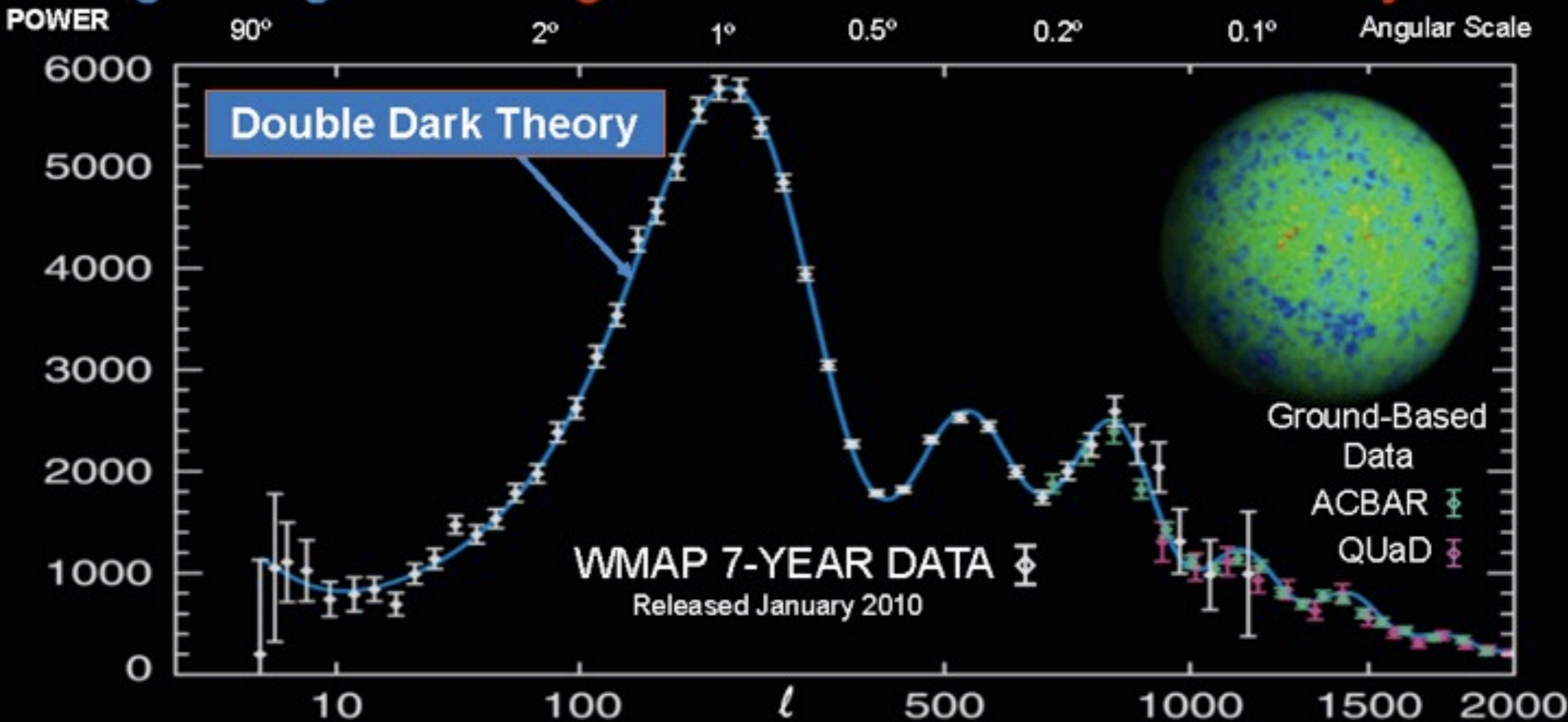
Fig. 12. The foreground-reduced Internal Linear Combination (ILC) map.

J. Dunkley, et.al. Five-Year Wilkinson Microwave Anisotropy Probe (WMAP) Observations: Likelihoods and Parameters from WMAP Data

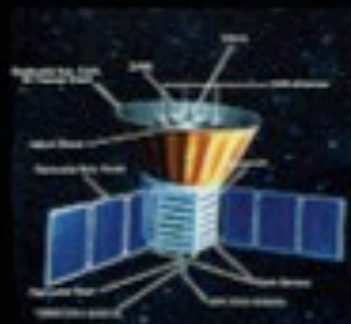
Final paragraph of Conclusions:

Considering a range of extended models, we continue to find that **the standard Λ CDM model is consistently preferred by the data**. The improved measurement of the third peak now requires the existence of light relativistic species, assumed to be neutrinos, at high confidence. The standard scenario has three neutrino species, but the three-year WMAP data could not rule out models with none. **The CDM model also continues to succeed in fitting a substantial array of other observations**. Certain tensions between other observations and those of WMAP, such as the amplitude of matter fluctuations measured by weak lensing surveys and using the Ly- α forest, and the primordial lithium abundance, have either been resolved with improved understanding of systematics, or show promise of being explained by recent observations. With further WMAP observations we will better probe both the universe at a range of epochs, measuring fluctuation characteristics to probe the initial inflationary process, or other non-inflationary scenario, improving measurements of the composition of the universe at the recombination era, and characterizing the reionization process in the universe.

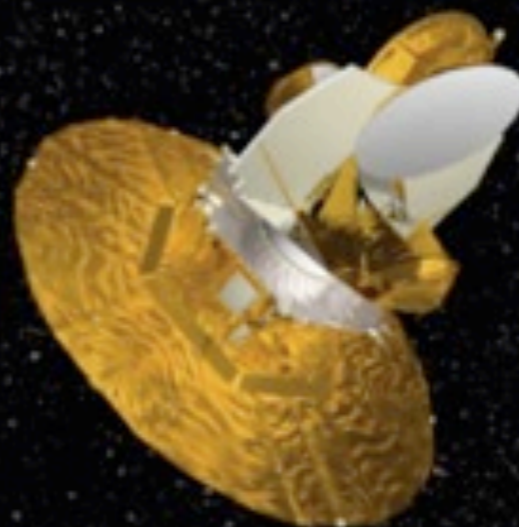
Big Bang Data Agrees with Double Dark Theory!



Cosmic Background Explorer
COBE
1992



Wilkinson Microwave Anisotropy Probe
WMAP
2003-



<http://lambda.gsfc.nasa.gov/product/space/>

Seven-Year Wilkinson Microwave Anisotropy Probe (WMAP) Observations:
Sky Maps, Systematic Errors, and Basic Results - N. Jarosik et al. - January 2010

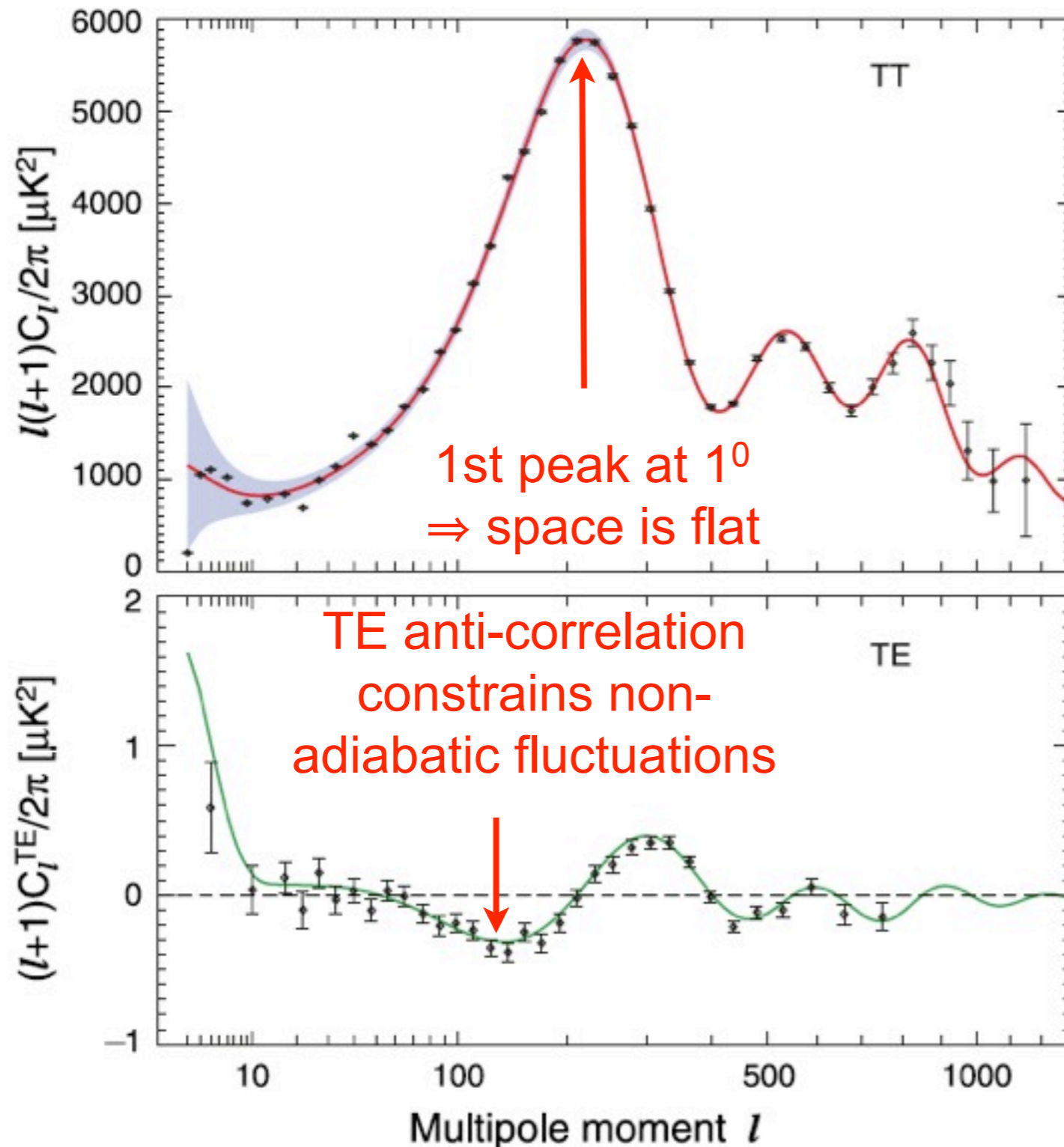


Fig. 9.— The temperature (TT) and temperature-polarization (TE) power spectra for the seven-year WMAP data set. The solid lines show the predicted spectrum for the best-fit flat Λ CDM model. The error bars on the data points represent measurement errors while the shaded region indicates the uncertainty in the model spectrum arising from cosmic variance.

Description	Symbol	WMAP -only	WMAP +BAO+ H_0
Parameters for Standard Λ CDM Model ^a			
Age of universe	t_0	13.75 ± 0.13 Gyr	13.75 ± 0.11 Gyr
Hubble constant	H_0	71.0 ± 2.5 km/s/Mpc	$70.4^{+1.3}_{-1.4}$ km/s/Mpc
Baryon density	Ω_b	0.0449 ± 0.0028	0.0456 ± 0.0016
Physical baryon density	$\Omega_b h^2$	$0.02258^{+0.00057}_{-0.00056}$	0.02260 ± 0.00053
Dark matter density	Ω_c	0.222 ± 0.026	0.227 ± 0.014
Physical dark matter density	$\Omega_c h^2$	0.1109 ± 0.0056	0.1123 ± 0.0035
Dark energy density	Ω_Λ	0.734 ± 0.029	$0.728^{+0.015}_{-0.016}$
Curvature fluctuation amplitude, $k_0 = 0.002$ Mpc ⁻¹ ^b	$\Delta_{\mathcal{R}}^2$	$(2.43 \pm 0.11) \times 10^{-9}$	$(2.441^{+0.088}_{-0.092}) \times 10^{-9}$
Fluctuation amplitude at $8h^{-1}$ Mpc	σ_8	0.801 ± 0.030	0.809 ± 0.024
Scalar spectral index	n_s	0.963 ± 0.014	0.963 ± 0.012
Redshift of matter-radiation equality	z_{eq}	3196^{+134}_{-133}	3232 ± 87
Angular diameter distance to matter-radiation eq. ^c	$d_A(z_{\text{eq}})$	14281^{+158}_{-161} Mpc	14238^{+128}_{-129} Mpc
Redshift of decoupling	z_*	$1090.79^{+0.94}_{-0.92}$	$1090.89^{+0.68}_{-0.69}$
Age at decoupling	t_*	379164^{+5187}_{-5243} yr	377730^{+3205}_{-3200} yr
Angular diameter distance to decoupling ^{c,d}	$d_A(z_*)$	14116^{+160}_{-163} Mpc	14073^{+129}_{-130} Mpc
Sound horizon at decoupling ^d	$r_s(z_*)$	$146.6^{+1.5}_{-1.6}$ Mpc	146.2 ± 1.1 Mpc
Acoustic scale at decoupling ^d	$l_A(z_*)$	302.44 ± 0.80	302.40 ± 0.73
Reionization optical depth	τ	0.088 ± 0.015	0.087 ± 0.014
Redshift of reionization	z_{reion}	10.5 ± 1.2	10.4 ± 1.2
Parameters for Extended Models ^e			
Total density ^f	Ω_{tot}	$1.080^{+0.093}_{-0.071}$	$1.0023^{+0.0056}_{-0.0054}$
Equation of state ^g	w	$-1.12^{+0.42}_{-0.43}$	-0.980 ± 0.053
Tensor to scalar ratio, $k_0 = 0.002$ Mpc ⁻¹ ^{b,h}	r	< 0.36 (95% CL)	< 0.24 (95% CL)
Running of spectral index, $k_0 = 0.002$ Mpc ⁻¹ ^{b,i}	$dn_s/d \ln k$	-0.034 ± 0.026	-0.022 ± 0.020
Neutrino density ^j	$\Omega_\nu h^2$	< 0.014 (95% CL)	< 0.0062 (95% CL)
Neutrino mass ^j	$\sum m_\nu$	< 1.3 eV (95% CL)	< 0.58 eV (95% CL)
Number of light neutrino families ^k	N_{eff}	> 2.7 (95% CL)	$4.34^{+0.86}_{-0.88}$

Table 8. WMAP Seven-year Cosmological Parameter Summary

The parameters reported in the first section assume the 6 parameter flat CDM model, first using WMAP data only (Larson et al. 2010), then using WMAP+BAO+ H_0 data (Komatsu et al. 2010). The H_0 data consists of a Gaussian prior on the present-day value of the Hubble constant, $H_0 = 74.2 \pm 3.6$ km s⁻¹ Mpc⁻¹ (Riess et al. 2009), while the BAO priors on the distance ratio $r_s(z_d)/D_V(z)$ at $z = 0.2, 0.3$ are obtained from the Sloan Digital Sky Survey Data Release 7 (Percival et al. 2009). **Uncertainties are 68% CL unless otherwise noted.**

SEVEN-YEAR WILKINSON MICROWAVE ANISOTROPY PROBE (WMAP) OBSERVATIONS: COSMOLOGICAL INTERPRETATION - E. Komatsu, et al. - January 2010

The combination of 7-year data from *WMAP* and improved astrophysical data rigorously tests the standard cosmological model and places new constraints on its basic parameters and extensions. By combining the *WMAP* data with the latest distance measurements from the Baryon Acoustic Oscillations (BAO) in the distribution of galaxies (Percival et al. 2009) and the Hubble constant (H_0) measurement (Riess et al. 2009), we determine the parameters of the simplest 6-parameter Λ CDM model. The power-law index of the primordial power spectrum is $n_s = 0.963 \pm 0.012$ (68% CL) for this data combination, a measurement that excludes the Harrison-Zel'dovich-Peebles spectrum by more than 3σ . The other parameters, including those beyond the minimal set, are also consistent with, and improved from, the 5-year results. We find no convincing deviations from the minimal model. The 7-year temperature power spectrum gives a better determination of the third acoustic peak, which results in a better determination of the redshift of the matter-radiation equality epoch. Notable examples of improved parameters are the total mass of neutrinos, $\sum m_\nu < 0.58$ eV (95% CL), and the effective number of neutrino species, $N_{\text{eff}} = 4.34^{+0.86}_{-0.88}$ (68% CL), which benefit from better determinations of the third peak and H_0 . The limit on a constant dark energy equation of state parameter from *WMAP*+BAO+ H_0 , without high-redshift Type Ia supernovae, is $w = -1.10 \pm 0.14$ (68% CL). We detect the effect of primordial helium on the temperature power spectrum and provide a new test of big bang nucleosynthesis by measuring $Y_p = 0.326 \pm 0.075$ (68% CL). We detect, and show on the map for the first time, the tangential and radial polarization patterns around hot and cold spots of temperature fluctuations, an important test of physical processes at $z = 1090$ and the dominance of adiabatic scalar fluctuations. The 7-year polarization data have significantly improved: we now detect the temperature-*E*-mode polarization cross power spectrum at 21σ , compared to 13σ from the 5-year data. With the 7-year temperature-*B*-mode cross power spectrum, the limit on a rotation of the polarization plane due to potential parity-violating effects has improved by 38% to $\Delta\alpha = -1.1^\circ \pm 1.3^\circ$ (statistical) $\pm 1.5^\circ$ (systematic) (68% CL). We report a significant (8σ) detection of the Sunyaev-Zel'dovich (SZ) effect at the locations of known clusters of galaxies, and show that the measured SZ signal is a factor of 0.5 to 0.7 times the predictions from analytical models, hydrodynamical simulations, and X-ray observations. This lower amplitude is consistent with the lower-than-expected SZ power spectrum recently measured by the South Pole Telescope collaboration.

SEVEN-YEAR WILKINSON MICROWAVE ANISOTROPY PROBE (WMAP) OBSERVATIONS:
COSMOLOGICAL INTERPRETATION - E. Komatsu, et al. - January 2010

TABLE 1
SUMMARY OF THE COSMOLOGICAL PARAMETERS OF Λ CDM MODEL

Class	Parameter	WMAP 7-year ML ^a	WMAP+BAO+ H_0 ML	WMAP 7-year Mean ^b	WMAP+BAO+ H_0 Mean
Primary	$100\Omega_b h^2$	2.270	2.246	$2.258^{+0.057}_{-0.056}$	2.260 ± 0.053
	$\Omega_c h^2$	0.1107	0.1120	0.1109 ± 0.0056	0.1123 ± 0.0035
	Ω_Λ	0.738	0.728	0.734 ± 0.029	$0.728^{+0.015}_{-0.016}$
	n_s	0.969	0.961	0.963 ± 0.014	0.963 ± 0.012
	τ	0.086	0.087	0.088 ± 0.015	0.087 ± 0.014
	$\Delta_{\mathcal{R}}^2(k_0)^c$	2.38×10^{-9}	2.45×10^{-9}	$(2.43 \pm 0.11) \times 10^{-9}$	$(2.441^{+0.088}_{-0.092}) \times 10^{-9}$
Derived	σ_8	0.803	0.807	0.801 ± 0.030	0.809 ± 0.024
	H_0	71.4 km/s/Mpc	70.2 km/s/Mpc	71.0 ± 2.5 km/s/Mpc	$70.4^{+1.3}_{-1.4}$ km/s/Mpc
	Ω_b	0.0445	0.0455	0.0449 ± 0.0028	0.0456 ± 0.0016
	Ω_c	0.217	0.227	0.222 ± 0.026	0.227 ± 0.014
	$\Omega_m h^2$	0.1334	0.1344	$0.1334^{+0.0056}_{-0.0055}$	0.1349 ± 0.0036
	z_{reion}^d	10.3	10.5	10.5 ± 1.2	10.4 ± 1.2
	t_0^e	13.71 Gyr	13.78 Gyr	13.75 ± 0.13 Gyr	13.75 ± 0.11 Gyr

^aLarson et al. (2010). “ML” refers to the Maximum Likelihood parameters.

^bLarson et al. (2010). “Mean” refers to the mean of the posterior distribution of each parameter. The quoted errors show the 68% confidence levels (CL).

^c $\Delta_{\mathcal{R}}^2(k) = k^3 P_{\mathcal{R}}(k)/(2\pi^2)$ and $k_0 = 0.002 \text{ Mpc}^{-1}$.

^d“Redshift of reionization,” if the universe was reionized instantaneously from the neutral state to the fully ionized state at z_{reion} . Note that these values are somewhat different from those in Table 1 of Komatsu et al. (2009b), largely because of the changes in the treatment of reionization history in the Boltzmann code CAMB (Lewis 2008).

^eThe present-day age of the universe.

The constraint on N_{eff} can also be interpreted as an upper bound on the energy density in primordial gravitational waves with frequencies $> 10^{-15}$ Hz. Many cosmological mechanisms for the generation of stochastic gravitational waves exist, such as certain inflationary models, electroweak phase transitions, and cosmic strings.

With the current WMAP+BAO+ H_0 data combination, we define $N_{\text{gw}} = N_{\text{eff}} - 3.04$, and find limits of

$$N_{\text{gw}} < 2.85, \quad \Omega_{\text{gw}} h^2 < 1.60 \times 10^{-5} \text{ (95\%CL)}$$

for adiabatic initial conditions, imposing an $N_{\text{eff}} \geq 3.04$ prior.